INSTITUUT VOOR MATERIAALONDERZOEK

LIMBURGS
UNIVERSITAIR
CENTRUM
Faculteit Wetenschappen

NMR onderzoek naar de moleculaire structuur en dynamica van ethyleen-propyleen copolymeren

Proefschrift voorgelegd tot het bekomen van de graad van
Doctor in de Wetenschappen
aan het Limburgs Universitair Centrum
te verdedigen door

Carla Jansen

Promotoren : Prof. Dr. J. Gelan
Prof. Dr. R. Dommisse

Diepenbeek 1998

INSTITUUT VOOR MATERIAALONDERZOEK

LIMBURGS UNIVERSITAIR CENTRUM
Faculteit Wetenschappen

NMR onderzoek naar de moleculaire structuur en dynamica van ethyleen-propyleen copolymeren

Proefschrift voorgelegd tot het bekomen van de graad van
Doctor in de Wetenschappen
aan het Limburgs Universitair Centrum
te verdedigen door

Carla Jansen

Promotoren : Prof. Dr. J. Gelan
Prof. Dr. R. Dommisse

Diepenbeek 1998

ACKNOWLEDGEMENT

This work was not possible without the aid of many people who I would like to thank.

I express my sincere thanks to my two promotors Prof. Dr. R. Dommisse and Prod. Dr. J. Gelan for the opportunity they gave me and for the scientific assistance.

I owe especially much gratitude to Dr. P. Adriaensens for his support, his encouragement and the scientific discussions.

I also thank the PhD students and the personnel of the RUCA as well as the LUC for the pleasant working atmosphere, the support and the computer assistance.

I am Prof. Dr. H. Desseyn, J. Jansens, Prof. Dr. J. Mullens and G. Reggers thankful for the DSC measurements and I thank Prof. E. Vansant and H. Nys for the WAXS measurements.

I also thank the people from Borealis and Neste (R. Van Der Linden, N. Ackermans, A. Luyten, A.Coomans and T. Vaänänen) for the samples, the measurements and the general information about the polymers.

Finally, I would like to express my thanks to my parents, family, friends and Wim for their support and encouragements.

CONTENTS

1. Focusing the research **7**

1.1. Introduction 7

1.2. Polypropylene: synthesis and properties 7

1.3. Ethylene-propylene copolymers: synthesis and properties 9

1.4. Purpose of the research 10

1.5. Overview of the content 11

1.6. References 13

2. NMR **15**

2.1. Introduction 15

2.2. Some general aspects of solid-state NMR 15

- 2.2.1. Fundamental principles 15
- 2.2.2. Spin diffusion and molecular diffusion 19
- 2.2.3. Relaxation times as function of the correlation times and the magnetic field 20
- 2.2.4. The utility of some relaxation times 22
  - 2.2.4.1. The carbon spin lattice relaxation time, T_{1C} 23
  - 2.2.4.2. The carbons spin lattice relaxation time in the rotating frame, $T_{1\rho C}$ 23
  - 2.2.4.3.The carbon spin spin relaxation time, T_{2C} 24
  - 2.2.4.4. The proton spin lattice relaxation time, T_{1H} 24
  - 2.2.4.5. The proton spin lattice relaxation time in the rotating frame, $T_{1\rho H}$ 25
  - 2.2.4.6. The proton spin spin relaxation time, T_{2H} 25
  - 2.2.4.7. The cross polarisation time, T_{CH} 25

2.3. ^{13}C high resolution solid-state NMR 26

- 2.3.1. Line width 26
- 2.3.2. Sensitivity enhancement by cross polarisation 29
- 2.3.3. The pulse sequences 33
  - 2.3.3.1. The $T_{1\rho H}$ or spin lock experiment 33
  - 2.3.3.2. The cross depolarisation experiment 35
  - 2.3.3.3. The inversion recovery experiment 37
  - 2.3.3.4. The saturation recovery experiment 38

2.3.3.5. The proton T_2 experiment 39

2.4. ^{1}H wideline NMR 41

2.4.1. The measurement of the proton spin spin relaxation time, T_{2H} 41

2.4.1.1. The solid echo pulse sequence 41

2.4.1.2. The Hahn echo pulse sequence 43

2.4.1.3. The CPMG pulse sequence 44

2.4.2. The measurement of the proton spin lattice relaxation time, T_{1H} 45

2.4.3. The measurement of the $T_{1\rho H}$ relaxation time 46

2.5. Conclusions 46

2.6. References 47

3. Macroscopic properties **49**

3.1. Introduction 49

3.2. Preliminary characterisation of the samples 49

3.3. Fractionation with xylene 51

3.4. Crystallinity 52

3.4.1. The crystalline forms of polypropylene 52

3.4.2. The crystallinity of the samples 53

3.4.3. The effect of annealing on the crystallinity 56

3.5. Glass transition temperature 58

3.6. Mechanical testing 60

3.7. Conclusions 61

3.8. References 62

4. Liquid-state NMR: a sequence analysis **65**

4.1. Introduction 65

4.2. Chemical shift assignment 65

4.3. Sequence analysis 67

4.3.1. Quantitative ^{13}C liquid-state NMR spectra 69

4.3.2. Reproducibility 70

4.3.2.1. The influence of integration of the signals 70

4.3.2.2. The influence of a NMR experiment 72

4.3.2.3. The influence of the solution 73
4.3.2.4. Conclusions 73
4.3.3. Micro-structure of some ethylene-propylene copolymers 73
4.3.4. Micro-structure of the fractionated samples 75
4.3.4.1. The xylene soluble fraction 77
4.3.4.2. The amorphous xylene soluble fraction 79
4.3.4.3. The xylene insoluble fraction 79
4.3.4.4. A comparison between the xylene insolubles and the xylene soluble fraction 80
4.4. Conclusions 81
4.5. References 83

5. High resolution ^{13}C solid-state NMR **85**
5.1. Introduction 85
5.2. The MAS and CP/MAS spectra of polypropylene and ethylene-propylene random and block copolymers 85
5.2.1. The influence of the temperature on the MAS NMR spectrum and a chemical shift assignment 87
5.2.1.1. The influence of the temperature on MAS NMR spectrum of polypropylene 87
5.2.1.2. The influence of the temperature on the solid-state spectrum of true ethylene-propylene copolymer 90
5.2.1.3. The influence of the temperature on the solids-state NMR spectrum of ethylene-propylene heterophasic copolymers and an accurate chemical shift assignment 92
5.2.1.4. Conclusions 94
5.2.2. Selectivity of the MAS and CP/MAS spectrum with regard to the mobile and rigid phase in the ethylene-propylene copolymer 95
5.2.2.1. Selectivity of the ^{13}C MAS spectrum of ethylene-propylene copolymers 95
5.2.2.2. The influence of the length of the contact time on CP/MAS spectra 97
5.2.3. The influence of the thermal pretreatment of the samples on the solid-state NMR spectrum 98
5.2.3.1. The influence of the annealing temperature on the spectrum of polypropylene 99

5.2.3.2. The influence of the annealing temperature on the spectrum of ethylene-propylene copolymers 103
5.2.3.3. Conclusions 105
5.2.4. Conclusions 106
5.3. A study of the relaxation times at different temperatures 107
5.3.1. A $T_{1\rho H}$ relaxation study 107
5.3.1.1. Choice of the $T_{1\rho H}$ equation 107
5.3.1.2. Determination of the T_{CH} time 108
5.3.1.3. The influence of the cross polarisation time on the $T_{1\rho H}$ relaxation 110
5.3.1.4. The $T_{1\rho H}$ behaviour of polypropylene and ethylene-propylene copolymers 112
5.3.1.5. Conclusions 119
5.3.2. T_{1H} relaxation time 119
5.3.2.1. T_{1H} measurements at room temperature 120
5.3.2.2. T_{1H} measurements at 90°C 122
5.3.2.3. Conclusions 123
5.3.3. T_{1C} study 124
5.3.3.1. T_{1C} relaxation of polypropylene 124
5.3.3.2. T_{1C} relaxation of the true ethylene-propylene copolymers 125
5.3.3.3. T_{1C} relaxation of ethylene-propylene block copolymer 126
5.3.4. A T_{2H} study 128
5.3.4.1. The T_{2H} relaxation behaviour of polypropylene 128
5.3.4.2. The T_{2H} relaxation behaviour of ethylene-propylene copolymers 129
5.3.5. Conclusions 130
5.4. $T_{1\rho H}$ relaxation time as a function of the annealing temperature and the annealing time 131
5.4.1. The influence of the annealing temperature and annealing time on the $T_{1\rho H}$ relaxation time of polypropylene 131
5.4.2. The influence of the annealing temperature on the $T_{1\rho H}$ relaxation time of ethylene-propylene copolymers 134
5.4.3. Conclusions 137
5.5. The influence of the magnetic field 137
5.6. Conclusions 139

5.7. References 141

6. ^{1}H wideline NMR 145

6.1. Introduction 145

6.2. The proton spin lattice relaxation time 145

6.3. The spin spin relaxation time 147

6.3.1. T_{2H} study with the solid echo pulse sequence 148

6.3.1.1. The spin spin relaxation of polypropylene 149

6.3.1.2. The T_{2H} relaxation of a block copolymers 151

6.3.1.3. The T_{2H} relaxation of the xylene soluble fractions 153

6.3.1.4. The spin spin relaxation behaviour of the xylene insoluble fractions 154

6.3.1.5. Conclusions 155

6.3.2. T_{2H} study with the Hahn echo pulse sequence 155

6.3.2.1. T_{2H} measurement of polypropylene 155

6.3.2.2. T_{2H} measurement of ethylene-propylene block copolymers 156

6.3.2.3. The spin spin relaxation time of different copolymer samples 159

6.3.3. T_{2H}study with the CPMG pulse sequence 160

6.3.3.1. A comparison of the T_{2H} relaxation of polypropylene and block copolymer 160

6.3.3.2. A comparison of the T_{2H} relaxation of the block copolymers 161

6.3.3.3. T_{2H} study of the xylene soluble fractions 162

6.3.4. The influence of the magnetic field on the spin spin relaxation times 163

6.4. $T_{1\rho H}$ relaxation time 164

6.5. Conclusions 166

6.6. References 169

7. Summary and general conclusions 171

8. Nederlandse samenvatting en algemene conclusies 175

9. Experimental part 181

1. FOCUSING THE RESEARCH

1.1. Introduction[1-3]

Commercial ethylene-propylene copolymers, which forms the subject of this research can be divided in ethylene-propylene block and random copolymers. For random copolymers the ethylene is randomly distributed in the polypropylene chains, while the term "block" implies that the copolymer is conceived as a sequential alteration of more or less long segments of ethylene and propylene.[4] In reality however, ethylene-propylene block copolymers are formed as multiphase structures comprised of polypropylene in which domains of true ethylene-propylene copolymer are dispersed. Other names that are used for the block copolymers are ethylene-propylene heterophasic copolymers, impact polypropylene copolymer or *in-situ* ethylene-propylene copolymers. The success of ethylene-propylene copolymers results out of the improved properties over polypropylene, polyethylene and their blends.[5]

1.2. Polypropylene: synthesis and properties[6-14]

Polypropylene is a semi-crystalline polymer that has been synthesised since the early 1950's. Since then it became possible to make stereo-specific polypropylene thanks to the work of Ziegler and Natta, who developed new polymerisation catalysts with stereo-regulating power.[15,16] Previously attempts to synthesise polypropylene from propylene by using the same low pressure process as for polyethylene were without any success because a mixture of the three possible stereo-isomers of polypropylene was synthesised. In the isotactic configuration the methyl groups lie on the same side of the plane of the main chain, that is in a fully extended planar zigzag conformation. For syndiotactic polypropylene the substituents lie alternately above and below the plane, while in atactic polypropylene the methyl groups are randomly positioned. Atactic polypropylene is amorphous and is not useful for technical applications, while isotactic polypropylene with the highest regularity can crystallise. The latter is the key to many of the desirable properties of polypropylene like its stiffness and its high tensile strength.

With the stereo-specific Ziegler-Natta catalysts it became possible to make highly isotactic polypropylene. The catalysts are formed by a combination of a transition-metal salt (e.g. $TiCl_4$) with an organometallic compound (e.g. $AlEt_3$). The catalysts are divided in four generations. The first-generation catalysts are those of Ziegler and Natta, that can produce polypropylene with an isotactic index of 83 to 93%. In the early 1970's an electron donor was added to the catalyst system. This can be regarded as the basis of the second-generation catalysts which were up to six times more active and the isotactic index was about 94 to 97%. The third-generation catalysts are supported on a inert porous material, like $MgCl_2$ particles. Internal and external modifiers are used to increase the stereo-regularity of the polymer. The advantage of the fourth-generation catalysts over the third ones is the controlled particle morphology, that is needed in certain polymerisation processes. During the last years, also metallocene catalysts[17] (or fifth-generation catalysts) were used and they introduced polymers with very narrow molecular weight distributions (a polydispersity index of 2) and narrow composition distributions. This means that all polymer chains have the same comonomer concentration and the same distribution. This improves the clarity in films and results also in a higher modulus, lower level of extractables, increased toughness,... These properties can be interesting for high speed spinning of fine fibres for non-woven fabrics and for thin biaxially oriented films. For general applications a broader molecular weight distribution is desirable as is produced with Ziegler-Natta catalysts (a polydispersity index of 4 to 6): the small amount of low molecular weight is necessary for a good processability and the very high molecular weight is needed to improve the impact strength.

For the production of polypropylene with Ziegler-Natta catalysts two different production processes exist: the slurry process and the spheriphol process.

The slurry process is the oldest and the polymerisation is carried out continuously in a five series reactor. Catalyst and its activator together with liquid propylene and diluent are added in the reactor under pressure and at increased temperature. The diluent is used to transport the heat of reaction to the reactor walls which are cooled with water. H_2 is used to control the molecular weight. Polypropylene is insoluble in the diluent and is formed as particles that can be removed from the reactor. The slurry of polypropylene particles is washed with an alcohol to deactivate the catalyst and activator and to make them soluble. Afterwards the polypropylene is dried and mixed with solid stabilisers in preparation for feeding into the pelletisers to get the finished product in the form of uniform pellets. This is a complicated process and the final polypropylene pellets can contain up to five percent of atactic material.

In the spheriphol process the polymerisation is carried out in liquid bulk with a high activity catalyst. The catalyst system comprises a titanium salt catalyst supported on an inert material in spherical form, an aluminium cocatalyst and a donor. The internal and external donor are used to increase the isotacticity. The catalyst package, the liquid polypropylene and the hydrogen are continuously fed to the loop reactor where the reaction takes place at increased temperature and under high pressure. The polymerisation pressure must be high enough to maintain the polypropylene in the liquid phase at the increased reaction temperature. The heat of polymerisation can easily be removed by the walls of the loop that has a high heat transfer surface to volume ratio. The slurry of polypropylene spheres that is synthesised in the liquid propylene is discharged from the loop reactor, dried and pelletised with specific additives, like antioxidants, UV-stabilisers, antistatics,...[18]

The highly isotactic polypropylene has a lot of interesting properties. This homopolymer has a specific gravity of 0.9; making it the lightest among the major plastics. Its high flex modulus makes polypropylene the stiffest of the polyolefins. Moreover, due to its high crystallinity polypropylene also has a high tensile strength and hardness. Besides polypropylene has the chemical inertness typical of hydrocarbon polymers. These properties together with its excellent processability and low cost make polypropylene to a versatile polymer that is used in a wide variety of markets: in the car industry for bumpers and battery cases, in the food industry for crates and transparent packaging films, in the housing market as filament and staple for carpeting, ...Oxley D.F.[19] claimed that polypropylene is replacing sulphuric acid as the barometer of the industrial world because of its wide range of applications. In 1995 about 19 125 000 ton was consumed over the world of which 4 960 000 ton in Western Europe and a growth rate of six percent is expected. The most important Western Europe polypropylene companies are Montell, BASF, Borealis and Hoechst.

Although polypropylene has many good properties, its major disadvantage is its low impact strength at low temperature. This can be improved by blending it up to 25% with ethylene-propylene copolymer (EPR) or with ethylene-propylene terpolymer (EPDM); or by adding ethylene during the second stage polymerisation process to make heterophasic ethylene-propylene copolymers. The latter will be discussed here.

1.3. Ethylene-propylene copolymers: synthesis and properties[1-3,10,20-25]

Ethylene-propylene random and block copolymers are synthesised with the same Ziegler-Natta catalysts as polypropylene. For the polymerisation of random copolymers with the spheriphol process, liquid ethylene together with liquid propylene, the catalyst system and hydrogen is fed to the loop reactor. For block copolymers, no ethylene is added to the first stage and only polypropylene is synthesised in the loop reactor. Afterwards, the polypropylene granules are fed in the gas-phase reactor where the copolymerisation takes place. This is a fluid-bed reactor where ethylene and propylene gases are continuously copolymerised. In the slurry polymerisation process, propylene is added in the first and second step of the five-step reactor. In the fourth and fifth step ethylene and propylene are added together to produce block copolymers. For random copolymers, ethylene is already added in the first and second step. Random copolymers can have up to 5% ethylene while heterophasic copolymers normally can contain up to 15% of ethylene.

Ethylene-polypropylene copolymers have an improved impact strength over polypropylene and they are used in auto interiors, for bumpers in cars, injection mouldings, seating, drain and irrigation pipes. Besides the better impact strength, a higher flexibility is also noted together with a decrease of crystallinity, tensile strength, stiffness and hardness. Random copolymers have a better clarity compared with polypropylene and the toughness is improved at the expense of stiffness.

The impact ethylene-propylene copolymers also have improved properties over blends of polypropylene and polyethylene because these two homopolymers are immiscible. The polymer blend has a phase-separated morphology. It was found that addition of ethylene-propylene rubber results in homogenisation of the material. Hence, the ethylene-propylene rubber can be considered as "interfacial" agent that improves the adhesion between the polyethylene dispersed phase and the polypropylene matrix. According to Stehling et al.[26] the dispersed phase in ternary blends (PP/EPR/PE) exists as layered sphere structures of spherical polyethylene occlusions that is covered by the ethylene-polypropylene rubber in the bulk polypropylene. Ethylene-propylene block copolymers are highly complicated composites of polypropylene, true ethylene-propylene copolymer and polyethylene. In these copolymers polyethylene combined with ethylene-polypropylene rubber forms a dispersed domain in the polypropylene matrix as can be seen with electron microscopy.[21,27]

1.4. Purpose of the research

Commercial ethylene-propylene copolymers have improved properties over polypropylene, polyethylene and their blends. These heterophasic copolymers are synthesised by adding ethylene during the second stage of the polymerisation process of polypropylene. Until now the characteristics of the synthesised polymer can be checked in the laboratory only after the polymerisation. This takes quite some time however. It would be more economic to check the product directly during the polymerisation. The question that came from the industry was: should it be possible to control the polymerisation with an *on-line* industrial NMR? To introduce such a NMR in the production process, the NMR results of the ethylene-propylene copolymers have to be clearly understood and a detailed solid-state NMR study of the complex polymer is needed.

For this study, a few ethylene-propylene heterophasic copolymer samples were supplied by Borealis. All the samples contain less than fifteen percent of ethylene as is typical for such copolymers. Although it is a small range of ethylene content the copolymers can have very different macroscopic properties. It is not only important how much ethylene the polymer contains, but also how the ethylene is divided among the polypropylene chains and this can be studied with liquid-state NMR. In addition, with solid-state NMR it is possible to study the molecular mobility of the polymer chains which can be correlated with the macroscopic properties.

The purpose of this research was to investigate the ethylene-polypropylene copolymers (supplied by Borealis) with NMR to get a better understanding of the molecular structure and molecular dynamics of the copolymers so that the results of an industrial NMR can be interpreted correctly.

1.5. Overview of the content

Chapter 1 contains a general introduction about ethylene-propylene copolymers. A brief summary of the synthesis and properties of polypropylene and ethylene-propylene copolymers is given. Eventually the purpose of the research is formulated.

In chapter 2 some solid-state NMR topics are explained. The line width of signals in a solid-state NMR spectrum and the relaxation times are function of the molecular dynamics of a polymer and this is pointed out in this chapter.

The polymerisation process has an influence on the mechanical properties, the crystallinity, the molecular weight and its distribution, the ethylene content and its distribution,... A characterisation of the polymers is given in chapter 3: the polymerisation process, the melt index, crystallinity, glass transition temperature, fractionation with xylene and the mechanical properties are summarised in this chapter. Liquid-state NMR is used to study the ethylene content and the sequence distribution of the copolymers, the xylene soluble and insoluble fractions. These results are discussed in chapter 4.

In chapter 5 the ^{13}C solid-state NMR spectra are studied and the relaxation times of ethylene-propylene copolymers are discussed in terms of their molecular mobility. The influence of the measuring temperature as well as the influence of the annealing temperature and the magnetic field are studied in order to find the best measuring conditions.

In chapter 6 the ^{1}H wideline results are discussed and attention is focused on T_{2H} relaxation. The wideline results were compared with the ^{13}C MAS NMR results of chapter 5.

Chapter 7 gives a summary and some general conclusions. A Dutch summary is given in chapter 8.

The experimental part is given in chapter 9.

1.6. References

1. Mirabella Jr, F.M.; Polymer, 34(8) (1993), 1729.

2. Flaris, V.; Stachurski, Z.H.; J. Appl. Polym. Sci., 45 (1992), 1789.

3. Ito, J.; Mitani, K.; Mizutani, Y.; J. Appl. Polym. Sci., 46 (1992), 1221.

4. Simonazzi, T.; Pure and Appl. Chem., 56(5) (1984), 625.

5. Prasad, J.V.; J. Polym. Sci.: Part A: Polym. Chem., 30 (1992), 2033.

6. Van der Vegt, A.K.; "Polymeren: van keten tot kunststof", Delftsche Uitgevers Maatschappij, Delft, 1994.

7. Billmeyer Jr., F.W.; "Textbook of Polymer Science", John Wiley & Sons, Singapore, 1994.

8. Arzounamidis, G.G.; karayannis, N.M.; Chemtech, 23 (1993), 43.

9. Galli, P.; Haylock, J.C; Makromol. Chem., Macromol. Symp., 63 (1992), 19.

10. Short, J.N.; Chemtech., 11 (1981), 238.

11. Soga, K.; Makromol. Chem., Macromol. Symp., 66 (1993), 43.

12. Zucchini, U.; Makromol. Chem., Macromol. Symp., 66 (1993), 25.

13. Frank, H.P.; "Polypropylene", Macdonald & Co., London, 1969.

14. Raff, R.A.V.; Doak, K.W.; "Crystalline Olefin Polymers", Part 1, Wiley-Interscience, New York, 1965.

15. Natta, G.; J. Am. Chem. Soc., 77 (1955), 1708.

16. Natta, G., J. Polym. Sci.; 16 (1955), 143.

17. Resconi, L.; Jones, R.L.; Rheingold, A.L.; Yap, G.P.A.; J. Am. Chem. Soc., 15 (1996), 998.

18. Stevens, M.P.; J. Chem. Education, 70(9) (1993), 713.

19. Oxley, D.F.; Chem. Ind., 15 (1996), 535.

20. Teh, J.W.; Rudin, A.; Keung, J.C.; Adv. Polym. Techn., 13(1) (1994), 1.

21. Sun, Z.; Yu, F.; Qi, Y.; Polymer, 32(6) (1991), 1059.

22. Ronarc'h D.; Audren, P.; Moura, J.L.; J. Appl. Phys., 58(1) (1985), 466.

23. Brydson, J.A., "Plastics materials", the Butterworth Group, London, 1975.

24. Prabhu, P.; Schindler, A.; Gilbert, R.D.; Polym. Prepr., 19 (1978), 642.

25. Prentice, P.; Polymer, 23 (1982), 1189.

26. Stehling, F.C.; Huff, T.; Speed, C.S.; Wissler, G.; J. Appl. Polym. Sci., 26 (1981), 2693.

27. Karger-Kocsis, J.; Kiss, L.; Polym. Eng. Sci., 27(4) (1987), 254.

2. SOLID-STATE NMR: A TECHNIQUE TO STUDY THE MOLECULAR DYNAMICS OF POLYMERS

2.1. Introduction

NMR is mainly known from liquid-state NMR because it gives information about the structure, the composition, the micro-structure, the conformation and the branching of the polymer,... On the other hand, solid-state NMR is also often used. The analysis of polymers in their solid state is interesting

(1) for polymers which are insoluble,

(2) to study the polymer in the aggregation state in which they are mostly used,

(3) to know the influence of molecular dynamics and domains on the macroscopic properties.

In this chapter a discussion is given about the use of some typical solid-state NMR parameters i.e. relaxation times, line broadening and spin diffusion. The methods to study these parameters with high-resolution ^{13}C solid-state NMR as well as with ^{1}H wideline NMR are discussed.

2.2. Some general aspects of solid-state NMR

2.2.1. Fundamental principles[1,2]

When a molecule is placed in a magnetic field B_0 the magnetic moments μ of the individual nuclei undergo precession around the direction of B_0 with the Larmor frequency $\omega_0 = \gamma B_0$. Due to this Zeeman interaction the nuclear magnetic moments of atoms with an odd mass number like ^{1}H and ^{13}C can have two orientations (parallel and antiparallel to B_0) with specific amount of energy each. The energy separation between the two magnetic energy levels in the magnetic field B_0 is given by:

$$\Delta E = h\nu_0 = \frac{\mu B_0}{I} \qquad \text{with I the nuclear spin quantum number} \qquad (2.1)$$

The population ratio of the two levels can be calculated from the Boltzmann equation. The sum of all magnetic moments results in a magnetisation in the direction of the magnetic field B_0.

In a NMR experiment a second magnetic field B_1 is applied at right angle to B_0. This causes the nuclear spins to flip over between the two levels and the sum magnetisation rotates around the B_1 field. This is shown in Figure 2.2a-c. The rotation around the B_1 field vector is only possible when the B_1 field rotates with the same Larmor frequency ω_0 around the B_0 field as the magnetic moments. Therefore the diagram shown in Figure 2.2 is for convenience drawn in the rotating frame. The rotating frame rotates at the angular frequency ω_0 with respect to the laboratory frame. The axes X, Y, Z label the rotating frame while another set X', Y' and Z' are appropriate to the laboratory frame in Figure 2.1. In both frames the Z and Z' axis coincide with the B_0 field. In NMR theory the rotating frame has been used frequently because it can remove the time dependence of some quantities. In the rotating frame the B_1 field is static and there is no precession of the sum magnetisation M around the B_0 field. In presence of the rf field B_1 the magnetisation M can be rotated around the field axis in the yz plane (Figure 2.2b). The angle of precession (α) depends on the strength (B) and the duration (t) of the pulse according to the equation:

$\alpha = \gamma B_1 t$ with γ the magnetogyric ratio (2.2)

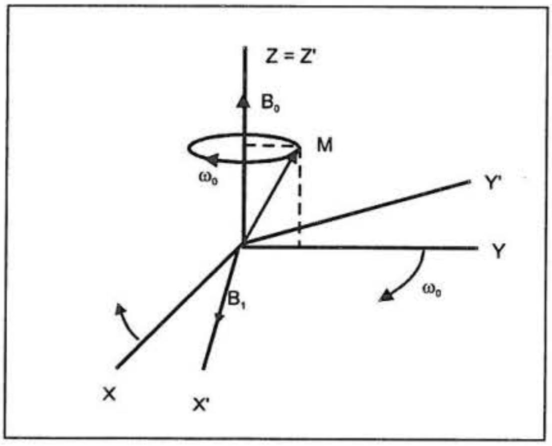

Figure 2.1: The rotating frame XYZ rotates with the Larmor frequency ω_0 around the Z' axis in the laboratory frame X'Y'Z'. B_1 and M are static in the rotating frame.

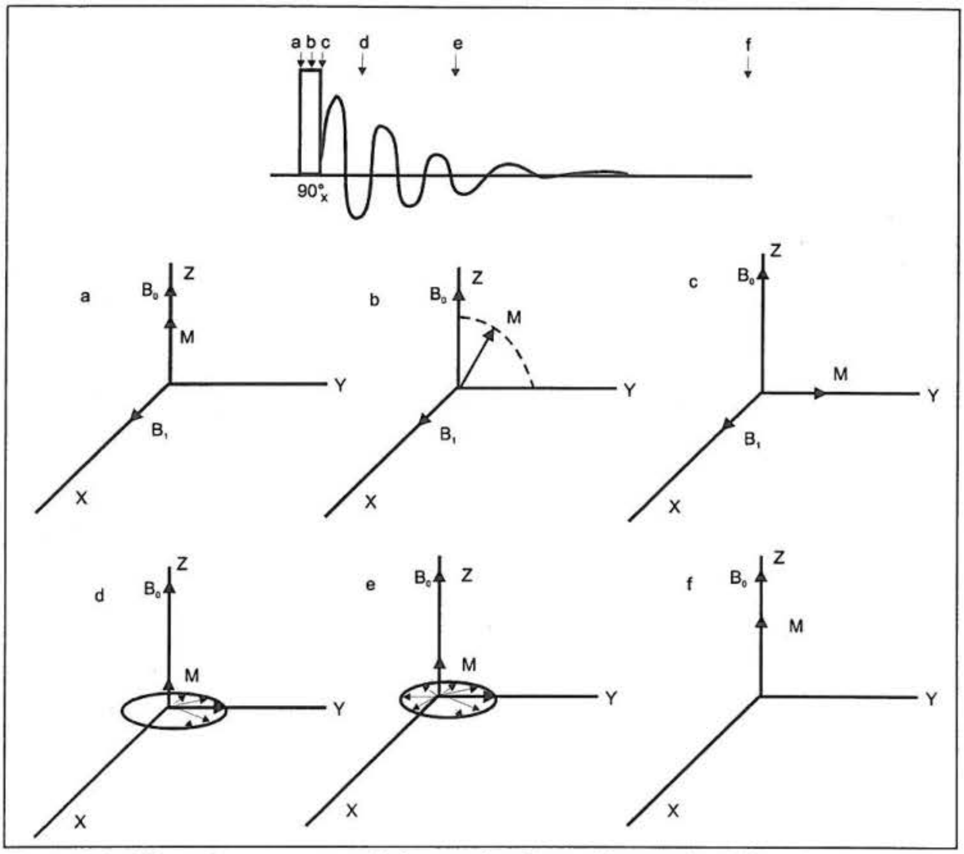

Figure 2.2: The pulse sequence and the rotating frame diagram describing the normal NMR experiment.

After the 90° pulse the spins relax in the xy plane by spin spin or T_2 relaxation and in the z direction by spin lattice or T_1 processes and eventually the equilibrium magnetisation is attained along the z axis (Figure 2.2d-f). This relaxation can be expressed by the Bloch[3] equations. The longitudinal relaxation is the relaxation of the z component toward an equilibrium value M_0:

$$\frac{dM_z}{dt} = \frac{M_z - M_0}{T_1} \tag{2.3}$$

The transverse relaxation is the change of the magnetisation in the xy plane as a function of the time:

$$\frac{dM_x}{dt} = \frac{-M_x}{T_2} \tag{2.4}$$

$$\frac{dM_y}{dt} = \frac{-M_y}{T_2} \tag{2.5}$$

The decay in the xy plane provides the observed signal and is called the free induction decay (FID). After Fourier transformation the frequency domain spectrum is obtained.

The relaxation in the x, y and z direction can also be described in terms of energy states. In absence of an external field B_1 the distribution of the spins in a magnetic field B_0 is given by the Boltzmann equation:

$$\frac{N_{+1/2}}{N_{-1/2}} = \exp\left(\frac{2\mu B_0}{kT}\right) \quad \text{for spins with I=1/2.} \tag{2.6}$$

$N_{+1/2}$ and $N_{-1/2}$ represent the population in respectively the lower and upper states and T is the spin temperature. At equilibrium $N_{+1/2}/N_{-1/2}$ is only slightly larger than 1.

In the presence of a field B_1 there is a transfer of spins for the lower energy state to the upper state and eventually the spins are equally distributed over the two states. This condition of saturation is correlated with a high spin temperature. To get the equilibrium state, the spin system has to be cooled or energy has to be transferred from the spin system. As the energy separation between the upper and lower state is very small, the energy dissipation does not occur spontaneously. Oscillating magnetic fields are necessary to stimulate the relaxation. This can be caused by modulation of the local magnetic field by molecular motions. This fluctuating magnetic field can be induced by the motion of nearby magnetic nuclei. Nuclei are thermally coupled to their surroundings or lattice and energy can be transferred. As the coupling is weak the thermal relaxation is slow. This process is the *spin lattice relaxation*. On the other side, the *spin spin relaxation* is an energy conserving process. T_2 is a pure entropy relaxation. This relaxation occurs because all the spins do not feel exactly the same magnetic field as a result of inhomogeneity of the external magnetic field B_0 and interactions in the system (i.e. dipolar coupling between nuclear magnetic moments). This causes the spins not to precess with the same frequency and the spins get out of phase. Eventually no net magnetisation is found in the xy plane. This T_2 relaxation is also related to the line width $\delta\nu$:

$$T_2 = \frac{1}{\pi \delta\nu} \tag{2.7}$$

This equation is true in absence of inhomogeneous line broadening effects (i.e. B_0 inhomogeneity and slightly different chemical shifts).

Besides T_1 and T_2 relaxation a third relaxation exists: $T_{1\rho}$. This is the spin lattice relaxation in the rotating magnetic field B_1. $T_{1\rho}$ describes the relaxation in the rotating frame in the direction of B_1. The magnetic field B_1 is 90° out of phase compared to B_0 and it is much smaller than B_0. As for T_1 $T_{1\rho}$ relaxation is also influenced by molecular motions of the surrounding. Molecular motions stimulate this relaxation most efficiently when their frequencies for molecular motions are at or near the transmitter frequency ($\omega_1 = \gamma B_1$). This causes T_1 and $T_{1\rho}$ to be influenced by different molecular motions.

2.2.2. Spin diffusion and molecular diffusion[4,5]

In solid-state NMR the relaxation can be averaged out over certain domains as a result of spin diffusion and molecular diffusion. In this way it is possible to detect the existence of distinct domains and to measure domain sizes in heterogeneous systems like blends and semi-crystalline polymers. Molecular diffusion occurs in very mobile domains while spin diffusion is most efficient in rigid systems. Spin diffusion is the transfer of magnetisation over a distance among coupled spins as a result of magnetisation gradients. If two nuclei which are coupled by dipolar interaction have antiparallel magnetic moments both nuclei flip or change their moments simultaneously. As the dipolar coupling connects many nuclei, the diffusion processes causes a distribution of the excess of magnetisation over the coupled spin system. This energy-conserving process occurs very rapidly among neighbouring protons because of their large gyromagnetic ratio and high isotopic abundance. Besides, the internuclear distance has to be short and a good mixing of domains with fast and slow relaxation times are needed to generate a magnetisation gradient which is the cause of diffusion. The spin diffusion process can be described as a function of the magnetisation M(r,t) on a certain place r and in a time t:

$$\frac{\partial M(r,t)}{\partial t} = D\frac{\partial^2 M(r,t)}{\partial r^2} \qquad (2.8)$$

with $D = \nu_0\langle l_0{}^2\rangle$ the spin diffusion coefficient where ν_0 is the jump frequency and l_0 is the distance between the neighbouring nuclei.

Spin diffusion occurs fast in rigid systems in comparison with T_1 and $T_{1\rho}$ relaxation. Both the magnitude and the intensity of T_1 and $T_{1\rho}$ are affected by spin diffusion. The maximum linear scale L over which spin diffusion occurs depends on the relaxation time t and is related by the equation: $L = \sqrt{6Dt}$ with t the relaxation time (T_1 or $T_{1\rho}$).

Generally, T_1 is longer than $T_{1\rho}$ and this implies that T_1 is averaged out over larger regions. Mostly spin diffusion occurs over 2-100 nm during these relaxation times.

2.2.3. Relaxation times as function of the correlation times and the magnetic field[1,2,6]

The relaxation times are influenced by molecular motions, internuclear distances and the magnetic field. The dependence is expressed in the equations developed by Bloembergen, Purcell and Pound.[7] They give the dipolar relaxation rates for two equal spins at distance r from each other as a function of the spectral density J(ω) which describes the molecular motion:

$$J(\omega) = \frac{2\tau_c}{1+\omega^2\tau_c^{\,2}} \qquad (2.9)$$

with τ_c the correlation time for isotropic rotational motions. It describes the probability available at angular frequency ω from the fluctuating interaction.
The dipolar relaxation rates are expressed as follows:

$$\frac{1}{T_1} = \frac{3}{10}\frac{\gamma^4\hbar^2}{r^6}\left[J(\omega_0) + 4J(2\omega_0)\right] \qquad (2.10)$$

$$\frac{1}{T_2} = \frac{3}{20}\frac{\gamma^4\hbar^2}{r^6}\left[3J(0) + 5J(\omega_0) + 2J(2\omega_0)\right] \qquad (2.11)$$

$$\frac{1}{T_{1\rho}} = \frac{3}{10}\frac{\gamma^4\hbar^2}{r^6}\left[\frac{5}{2}J(\omega_0) + J(2\omega_0) + \frac{3}{2}J(\omega_1)\right] \qquad (2.12)$$

From this equations it is known that molecular motions at the Larmor frequency or twice the Larmor frequency influence the three relaxation rates. The T_1 minimum is found when $\nu_c \cong \sqrt{2}\nu_0$ which is a *MHz frequency*. On the other hand, $T_{1\rho}$ has a term $J(\omega_1)$ and $T_{1\rho}$ has a minimum when $\nu_c \cong B_1\gamma / 2\pi$. Therefore $T_{1\rho}$ is sensitive to motions in the *kHz region*. T_2 contains a static term J(0) which causes the transverse relaxation. This term describes the spin diffusion and is mostly efficient for *slow molecular motions of 100-1000 Hz*. A T_2 transition occurs at a frequency $\nu_c \cong 1/\pi T_2$. Due to the terms $J(\omega_0)$ and $J(2\omega_0)$ the spin spin relaxation time is also affected by motions in the *MHz region*.

The spectral density J(ω) is a function of the frequency ω as is shown in Figure 2.3. The dependence of the relaxation times on the correlation time τ_c is given in Figure 2.4. The relaxation times are discussed here for atoms according to their molecular motion.

a) *Short τ_c times* ($\omega_0 < 1/\tau_c$) is characteristic to small mobile molecules. In this case the molecular motions are spread over a wide frequency region, as is shown in Figure 2.3(a). J(ω) is small for every value of ω and therefore all frequencies have a small probability. In Figure 2.4 T_1, $T_{1\rho}$ and T_2 have the same value for short τ_c times, i.e.:

$$\frac{1}{T_{1\rho}} = \frac{1}{T_1} = \frac{1}{T_2} = C\frac{\gamma^4\hbar^2}{r^6}\tau_c \quad \text{with C a constant} \qquad (2.13)$$

This region is termed the "extreme narrowing region" and the efficiency of the relaxation is independent of the resonance frequency B_0. On the other hand, with increasing resonance frequency the range of correlation times that satisfies the extreme narrowing conditions, is reduced.

b) For $\tau_c = 1/\omega_0$ the spectral density J(ω) is high at or near the Larmor frequency (Figure 2.3b). At this frequency the T_1 relaxation is the most efficient and $T_{1\rho}$ and T_2 have a twist in the curve around that correlation time.

As $J(\omega) \approx \tau_c = 1/\omega_0$ the T_1 minimum is proportional to the Larmor frequency $\omega_0 = \gamma B_0$. This implies that for higher magnetic fields the T_1 minimum is influenced more by faster molecular motions.

c) For *long τ_c times* ($\omega_0 > 1/\tau_c$) most of the molecular motions have a low frequency and high frequency motions are absent (Figure 2.3c). This situation is typical for immobile molecules like polymers. For $\omega_0\tau_c > 1$, $J(\omega_0)$ and $J(2\omega_0)$ are small and the relaxation as T_1 which is influenced by motions near the Larmor frequency are less efficient. In this case $J(\omega_0)$ and $J(2\omega_0)$ in T_2 are negligible compared with the static term J(0) and the spin spin relaxation is determined more by static dipolar interactions. In this region the $T_{1\rho}$ minimum is found when $\tau_c = 1/\omega_1$ with $\omega_1 = \gamma B_1$. As the field B_1 is much smaller than B_0 the $T_{1\rho}$ minimum is influenced by motions in the kHz region while T_1 is affected by MHz motions. Motions in the kHz region are generally found in polymers and therefore $T_{1\rho}$ is often used to study macromolecules.

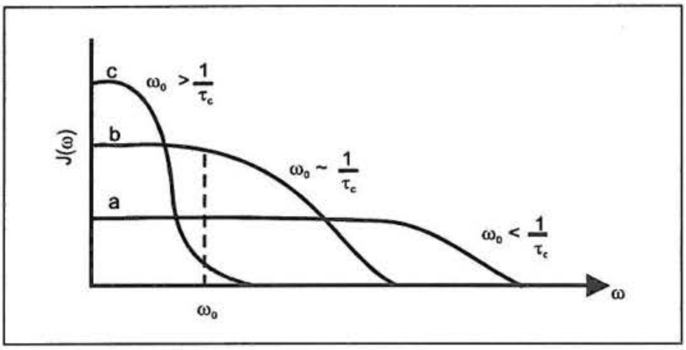

Figure 2.3: The spectral density J(ω) as a function of the frequency ω for (a) mobile, (b) moderate and (c) rigid molecules. The Larmor frequency is given as ω_0.

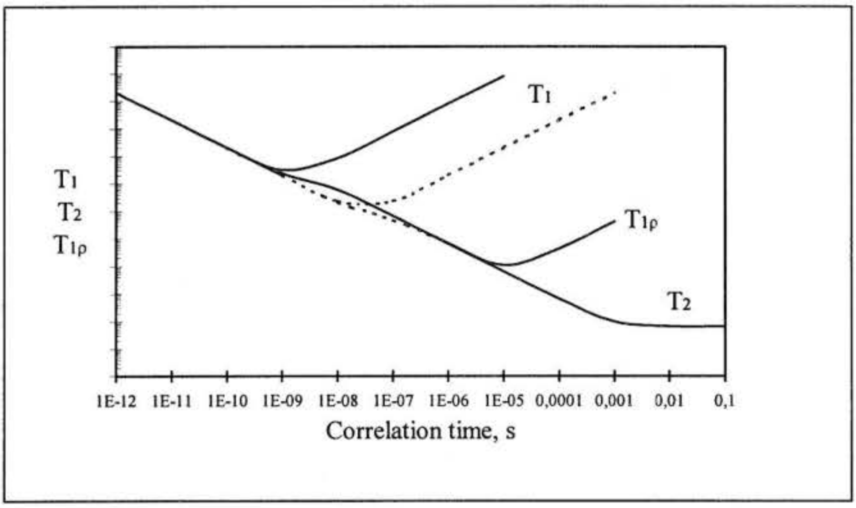

Figure 2.4: The T_1, T_2 and the $T_{1\rho}$ relaxation times as function of the correlation time for molecular motion, τ_c, at different field strength (___ 400MHz, ----- 20MHz).

2.2.4. The utility of some relaxation times[8]

As was seen in previous section the efficiency of the different relaxation processes is determined by the correlation time τ_c which describes the mobility of the atoms. In this section the different relaxation times for carbons and protons are discussed concerning their use to study molecular mobilities.

2.2.4.1. The carbon spin lattice relaxation time, T_{1C}[5,9]

Since ^{13}C has a low gyromagnetic ratio and natural abundance, carbon relaxation is dominated by dynamic contributions and spin diffusion has a minor effect. This means that T_{1C} can be interpreted in terms of local molecular motions with frequencies in the MHz region. Such high frequency motions are only found for polymers well above their glass transition temperature. Below T_g rigid systems can have very long T_{1C} times so that spin diffusion still influences these long relaxation times.[10] In such polymers T_{1C} is often dominated by chain end reorientations or side chain processes. This effect decreases when the distance between the carbon atom under investigation and the methyl group increases. As the backbone and side chains can have a different T_{1C} time one has to be careful with the interpretation in terms of mobile and rigid phases. Thus, in this case, T_{1C} is not a phase property. In absence of mobile side chains the carbon spin lattice relaxation time can be used to obtain any domain selectivity in the spectrum with respect to mobile or amorphous and rigid or crystalline phases. This is the result of the rapid relaxation of the carbons in the amorphous domain compared with the immobile crystalline domain.[11]

2.2.4.2. The carbon spin lattice relaxation time in the rotating frame, $T_{1\rho C}$[8,9, 12-14]

While T_{1C} is often dominated by motions of the end group and side chains, $T_{1\rho C}$ can be used to study backbone motions. The reason is that $T_{1\rho C}$ is determined by motions in the kHz region and polymers have many important motions in this region. This makes $T_{1\rho C}$ to an important relaxation parameter for the study of polymers.

The interpretation of $T_{1\rho C}$ data is very complex because this relaxation is caused by the fluctuating dipole fields of the protons. This fluctuation can result from reorientation of the ^{13}C-^{1}H internuclear vectors and the relaxation is affected by the spectral density J at the frequency ω_{1C} of the fluctuating fields. This process is termed the spin lattice relaxation and it reflects the local molecular dynamics. On the other hand, the observed $T_{1\rho C}$ can also be influenced by the spin spin contribution. During the spin locking time of the carbons ($\omega_{1C} = \gamma H_1$) there is a magnetisation transfer between the carbons and the protons which have lost their magnetisation via dipolar interactions. The observed $T_{1\rho C}$ can be written as:

$$\frac{1}{T_{1\rho C}} = \left(\frac{1}{T_{1\rho C}}\right)_{\text{spinlattice}} + \frac{1}{T_{CH}{}^{D}} \qquad (2.14)$$

In rigid systems with strongly coupled protons like crystalline polymers there is nearly no motion and $T_{1\rho C}$ is dominated by the spin spin relaxation: $T_{1\rho C} = T_{CH}^{D}$ which is a heteronuclear spin diffusion.[15] The $T_{1\rho C}$ data however can be interpreted in terms of molecular dynamics if $T_{CH}^{D} >> (T_{1\rho C})_{\text{spin lattice}}$. In mobile systems like amorphous polymers the relaxation is dominated by spin lattice relaxation and $T_{1\rho C}$ results of such polymers give information about the local molecular mobility.[16]

2.2.4.3. The carbon spin spin relaxation time, T_{2C}[17,18]

The carbon spin spin relaxation time, T_{2C} arises from the motional modulation of the ^{13}C-^{1}H dipolar interaction and it is influenced by $J(\omega_{1H})$ which is the spectral density at the frequency corresponding to the intensity of the ^{1}H rf field. On the other hand, $T_{1\rho C}$ is affected by the spectral density at the frequency ω_{1C} and in the CP/MAS experiment ω_{1H} equals ω_{1C} during the cross polarisation time (section 2.3.2). Therefore, $T_{1\rho C}$ and T_{2C} are affected by the same spectral density $\omega_{1C} = \omega_{1H}$. Besides, T_{2C} determines the line width in the ^{13}C NMR spectrum. A maximum in the line width due to T_{2C} is reached when the molecular dynamics have the same frequency as the proton decoupling frequency ω_{1H}.[19]

2.2.4.4. The proton spin lattice relaxation time, T_{1H}[18-20]

The spin lattice relaxation time is dominated by motions in the MHz region. As for T_{1C} the proton spin lattice relaxation times for polymers below T_g is dominated by end group and side chain processes and methyl reorientation, while well above the glass transition temperature the relaxation via backbone motions becomes more important.

T_{1H} is a phase property for solids because spin diffusion is very efficient for the high abundant ^{1}H protons which have a high gyromagnetic ratio. This means that all the protons in the region over which spin diffusion takes place have the same T_{1H} relaxation time. Spin lattice relaxation generally is a slow process and the relaxation is averaged out over large domains. Often only one T_{1H} relaxation time is found for a polymer although there are crystalline and amorphous regions. The protons of the crystalline domain relax via the protons of the amorphous domain due to spin diffusion. If the crystalline and amorphous domains of a polymer have a different T_{1H} time, it can be used to achieve any selectivity in the spectrum with regard to one of these phases. It has to be noticed here that chemical and structural heterogeneity can also cause different T_{1H} relaxation times.

2.2.4.5. The proton spin lattice relaxation time in the rotating frame, $T_{1\rho H}$[5,16,23]

$T_{1\rho H}$ is an important relaxation parameter to investigate polymers because these relaxation times are affected by motions in the kHz region as is the case for $T_{1\rho C}$. The difference between $T_{1\rho C}$ and $T_{1\rho H}$ is that the proton relaxation time is influenced by spin diffusion. Strong dipolar coupling between protons, like in rigid crystalline or glassy domains, gives rise to efficient spin diffusion. Spin diffusion minimises the nonequilibrium magnetisation in a part of the proton spin system. That way it is possible to measure the homogeneity of mixing in a blend or a copolymer because the rate of spin diffusion is strongly influenced by the spatial mixing of polymer chains. Like T_{1H}, $T_{1\rho H}$ is also a volume property. $T_{1\rho H}$ is mostly shorter than T_{1H} which means that the relaxation time is averaged out over smaller regions. This often results in several $T_{1\rho H}$ components while for T_{1H} there is often only one relaxation time.

2.2.4.6. The proton spin spin relaxation time, T_{2H}

Compared with T_{1H} and $T_{1\rho H}$, T_{2H} is easier to interpret because a higher T_{2H} relaxation time always indicates a higher molecular mobility. With T_{2H} the local molecular mobility can be studied because during a T_{2H} relaxation time spin diffusion does not have the time to average out the relaxation over domains. Moreover, the value of T_{2H} is much less dependent on the magnetic field than is the case for T_{1H} and $T_{1\rho H}$. Below T_g, one small relaxation time is often found and the influence of methyl reorientation is not prominent in T_2 results. The T_{2H} study of semi-crystalline polymers above T_g are often highly informative.[24,25]

Above the glass transition temperature the mobility of the amorphous domain increases with temperature and T_{2H} also increases. Below T_g T_2 is more or less the same for crystalline and glassy amorphous domains and they are unresolvable. The glass transition temperature can often be deduced from T_2 measurements as function of the temperature.

2.2.4.7. The cross polarisation time constant, T_{CH}[12]

$1/T_{CH}$ describes the rate of magnetisation transfer from protons to carbons during the cross polarisation process in a CP/MAS experiment (section 2.3.2). It can be compared with spin diffusion between ^1H-^1H atoms. T_{CH} is determined by the effective strength of the heteronuclear dipolar interaction which is influenced by molecular motions, interatomic C-H distance and the number of the surrounding protons. T_{CH} is the shortest for protonated carbons in rigid systems. Sometimes in rigid systems cross polarisation between carbons and the directly bonded protons can not be conceived as a single-exponential process. The directly bonded protons are dipolarly coupled to other protons by spin diffusion. Spin diffusion transfers the polarisation between the spin pair (^{13}C-^{1}H) and the other proton spins. Sometimes the ^{1}H-^{1}H spin diffusion is a slower process compared to the ^{13}C-^{1}H transfer causing the carbon magnetisation to oscillate. Cross polarisation is a single exponential process if there are strong homonuclear H-H dipole interactions, i.e. a short T_{2H} relaxation time. In this case the protons can be conceived as a spin reservoir with a single spin temperature. This phenomenon will be discussed later in section 2.3.2.

2.3. ^{13}C high resolution solid-state NMR

One way to study the relaxation times of solids is by ^{13}C high-resolution NMR. The advantage of ^{13}C NMR compared with ^{1}H NMR is that the ^{13}C NMR signals are spread over 200ppm while this is only 10ppm for proton NMR spectra. Another advantage is that unprotonated carbon groups (i.e. C=O, C≡N) can be detected. Compared with liquid-state spectra, the spectral lines of a ^{13}C solid-state spectrum are broadened. The line width of a solid-state spectrum is discussed in this section. Besides the study of carbon relaxation times, it is also possible to study the proton relaxation times via the carbon spectrum by using the cross polarisation technique. This is described in section 2.3.2. Eventually, the pulse sequences to determine the relaxation times are given.

2.3.1. Line width[24-26]

The ^{13}C solid-state NMR spectrum can have spectral lines of some tens of kilohertz, while the line width in the liquid-state spectrum of the same product is 1 to 10 Hz. The major cause of line broadening is the *dipolar coupling* of the carbon with nearby protons. This interaction between a carbon and a proton is given in Figure 2.5. The proton magnetic moment generates a magnetic field B_z^H near the carbon. This field will be added to or subtracted from the external field B_0 and it causes an upfield or a downfield shift of the resonance line. The ^{13}C NMR spectrum of the C-H pair in a certain orientation is a doublet that is centred at the Larmor frequency with a splitting (given in Hz):

$$\Delta\nu = \frac{\gamma_C \gamma_H \hbar}{2\pi r^3}(1 - 3\cos^2\Theta_{CH}) \qquad (2.15)$$

The dipolar interaction is independent of the strength of the external magnetic field and it is strongly influenced by the distance between the carbon and the protons. Isolated C-H pairs are rarely found in polymers and the heteronuclear dipolar interaction is the sum of all carbons with its surrounding protons. The doublet shown in Figure 2.5II changes to a broad signal of some tens of kHz for a complete sample because the C-H coupling can have different distances and can have all possible angles with respect to the external magnetic field. That way a lot of information about the polymer under investigation (i.e. the fine structure) is lost. This strong dipolar coupling can be reduced by irradiation of the protons with a strong radio frequency field with a frequency equal to the resonance frequency of protons. This rf field causes the protons to flip between the two energy states and averages the effective field from the protons that is seen by the carbons. The decoupling field has to be larger than the C-H dipolar coupling and the strong H-H coupling. This decoupling in solid-state NMR is a factor 10 larger than in liquid NMR. In liquid-state NMR the dipolar coupling is averaged out by the very rapid rotational and translational motion and the effect of dipolar coupling is zero.

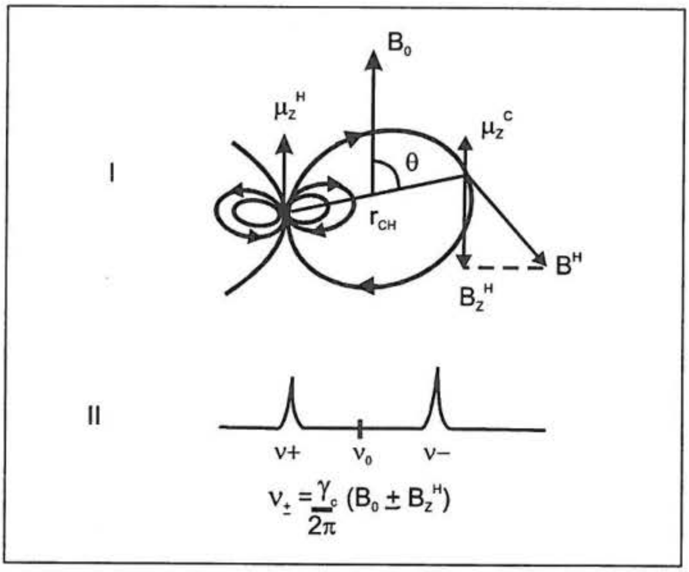

Figure 2.5: I) A model for the dipolar coupling between a carbon and a bonded proton. B_z^H is the z component of the proton dipolar field at the carbon. μ_z are the z components of the magnetic moments. II) The ^{13}C spectrum of a sample of and isolated C-H pair at one angle relative to the magnetic field.

The chemical shift anisotropy also contributes to the broadening of the spectral lines. The chemical shift of a certain carbon is influenced by its electronic environment and the electronic distribution about the nucleus depends on the orientation in the magnetic field. In mobile systems as in liquids this interaction is averaged out by the rapid molecular motions. In contrast, in a solid all orientations are possible and the signal is the sum of all chemical shifts of the different orientations. For some samples it can give useful information about the orientation of the sample but mostly the line shape is very complex.

The chemical shift of a nucleus with a certain orientation is given by the chemical shift tensor σ_{zz}:

$$\sigma_{zz} = \sum_{i=1}^{3} \sigma_i \cos^2 \theta_i \tag{2.16}$$

with σ_i the principal tensor component and θ_i the angle with respect to the external field. In solution the chemical shift is one third of the sum of the three principal tensor components and one isotropic chemical shift is found. In rigid systems the spatial term can be averaged out by physical spinning of the sample at the 'magic angle'. An isotropic shift is reached at an angle of 54.44°. The samples are spun at a rate of several kHz.

According to equation 2.15 the dipolar coupling is also orientation dependent but this effect can only be reduced partly by spinning at the magic angle. Dipolar decoupling is needed to reduce the broadening due to this strong coupling.

Eventually, the attainable line width of rigid solids is 10-100 Hz for high field NMR spectrometers. The line broadening mechanisms can be divided in two groups: the static and the motional contribution.[8,29,30] The *static* contribution includes conformational nonequivalence and packing effects. An atom in a molecule that can have different conformations gives rise to a broad signal in the solid state spectrum because of the freezing-in of the conformational states. Chemical shift dispersion can also be caused by packing variations by modifying bond dispersion or by variations in local susceptibility. These contributions cause different chemical shifts and thus line broadening. On the other hand, it can also give a lot of information about the polymer because conformations and packing can be studied if the signals are resolved. The *motional* contribution is the motional modulation of the C-H dipolar coupling and of the chemical shift anisotropy. If motions occur at frequencies comparable to the frequency of the decoupling field, the dipolar decoupling is insufficient to reduce the line width and it results in broad lines. This can be seen for elastomers above the glass transition temperature or for chain ends or side chains in polymers below T_g. Increasing the temperature causes motions with higher frequencies and the line width is reduced by rapid motional averaging. At lower temperatures the efficient dipolar decoupling of the C-H dipolar interactions provides a narrowing of the spectral lines. There is also broadening due to motional modulation of the chemical shift anisotropy, if motions occur with a frequency of the rotor. It concerns unsaturated carbons with a large chemical shift anisotropy. These motional contributions are much stronger than the static contributions which do not exceed 6ppm.

2.3.2. Sensitivity enhancement by cross polarisation[5,26,31]

The low sensitivity in ^{13}C DD/MAS spectra is a result of the ^{13}C low abundance and small magnetic moments. Moreover, the repetition time of a ^{13}C DD/MAS experiment is determined by the carbon spin lattice relaxation time (recycle delay = $5*T_{1C}$) which can be very long (some minutes).[11] In contrast, protons have a high gyromagnetic ratio and a natural abundance which results in a high sensitivity. On top, the proton spin lattice relaxation time is smaller. Thanks to a technique, known as *cross polarisation*, it is possible to use this high proton sensitivity and short relaxation time to increase the sensitivity of the carbon spectrum. During the cross polarisation time a small fraction of the proton magnetisation is transferred from protons to the carbon spin system. To understand the variation of the magnetisation during a cross polarisation experiment, shown in Figure 2.6, the concept of spin temperature has to be introduced.

When a solid is placed in a magnetic field B_0 the ^1H spins are divided among the two Zeeman energy levels according to the Boltzmann equation as was given in equation 2.6.

Due to the efficient spin diffusion among protons the equilibrium state is found for the protons and they can be conceived as a spin system with a single spin temperature T_s or an isolated spin reservoir (Figure 2.7). The protons can not exchange energy with the carbon spin system because the separation between the proton levels is four times that of the carbon levels, as is shown in Figure 2.8I. As the carbons and protons cannot undergo mutual energy conserving spin flip flops, both carbons and protons have their own specific relaxation times. Therefore they are isolated spin systems. After a time the proton reservoir comes to an equilibrium with the lattice by spin lattice relaxation and the proton spin temperature will equal the lattice temperature, T_l. The ^1H magnetisation is given by the Curie law:

$$M_{0H} = \frac{C_H B_0}{T_1} \qquad (2.17)$$

$$\text{with } C_H = \frac{N_H \gamma_H{}^2 \hbar^2}{4k} \qquad (2.18)$$

N_H is the number of protons and k is the Boltzmann constant.

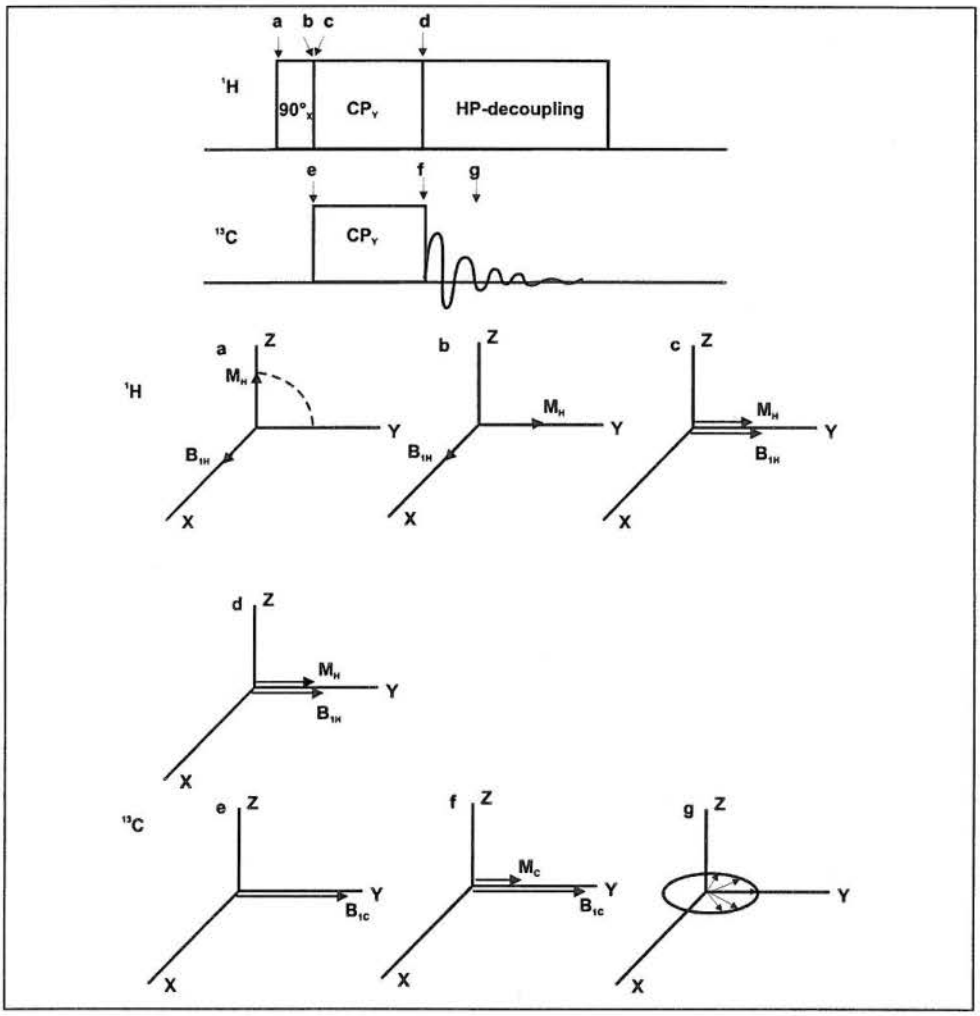

Figure 2.6: The pulse sequence of a cross polarisation experiment: The proton magnetisation vector is turned in the y direction by a rf field B_{1H} in the x direction. Afterwards, the B_{1H} field is shifted 90°. The proton spins are spin locked in the y direction by the field B_{1H}. The protons and carbons are brought in thermal contact with each other by fulfilling the Hartmann-Hahn conditions: a rf field B_{1C} with a strength that is 4 times bigger than the B_{1H} field, is used in the y direction. During this contact time magnetisation is transferred from protons to carbons. Eventually, the carbons have the spin temperature of the proton spin reservoir. After the cross polarisation time the FID can be measured.

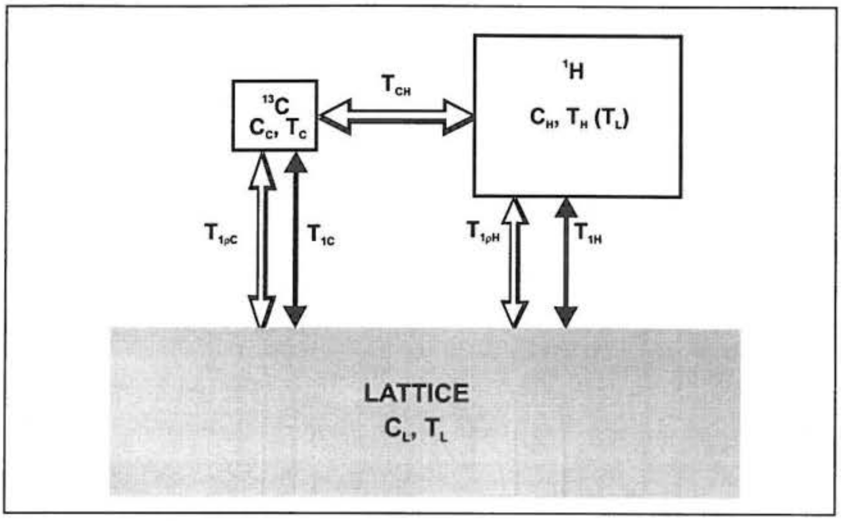

Figure 2.7: A schematic representation of the isolated spin systems of carbon and proton with each their own spin temperature and relaxation times.

In a cross polarisation experiment, as is shown in Figure 2.6, the 90° pulse is followed by a 90° phase shift of the rf field and the protons are spin locked along the B_{1H} field during the contact time. The proton magnetisation is conserved during the spin lock time and is determined by the rf field B_{1H}:

$$M_{0H} = \frac{C_H B_{1H}}{T_H} \tag{2.19}$$

with T_H the spin temperature in the rotating frame. A combination of equation 2.17 and 2.19 gives:

$$T_H = \frac{B_{1H}}{B_0} T_l \tag{2.20}$$

Since B_{1H} is much smaller than B_0 the spin temperature in the rotating frame must be low compared with T_l.

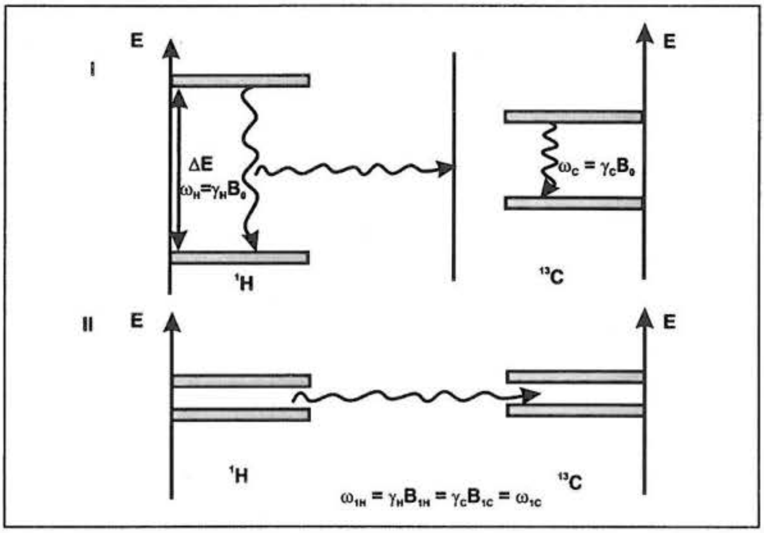

Figure 2.8: Schematic diagram of the cross polarisation process. I) The energy dissipation between the two proton energy levels is four times that of the carbon levels and it is not possible to transfer energy or magnetisation between the carbon and protons spin systems. II) Both spin systems are in the rotating frame with the same frequency and energy is transferred.

For carbons in an external magnetic field B_0 the magnetisation is much smaller. This means that according to the Curie law the carbon spin temperature must be large or the spin reservoir is hot. Cross polarisation occurs between the cold, large proton reservoir and the hot, small carbon reservoir if they are brought in contact. This can be done by irradiation of the carbons with an rf field B_{1C} according to the equation:

$$\gamma_C B_{1C} = \gamma_H B_{1H} \tag{2.21}$$

This is the Hartmann-Hahn[32] condition. The condition is satisfied if the strength of the field B_{1C} is four times that of B_{1H}. During this thermal contact the proton and carbon spins precess with the same frequency around the y direction and energy can be transferred from the proton reservoir to the carbon spin system (Figure 2.8II). The carbon magnetisation increases during the contact time and the equilibrium state is reached when carbons are cooled down to the spin temperature of the proton reservoir. As the proton reservoir is very large in comparison with the carbon system, the proton magnetisation is only slightly reduced at the end of the cross polarisation time.

During the contact time there is magnetisation transfer from protons to carbons but on the other hand the proton magnetisation in the rotating frame is reduced by proton spin lattice relaxation in the rotating frame, $T_{1\rho H}$. For rigid systems the relaxation is a slower process compared with the increase in carbon magnetisation. The carbon magnetisation as a function of the contact time can generally be given as follows[33]:

$$M(t) = M_0\beta^{-1}\left[1-\exp\left(\frac{-\beta t}{T_{CH}}\right)\right]\exp\left(\frac{-t}{T_{1\rho H}}\right) \tag{2.22}$$

$$\text{with } \beta = 1+\frac{T_{CH}}{T_{1\rho C}}-\frac{T_{CH}}{T_{1\rho H}} \tag{2.23}$$

In polymers, T_{CH} is often much smaller than the carbon and proton relaxation in the rotating frame and β equals 1. In this case the equation is simplified to:

$$M(t) = M_0\left[1-\exp\left(\frac{-t}{T_{CH}}\right)\right]\exp\left(\frac{-t}{T_{1\rho H}}\right) \tag{2.24}$$

It describes the increase of magnetisation according to T_{CH} and the depletion due to $T_{1\rho H}$ relaxation. The highest intensity in magnetisation is obtained after four to five times the cross polarisation time T_{CH} on condition that $T_{1\rho H}$ is much longer than T_{CH}.

2.3.3. The pulse sequences

In the previous section the pulse sequence of a normal cross polarisation experiment was described. With this pulse sequence it was possible to determine the T_{CH} time together with the $T_{1\rho H}$ time. When there are two $T_{1\rho H}$ and two T_{CH} times the analysis becomes too complex and both relaxation times have to be determined in separated pulse sequences: the cross depolarisation experiment and the proton $T_{1\rho}$ experiment.[34]

In this section only the pulse sequences that were used in this research are described. For the pulse sequence of T_{2C} and $T_{1\rho C}$ we refer to the literature.[13,15,35]

2.3.3.1. The $T_{1\rho H}$ or spin lock experiment

The $T_{1\rho H}$ or the spin lock pulse sequence is shown in Figure 2.9.

The pulse sequence starts with a rf field B_{1H} in the rotating frame of the protons which rotates the proton magnetisation vector M_H in the yz plane (Figure 2.9a&b). After the 90° pulse the rf field B_{1H} is phase shifted 90° in the direction of the magnetisation vector M_H (Figure 2.9c) and the protons are spin locked during a variable time t. During this spin lock time the initial proton magnetisation M_0 decreases exponential with a time constant $T_{1\rho H}$

(Figure 2.9c&d). After the variable time t the carbons are brought into contact with the protons during the cross polarisation time. The proton magnetisation is transferred to the carbon spin system (Figure 2.9e&f). Afterwards the carbon signal is detected under high-power proton decoupling conditions.

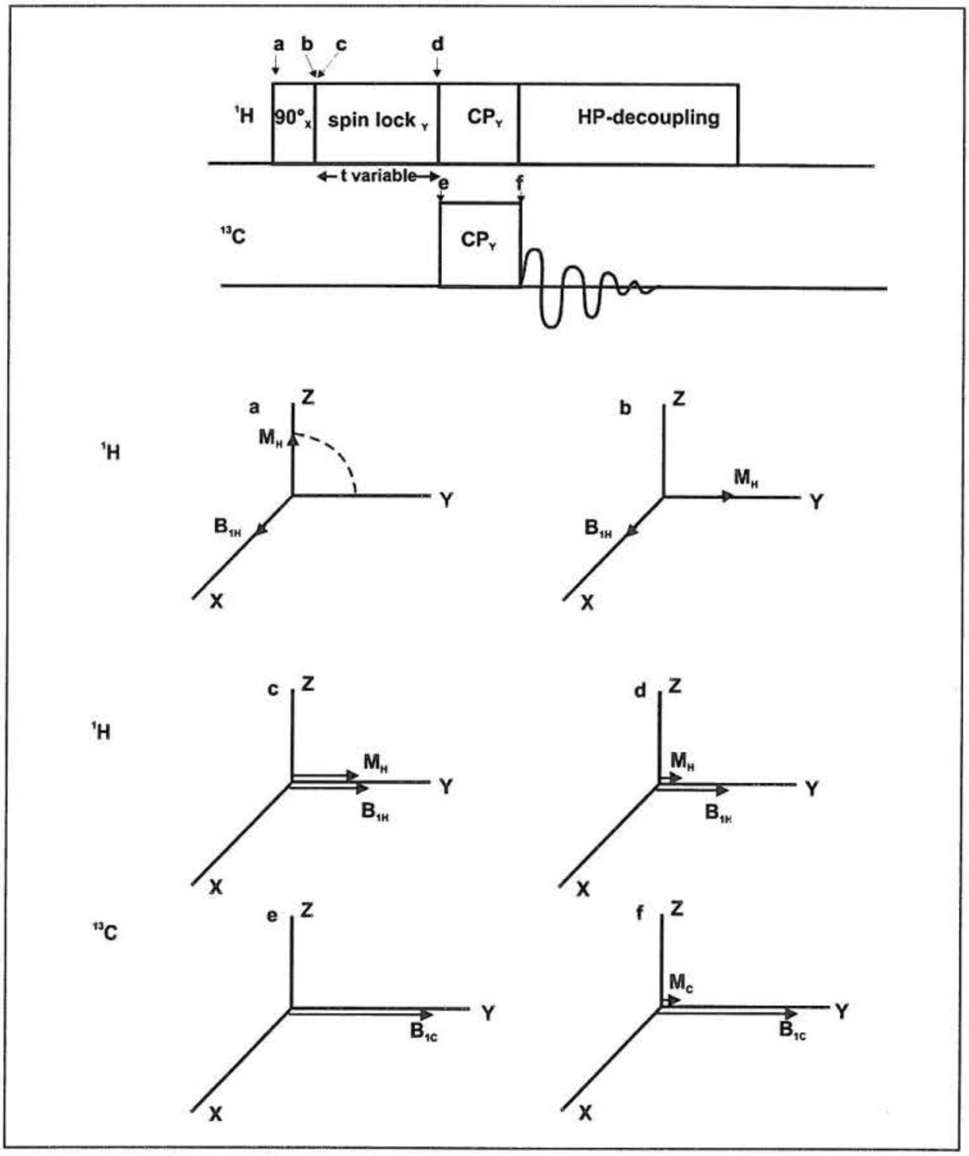

Figure 2.9: The schematic representation of the $T_{1\rho H}$ pulse sequence.

The carbon magnetisation that is acquired is determined by the proton magnetisation. The proton magnetisation at his turn is determined by the initial magnetisation and the relaxation during the spin lock time and the cross polarisation time. The spin lock time t is varied and the magnetisation as a function of t can be fitted to an exponential decay:

$$M(t) = M_0 \exp\left(-\frac{t + CP}{T_{1\rho H}}\right) \qquad (2.25)$$

with M_0 the magnetisation at equilibrium and CP the contact time. If the contact time is shorter than 5 times the longest T_{CH} time, then the increase in magnetisation during the cross polarisation time has to be charged to get quantitative results.

2.3.3.2. The cross depolarisation experiment

To determine the T_{CH} time the cross depolarisation experiment shown in Figure 2.10 can be used.

The first part of the pulse sequence is the same as for a normal cross polarisation experiment (Figure 2.6): a proton 90° pulse is followed by a cross polarisation time and the magnetisation is transferred from protons to carbons to increase the carbon magnetisation. After a time t_1 a rf field B_{1H} undergoes a 180° phase shift and it rotates the proton magnetisation vector in the -y direction. During the following variable time t_2 there is still contact between the proton and the carbon spin system. The carbon magnetisation is diminished in the positive y direction, goes through zero and eventually gets a magnetisation in the -y direction. Finally, the carbon FID is acquired during proton decoupling.

The carbon magnetisation M as a function of the time t_2, describes the cross depolarisation and the T_{CH} time can be deduced from this magnetisation evolution.

$$M(t) = -M_\infty + (M_\infty + M_0)\exp\left(\frac{-t_2}{T_{CH}}\right) \qquad (2.26)$$

In this equation M_0 describes the magnetisation at time $t_2 = 0$ and M_∞ the magnetisation at equilibrium.

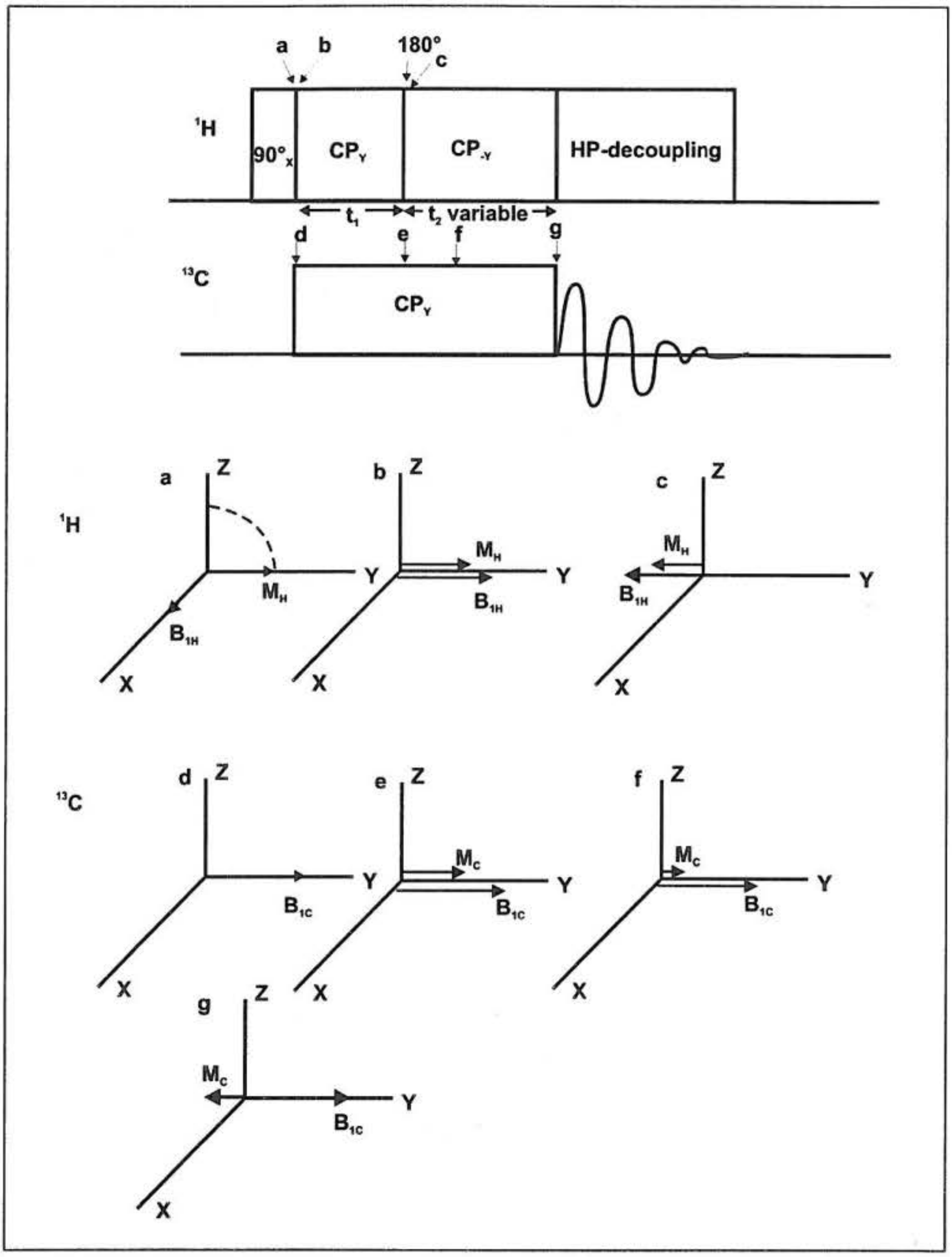

Figure 2.10: The cross depolarisation experiment.

2.3.3.3. The inversion recovery experiment

The inversion recovery experiment can be used to determine the proton spin lattice relaxation time, T_{1H} and the pulse sequence is shown in Figure 2.11.

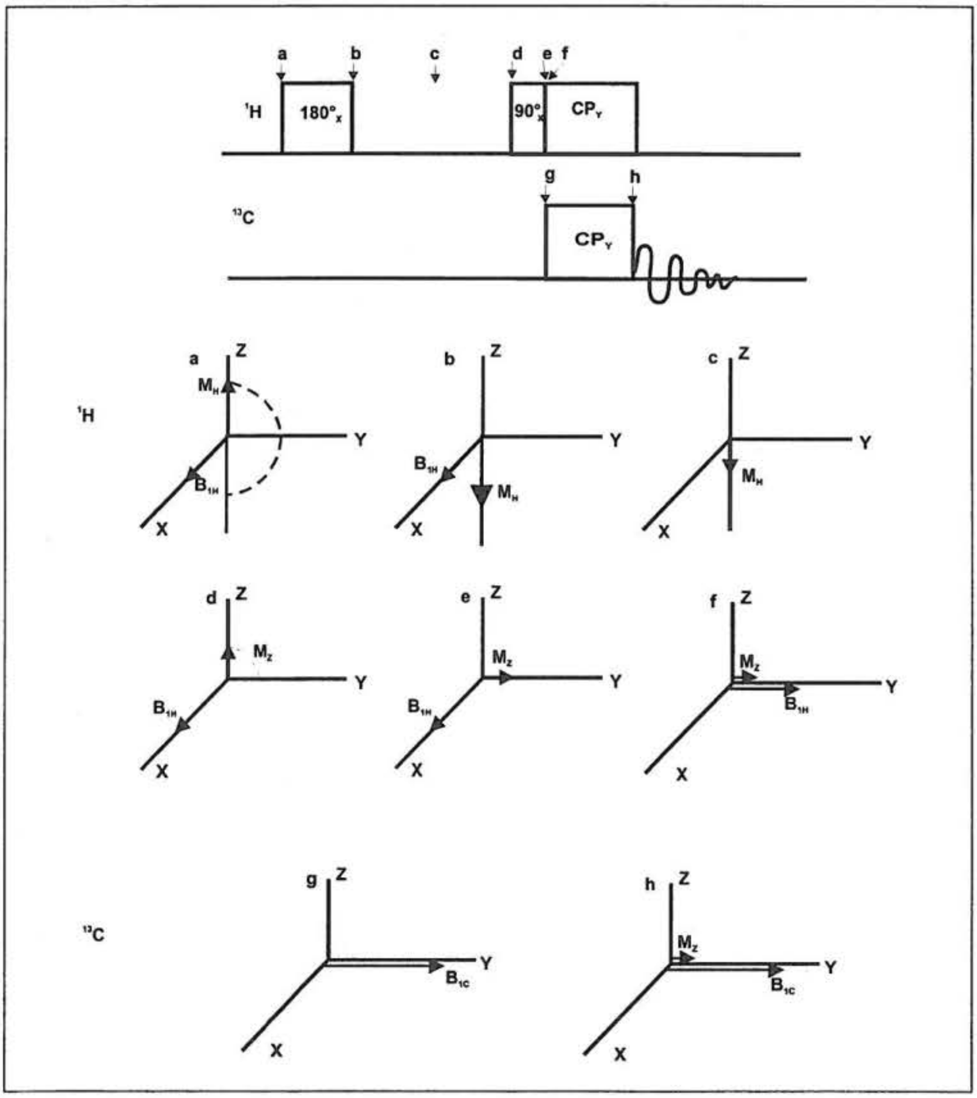

Figure 2.11: A schematic diagram of the inversion recovery pulse sequence.

A 180° pulse brings the proton magnetisation from the positive z direction into the negative z direction. Due to spin lattice relaxation in the external field B_0 the proton magnetisation decreases, becomes zero and increases in the positive z direction. After a variable time t the proton magnetisation is rotated in the y direction. The carbons are brought in contact with the protons and after a suitable cross polarisation time the carbon FID is acquired.

During the variable time t the proton magnetisation is relaxed exponentially according to the spin lattice relaxation time T_{1H} and goes from a magnetisation in the negative z direction M_0 to a positive magnetisation M_∞:

$$M(t) = M_\infty - (M_\infty - M_0)\exp\left(\frac{-t}{T_{1H}}\right) \tag{2.27}$$

2.3.3.4. The saturation recovery experiment

To determine the carbon spin lattice relaxation times several pulse sequences are available for instance the Torchia pulse sequence[36], the inversion recovery, the saturation recovery and the progressive saturation.[37] The saturation recovery pulse sequence[38] was used in this research and will be discussed here (Figure 2.12).

In this pulse sequence the carbon magnetisation is rotated into the xy plane by a 90° pulse. Afterwards this magnetisation is dispersed in the xy plane by a field gradient pulse along the z axis. During this homospoil time (HSP) the magnetisation in the xy plane is eliminated and only relaxation along the z direction is possible. During a variable time t the magnetisation in the z direction increases in an exponential process according to the carbon spin lattice relaxation time, T_{1C}. To detect this magnetisation a rf field is applied to rotate this magnetisation in the xy plane and the FID is acquired under high-power proton decoupling conditions.

The magnetisation can be described as an exponential increasing function with variable time t between the two 90° pulses:

$$M(t) = M_0 * \left[1 - \exp\left(-\frac{t + HSP}{T_{1C}}\right)\right] \tag{2.28}$$

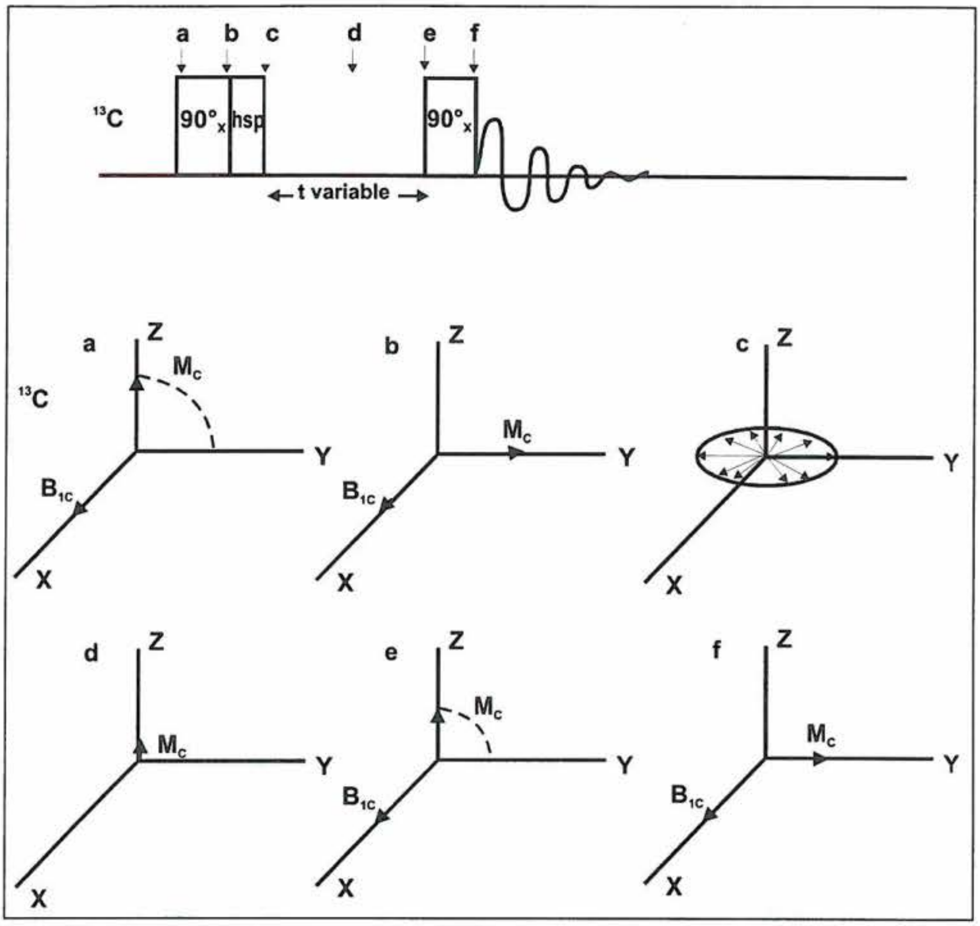

Figure 2.12: The saturation recovery pulse sequence.

2.3.3.5. The proton T_2 experiment

The pulse sequence to measure T_{2H} is given in Figure 2.13. After a 90° pulse of the protons the magnetisation is dispersed in the xy plane due to T_2 relaxation. After a variable time t and a 90° phase shift the proton magnetisation is transferred to the carbons and this magnetisation can be detected. The magnetisation at moment f (Figure 2.13) is determined by the proton spin spin relaxation during the time t. A set of experiments with increasing time t describes the T_{2H} relaxation according to the equation:

$$M(t) = M_0 \exp\left(\frac{-t}{T_{2H}}\right) \qquad (2.29)$$

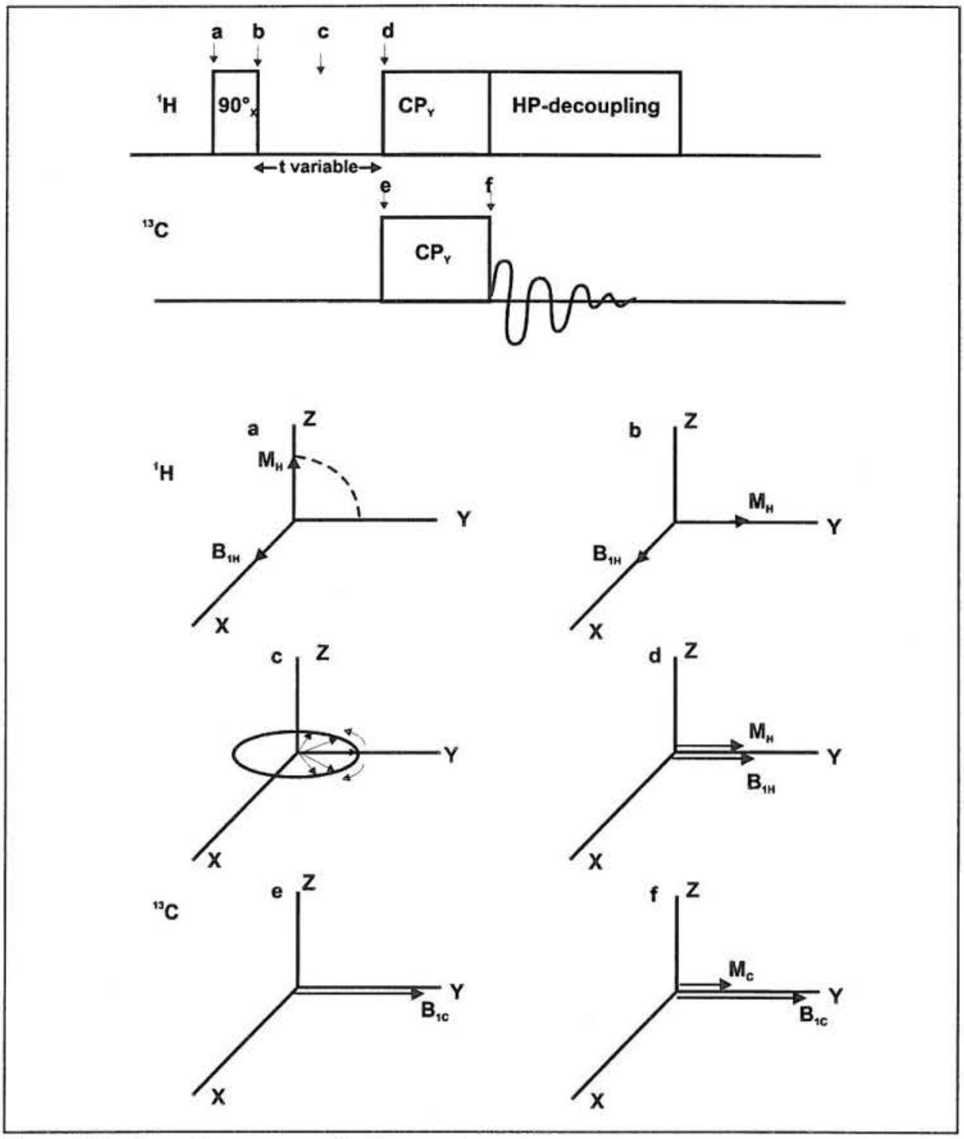

Figure 2.13: The pulse sequence of a T_{2H} experiment.

2.4. ^{1}H wideline NMR[39]

^{1}H wideline NMR is another technique that can be used to study the local mobility and molecular surroundings in a polymer.

The advantage of wideline NMR compared to high-resolution ^{13}C solid-state NMR is that it is a fast technique. For example a T_{2H} experiment takes only a few seconds while many hours are needed for a ^{13}C CP/MAS experiment. With wideline NMR the results are obtained from the FID or the proton spectrum. As in this technique no line narrowing techniques are used the proton spectrum consists of one broad signal. The disadvantage is that the broad proton signal or the FID consists the information of all domains in the sample. For many years this technique had less success compared to ^{13}C CP/MAS NMR because the results are difficult to interpret. This problem can partly be solved by comparing the results with high-resolution ^{13}C solid-state NMR results.

2.4.1. The measurement of the proton spin spin relaxation time, T_{2H}

Generally, the T_{2H} relaxation time can be determined directly from the free induction decay after a 90° pulse. When the relaxation time is very short or very long wrong relaxation times can be found. Hence, other pulse sequences are used like the solid-echo, the Hahn echo and the CPMG pulse sequence.[40]

2.4.1.1. The solid echo pulse sequence

In a standard NMR experiment the FID is acquired after the 90° pulse and the spin spin relaxation times can be determined from it. In such an experiment it is not possible to start the acquisition of the FID directly after the 90° pulse because of the dead time (t_d). The dead time is the time taken for the spectrometer to recover from the overload caused by the rf pulse. This implies that most of the FID is observed but the initial part of the FID is hidden by the dead time, as is shown in Figure 2.14I. This problem is more important in rigid solids than in mobile systems and liquids. The solid echo pulse sequence, introduced by Powles et al.[41], can be used to reduce the effect of the receiver recovery so that short T_{2H} relaxation times can precisely be measured. In this pulse sequence (Figure 2.14 II &III) a 90° pulse is followed by a waiting time τ of a few microseconds and then a second 90° pulse is applied which refocuses the magnetisation in the positive y direction. The second 90° pulse has to be 90° out of phase with respect to the first. The time τ has to be chosen in such way that the FID is not attenuated too much. An echo decay with the shape of the FID can be acquired a time τ after the second pulse. The amplitude of the echo approximates the initial amplitude of the FID. When the time τ is longer than the dead time and comparable to the T_{2H} relaxation time of a part of the sample, the echo decay is considerably attenuated. This situation has to be avoided.

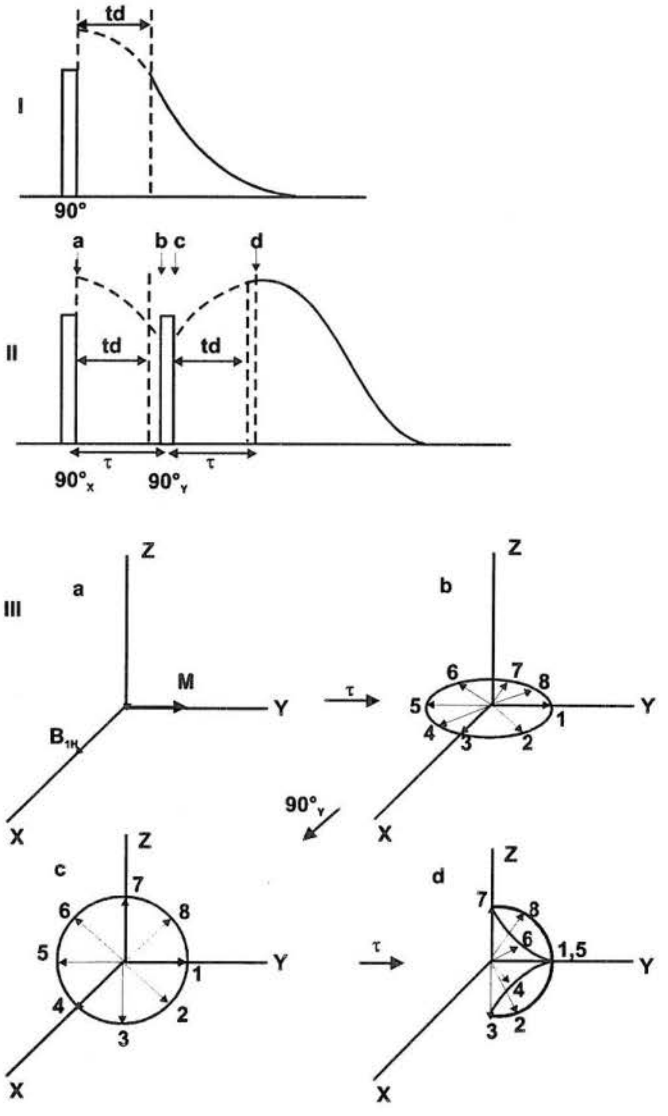

Figure 2.14: I) The free induction decay after a 90° pulse. The echo can be acquired after a dead time t_d after the pulse. II) The solid echo pulse sequence. The echo is acquired a time 2τ after the first pulse. III) A schematic representation of the magnetisation vectors during the solid echo pulse sequence.

For the analysis of the echo decay exponential, Gaussian, Weibullian or Abragamian functions are used. This will be further discussed in chapter 6.

2.4.1.2. The Hahn echo pulse sequence

For long relaxation times the relaxation can be influenced by field inhomogeneities. This contribution can be included in the experimental values of the T_2 relaxation time, T_2*:

$$\frac{1}{T_2^*} = \frac{1}{T_2} + \frac{\gamma \delta B_0}{2} \tag{2.30}$$

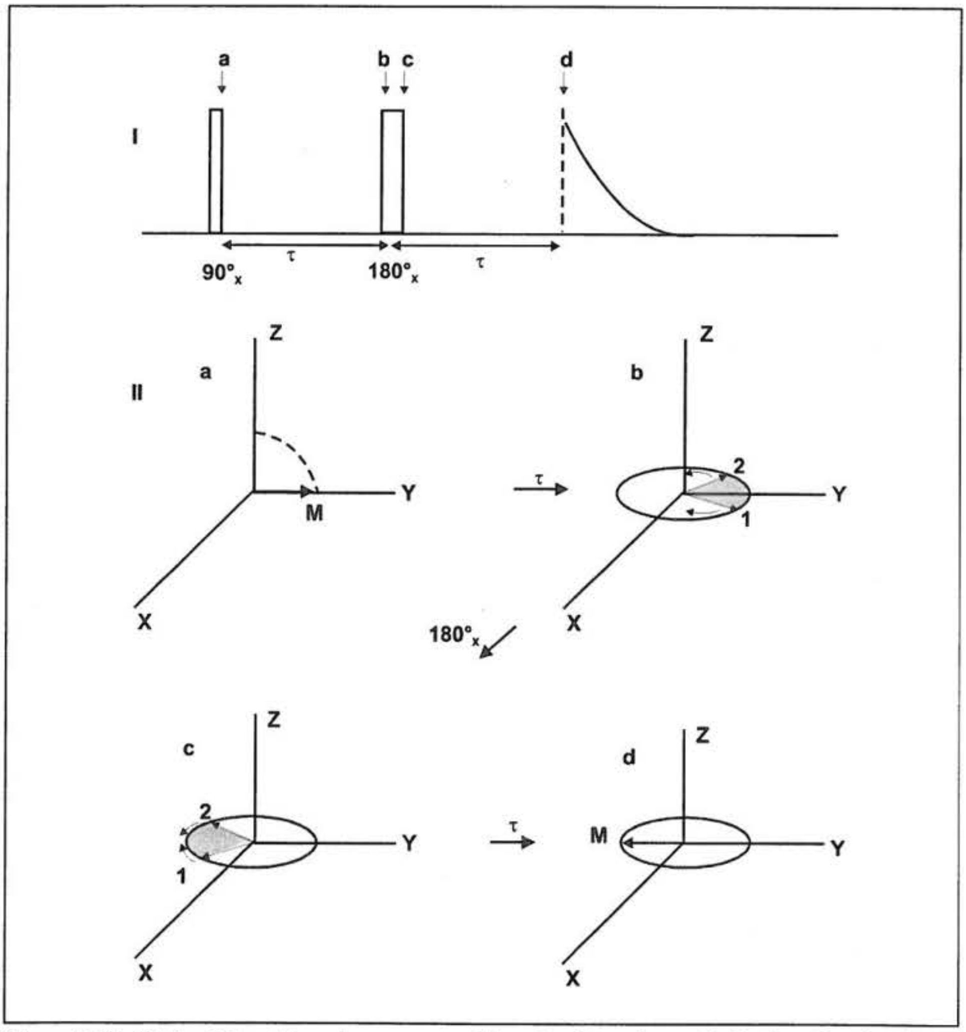

Figure 2.15: I) The Hahn echo pulse sequence. The echo decay is acquired a time 2τ after the 90° pulse. II) A schematic representation of the magnetisation vector during the pulse sequence.

To avoid this influence ($\gamma\delta B_0/2$), Hahn[42] proposed the pulse sequence shown in Figure 2.15. In this pulse sequence a first 90° pulse is followed by a variable waiting time τ. Due to magnetic field inhomogeneities over the probe nuclei at different locations see a slightly different magnetic field B_0. Therefore, they precess with a slightly different Larmor frequency (Figure 2.15 IIb). If after a variable time τ a 180° pulse is applied around the same axis, the spins are flipped around that axis (Figure 2.15IIc). After a second interval τ the spins coincide on the y axis and the echo has been formed.

2.4.1.3. The Carr Pulcell Meiboom Gill (CPMG) pulse sequence

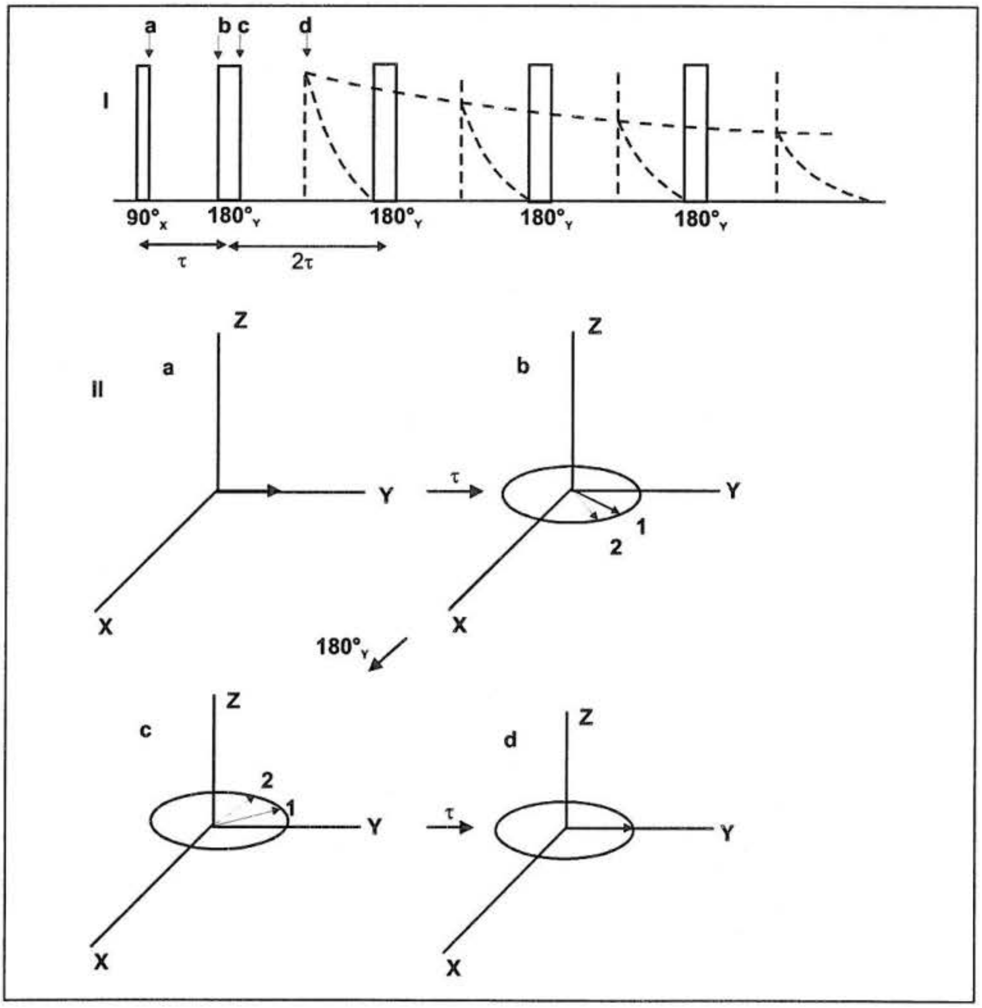

Figure 2.16: The CPMG pulse sequence. The 90° pulse in the x direction is followed by a variable set of 180 pulses in the y direction.

The spin echo method due to Hahn is only capable of refocusing the transverse spin magnetisation in spin systems when the magnetisation is lost through static inhomogeneous interactions such as field inhomogeneities. Homogeneous interactions such as spin diffusion cause a FID with an irreversible component due to mutual spin flips. Carr and Purcell[43] introduced a pulse sequence to reduce the error caused by homogeneous interactions. In this pulse sequence a lot of rf pulses are applied. The 90° pulse is followed by a series of 180° pulses and the time between the 180° pulses is twice the time interval between the 90° pulse and the first 180° pulse. The echoes are observed halfway between two 180° pulses. In this pulse sequence the amplitude adjustment of the 180° pulses is very critical because of the cumulative error of this amplitude in the results. In fact more 180° pulse are needed to eliminate the effect of diffusion. Moreover, the reproducibility of the measurements was low. Therefore Meiboom and Gill[44] modified the Carr Purcell pulse sequence: the 180° pulses are 90° out of phase of the 90° pulse and the successive pulses are coherent. This CPMG pulse sequence is shown in Figure 2.16. In contrast with the Carr Purcell pulse sequence all the echoes have the same phase and the amplitude deviation of the 180° pulses is not cumulative in its effect. This is the best pulse sequence for measuring very long spin spin relaxation times.

2.4.2. The measurement of the proton spin lattice relaxation time, T_{1H}

The proton spin lattice relaxation time can be measured with the inversion recovery method: after a 180° pulse a variable time interval is followed by a 90° pulse and the free induction decay can be acquired:

($180°_x$ - variable time - $90°_x$ - acquire)

This is a comparable pulse sequence as those for CP/MAS experiments described in section 2.3.3.3.

For rigid systems with short T_{2H} relaxation times this pulse sequence can be combined with the solid echo pulse sequence and the resulting pulse sequence is as follows:

($180°_x$ - variable time - $90°_x$ - τ -$90°_y$ - acquire)

This combination is only used when the sample is below its glass transition temperature or when the relaxation of the rigid part of the polymer has to be known. A preparation time of at least 5 times the longest T_1 time has to be respected. In both cases, i.e. with and without solid echo, the evolution of the magnetisation as a function of the variable time t can be described with the same equation as for the CP/MAS experiments, i.e. equation 2.27.

2.4.3. The measurement of the $T_{1\rho H}$ relaxation time

The $T_{1\rho H}$ relaxation can be studied by the solid echo train[45] or by applying a spin lock field after a 90° pulse. The latter pulse sequence was used in this research and will be discussed here. In this pulse sequence the 90° pulse tips the magnetisation to the xy plane. The rf field B_{1H} is shifted 90° so that it has the direction of the magnetisation vector. During a variable time the proton magnetisation is spin locked and afterwards the FID is acquired:

($90°_x$ - spin lock_y -acquire)

As for T_{1H} the $T_{1\rho H}$ pulse sequence can be combined with the solid echo pulse sequence for rigid polymers. The former pulse sequence will be used in this work.

The relaxation during the spin lock time t can be described as an exponential function:

$$M(t) = M_0 \exp\left(\frac{-t}{T_{1\rho H}}\right) \tag{2.31}$$

2.5. Conclusions

With high resolution ^{13}C CP/MAS NMR as well as with ^{1}H wideline NMR relaxation times can be determined which give information about the molecular dynamics and molecular domains in polymers.[46] The relaxation parameter that has to be used to study the motions of a polymer depends on the frequency of the motions. Spin lattice relaxation times in the rotating frame are sensitive to motions in the kHz region, while motions in the MHz region influence strongly the spin lattice relaxation in the laboratory frame. Spin spin relaxation is also influenced by these high frequency motions and also by slow motions of some 10-100Hz. Carbon relaxation parameters can be used to study the local molecular dynamics and proton relaxation is generally a phase property (except for T_{2H}).

In addition to the relaxation times the line width can also give interesting information concerning the mobility of the polymer chain, the packing, the conformations, ...

The applications of these solid state parameters on the ethylene-propylene copolymers are given in chapter 5 and 6.

2.6. References

1. Bovey, F.A.; "Nuclear Magnetic Resonance Spectroscopy", Academic Press, London, 1988.

2. Fyfe, C.A.; "Solid State NMR for Chemists", C.F.C. Press, Ontario, Canada, 1984.

3. Bloch, F.; Phys. Rev., 70 (1946), 460.

4. McBrierty, V.J.; Douglass, D.C.; J. Polym. Sci., Macromol. Rev., 16 (1981), 295.

5. Komoroski, "High Resolution NMR Spectroscopy of Synthetic Polymers in Bulk", VCH, Florida, 1986.

6. Mehring, M.; "High Resolution NMR spectroscopy in solids: Basic Principles and Progress", Springer-Verslag, Berlin, 1976.

7. Bloembergen, N.; Purcell, E.M.; Pound, R.V.; Phys. Rev., 73(7) (1948), 679.

8. Voelkel, R.; Angew. Chem. Int. Ed. Engl., 27 (1988), 1468.

9. Laupretre, F.; Prog. Polym. Sci., 15 (1990), 425.

10. Schaefer, J.; Stejskal, E.O.; Buchdahl, R.; Macromolecules, 8(3) (1975), 291.

11. Kitamaru, R.; Horii, F.; Murayama, K.; Macromolecules, 19 (1986), 636.

12. Havens, J.R.; Koenig, J.L.; Appl. Spectr., 37(3), (1983), 226.

13. Schaefer, J.; Stejskal, E.O.; Steger, T.R.; Sefcik, M.D.; Mckay, R.A.; Macromolecules, 13 (1980), 1131.

14. Garroway, A.N.; Vanderhart, D.L.; Earl, W.L.; Philos. Trans. R. Lond. A, 229 (1981), 609.

15. VanderHart, D.L.; J. Chem. Phys., 71(7) (1979), 2773.

16. Schaefer, J.; Stejskal, E.O.; Buchdahl, R.; Macromolecules, 10(2) (1977), 384.

17. Rothwell, W.P.; Waugh, J.S.; J. Chem. Phys., 74(5) (1981), 2721.

18. Lauprêtre, F.; Monnerie, L.; Virlet, J.; Macromolecules, 17 (1984), 1397.

19. Laupretre, F.; Monnerie, L.; Virget, J.; Macromolecules, 17 (1984), 1397.

20. McCall, D.W.; Acc. Chem. Res., 4 (1971), 223.

21. Connor, T.M.; NMR Basic Principles And Progr., 17(4) (1971), 250.

22. Powles, J.G.; Mansfield, P.; Polym. Comm. , 3 (1962), 339.

23. Stejskal, Macromolecules, 14 (1981), 275.

24. McCall, D.W.; Douglass, D.C.; Polymer, 4 (1963), 433.

25. McCall, D.W.; Anderson, E.W.; J. Chem. Phys., 32 (1962), 237.

26. Yannoni, C.S.; Acc. Chem. Res., 15 (1982), 201.

27. Bovey, F.A.; Polym. Engin. Sci., 26(20) (1986), 1419.

28. Lauprêtre, F.; Prog. Polym. Sci., 15 (1990), 425.

29. Vanderhart, D.L.; Earl, W.L.; Garroay, A.N.; J. Magn. Res., 44 (1981), 361.

30. Dechter, J.J.; Komoroski, R.A.; Axelson, D.E.; Mandelkern, L.; J. Polym. Sci.: Polym. Phys. Edn., 19 (1981), 631.

31. Pines, A.; Gibby, M.G.; Qaugh, J.S.; J. Chem. Phys., 59(2) (1973), 569.

32. Hartmann, S.R.; Hahn, E.L.; Phys. Rev., 128(5) (1962), 2042.

33. Yu, T.; Guo, M.; Prog. Polym. Sci.; 15 (1990), 825.

34. Aujila, R.S.; Harris, R.K.; Packer, K.J.; Parasneswaran, M.; Say, B.J.; Polym. Bull., 8 (1982), 253.

35. Hirai, A.; Horii, F.; Kitamaru, R.; Macromolecules, 23 (1990), 2913.

36. Torchia, D.A.; J. Magn. Res. Comm., 30 (1978), 613.

37. Wehrli, F.W.; Werthlin, T.; "Interpretation of Carbon-13 NMR Spectra", Heyden & Son Ltd., London, 1976.

38. McDonald, G.G.; Leigh Jr., J.S.; J. Magn. Res., 9 (1973), 358.

39. Ibbett, R.N.; "NMR Spectroscopy of Polymers", Chapman & Hall, London, 1993.

40. Fujimoto, K.; Nishi, R.; kado, R.; Polym. J., 3(4) (1972), 448.

41. Powles, J.G.; Stange, J.H.; Proc. Phys. Soc., 82 (1963), 6.

42. Hahn, E.L.; Phys. Rev., 80(4) (1950), 580.

43. Carr, H.Y.; Purcell, E.M.; Phys. Rev., 94 (1954), 630.

44. Meiboom, S.; Gill, D.; Rev. Sci. Instr., 29(8) (1958), 688.

45. Waugh, J.S.; Wang, C.H.; Phys. Rev., 162(2) (1967), 162.

46. Fedotov, V.D.; Schneider, H.; "Structure and Dynamics of Bulk Polymers by NMR-methods", Springer-Verslag, Berlin, (1989).

3. MACROSCOPIC PROPERTIES

3.1. Introduction

The possible polymerisation processes of polypropylene and ethylene-propylene copolymers were described in chapter 1. These polymerisation processes and conditions have an influence on the final macroscopic properties of the polymer. In this chapter the macroscopic properties of the ethylene-propylene copolymers are given in order to correlate them later with the NMR results (chapter 4, 5 and 6).

In the first paragraph an initial characterisation of the samples is given with regard to the polymerisation process and the melt index.

In paragraph 3.3 a discussion is given concerning the fractionation of the samples with xylene to separate the bulk polypropylene from the true ethylene-propylene copolymer and the low molecular weight part, since the ethylene-polypropylene heterophasic copolymers are complex mixtures of polypropylene, true ethylene-polypropylene copolymer and polyethylene. In addition to the total samples the different fractions were also analysed with liquid-state as well as with solid-state NMR to get a better understanding of the influence of every component (the bulk polypropylene and the ethylene-propylene copolymer) of the copolymer samples on the NMR results. These NMR results are reported in chapter 4, 5 and 6.

The influence of the thermal history on the crystallinity is discussed in section 3.4. In section 3.5 the glass transition temperature of a polypropylene sample, a random and a block copolymer are compared.

Ultimately in the last paragraph, the mechanical properties of the block copolymers are given.

3.2. Preliminary characterisation of the samples

Three ethylene-polypropylene heterophasic copolymers were supplied by Borealis, i.e. H, I and I*. The samples I and I* have the same ethylene content of about 15%, while sample H and I have the same xylene soluble fraction as will be seen in the following paragraphs. Two polypropylene homopolymer samples A and B, were used as a reference. A random copolymer J, was also taken to study the difference between random and block copolymers.

The copolymers were synthesised in different ways and the polymerisation process of the samples is given in Table 3.1. The total ethylene content, determined with liquid-state NMR (chapter 4) and the melt index are also mentioned. The melt index or the melt flow rate gives information about the average molecular weight of a polymer. A low melt index indicates a high molecular weight. The average molecular weight of all the samples is of the size of 10^5. All the samples contain less than 5% atactic material. Sample B and sample H have a broader molecular weight distribution than the other samples as is known from the catalyst system.

It is known from the literature that polypropylene and ethylene-propylene copolymers are not stable at high temperature.[1-4] Hence antioxidants were added to all polymers after polymerisation to be sure that they are stable during processing at high temperatures (>250°C).

	sample name	polymerisation process	ethylene content (%)	melt index (g/10min.)
polypropylene	A	spheriphol	-	3.4
polypropylene	B	slurry	-	3.0
random copolymer	J	spheriphol	3.4(.3)	6.0
heterophasic copolymer	H	slurry	8.5(.7)	0.4
heterophasic copolymer	I	spheriphol	14(2)	3.5
heterophasic copolymer	I*	spheriphol	15.5(.9)	2.6

Table 3.1: The polymerisation process, the melt index and the total ethylene content (determined with liquid-state NMR: Table 4.3) of the different samples.

Sample preparation

For the measurements of the samples in their solid state such as solid-state NMR measurements, the influence of the sample preparation was studied. The samples were pressed in a hot press, quenched in ice water and the quenched films were annealed at different temperatures. Annealing of a polymer has an influence on the crystallinity and this effect was studied with DSC, WAXS (section 3.4) and solid-state NMR (chapter 5).

To compare the different ethylene-propylene copolymers, the sample preparation has to be the same for all of them: an annealing temperature of 100°C was chosen just to remove any smectic form[5] and to avoid any crystallisation during the high temperature measurements[6].

3.3. Fractionation with xylene[7,8]

The ethylene-propylene block and random copolymers were fractionated with xylene to separate the bulk polypropylene from the true ethylene-propylene copolymer. The xylene insoluble fraction is the crystallisable isotactic polypropylene and polyethylene, while the xylene soluble fraction consists of the ethylene-propylene copolymer, the atactic polypropylene and the low molecular weight fraction. The xylene soluble fraction was further fractionated with acetone to divide the low molecular weight or oil fraction from the ethylene-propylene copolymer and atactic polypropylene (the amorphous fraction). The purpose of the fractionation is to study each fraction with NMR and to compare these results with the NMR data of the total samples in order to know the influence of the different components on each other. Besides, these xylene soluble fractions can be conceived as samples with extremely high ethylene content, when they are compared with the total samples: H, I and I*.

The fractions are expressed as weight percentages, by the general formula:

$$F\% = \frac{100 * m_1 * V_0}{m_0 * V_1} \qquad (3.1)$$

with: m_0 the sample weight and m_1 the polymer fraction weight (g)

V_0 the initial volume and V_1 the volume of the analysed aliquot (ml)

The results of the fractionation of the copolymers are given in Table 3.2. The oil fraction is for all the samples more or less the same. This means that all the samples have more or less the same amount of low molecular weight. The amorphous fraction with the true ethylene-propylene copolymer depends on the total ethylene content of the sample (Table 3.1), although there is no linear relation between the amorphous fraction and the total ethylene content. For example sample I and I* have approximately the same ethylene content and a significant difference in their amorphous fraction is found. This will be further discussed in chapter 4 in terms of the sequence distribution of the total samples and their fractions. The xylene soluble fraction exhibits the same trend as the amorphous fraction as it equals the sum of the amorphous fraction and the oil fraction.

Sample name	Amorphous fraction (%)	oil (%)	xylene soluble fraction (%)
J	6.1(.8)	1.8(.1)	7.7(.5)
H	13.8(1.1)	1.5(.2)	15.2(.3)
I	15.4(.3)	1.3(.2)	16.5(.4)
I*	23(1)	1.25(.07)	23.95(.07)

Table 3.2: Weight percentages of the amorphous, the oil and the xylene soluble fraction of the ethylene-propylene copolymers. The standard deviation is given between brackets.

3.4. Crystallinity

3.4.1. The crystalline forms of polypropylene

For polypropylene two stereo-regular forms exist, i.e. isotactic (i-PP) and syndiotactic (s-PP) polypropylene. They are both crystalline, but with distinct helical conformations (Figure 3.1). Isotactic polypropylene adopts a ...(gt)(gt)(gt)... 3_1 helical conformation in the crystal, while a 4_1 helix with a repeating ...(gg)(tt)(gg)(tt)... conformation is assumed by the syndiotactic polypropylene. The difference between the two stereo-regular forms can be seen with X-ray diffraction[9], by solid-state NMR[10-13] and by liquid-state NMR.[14] Polypropylene synthesised with Ziegler-Natta catalysts are for more than 90% isotactic. The remaining atactic fraction is amorphous. Four different crystalline forms of isotactic polypropylene exist:[15] a monoclinic α-form, a less stable hexagonal β-form[16], a lower ordered smectic form and a triclinic γ-form.[17,18] The triclinic γ-phase is rarely observed, being found only in low molecular weight and stereoblock fractions of polypropylene or by copolymerisation with a minor amount of ethylene.[19,20] A distinction between these crystal forms can be made with wide-angle X-ray diffraction. The characteristic peaks are found in the 2θ plot between the angles 18 -19°, 15-16° and 19.2-20.5° for the α-, β- and γ-crystals respectively.[21,22] Two diffuse reflections centred at 2Θ=15.2° and 21.3° are characteristic for smectic i-polypropylene.

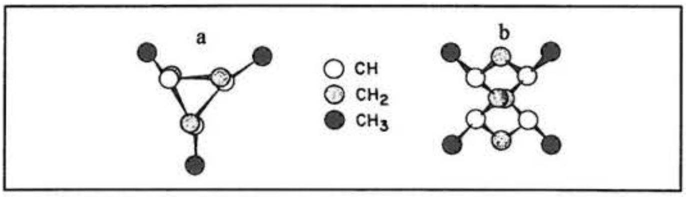

Figure 3.1: Representation of the helical conformation of isotactic (a) and of syndiotactic (b) polypropylene.[14]

3.4.2. The crystallinity of the samples

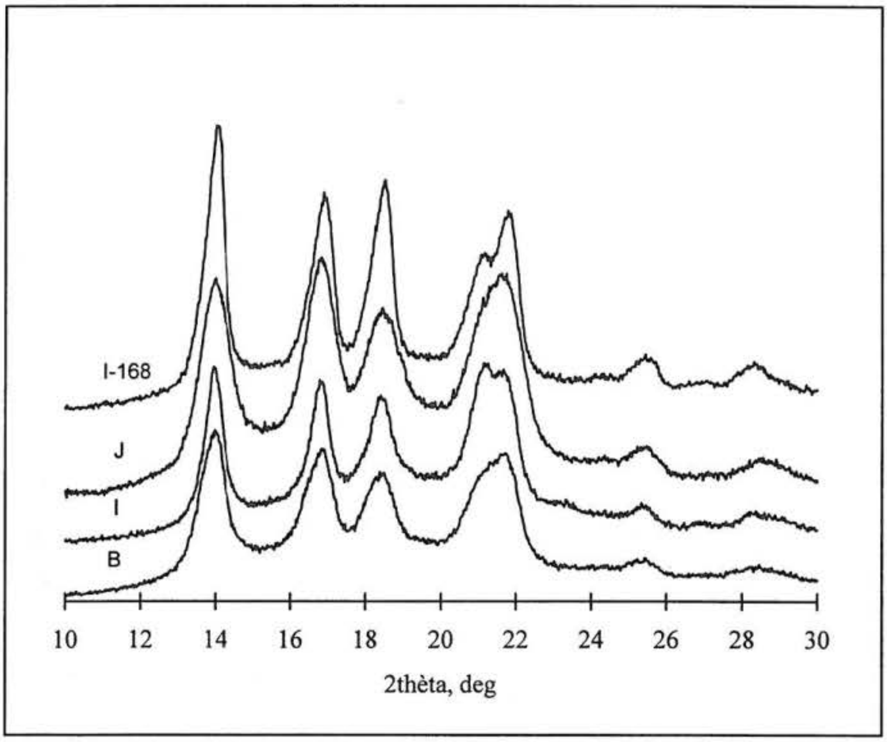

Figure 3.2: X-ray diagrams of polypropylene sample B, the random copolymer J, and the block copolymer sample I. The polymer samples were melt pressed, quenched in ice water and heated at100°C. Sample I-168 indicates the sample film I that is annealed at 168°C.

In Figure 3.2 the wide-angle X-ray diffraction patterns of a polypropylene sample, a random and a block copolymer sample are given. The wide-angle X-ray diffractogram of the α monoclinic form is characterised by five strong reflections at $2\theta = 14.0°$ (110), 16.8° (040), 18.6° (130), 21.1° (111) and 21.7° (131, 041) and all reflections are found in the diffractograms Figure 3.2. This indicates that all the samples have an α-crystalline form and there is no indication of another crystalline form. The reflections at 21.1° and 21.7° are too broad to be detected separately. For the sample annealed at 168°C (sample preparation: see chapter 9) these lines are better resolved compared with the other samples. This is an indication for a more perfect crystalline form. The crystal structure of this α crystalline form is given in Figure 3.3.

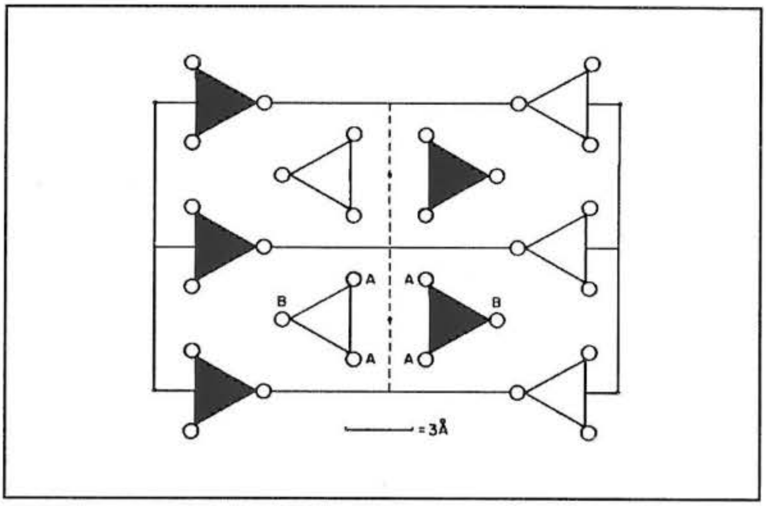

Figure 3.3: The crystal structure of the α-form. The 3_1 helical polypropylene chains of different handedness are represented by full and open triangles. A and B indicates the inequivalent sites between the helices.

It has to be pointed out here that there can also be some reflections due to the crystalline polyethylene. Two sharp peaks at 21.3° and 23.7° are characteristic for crystalline polyethylene and a broad signal at 19.5° characterise the diffractogram of amorphous polyethylene.[23] The most intense signal at 21.3° can't be seen in Figure 3.2 because there are also reflections of the crystalline polypropylene. The small signal at 23.7° is not visible in Figure 3.2 and this indicates that there is little or no crystalline polyethylene in the ethylene-propylene copolymers or that the crystals are not perfect enough to give small reflections. This can be checked with differential scanning calorimetry. The DSC scans of a homopolymer, a random copolymer, three block copolymers and a xylene insoluble fraction are compared in Figure 3.4.

For the homopolymer (B) one endotherm is found, i.e. the melting peak of polypropylene at 165°C. For random copolymers (J) in stead, the melting temperature depends on the fraction of the crystallisable component and is determined by the percentage of ethylene. For sample J the melting peak is decreased from 165°C for pure polypropylene to 150.7°C as a result of the three percent of ethylene. For the block copolymers two melting peaks are found:

one around 167°C for the crystalline polypropylene and the other around 110-120°C for the crystalline polyethylene. Normally, one should expect a melting peak of polyethylene around 127°. A lower melting peak indicates that the crystalline structure is not perfect. This can be explained by the fact that the samples contain only a few percentages of crystalline polyethylene (Table 3.3) which results in small crystalline domains. This can also explain the fact that the reflections of crystalline PE are not visible in the wide-angle x-ray diffractograms (Figure 3.2).

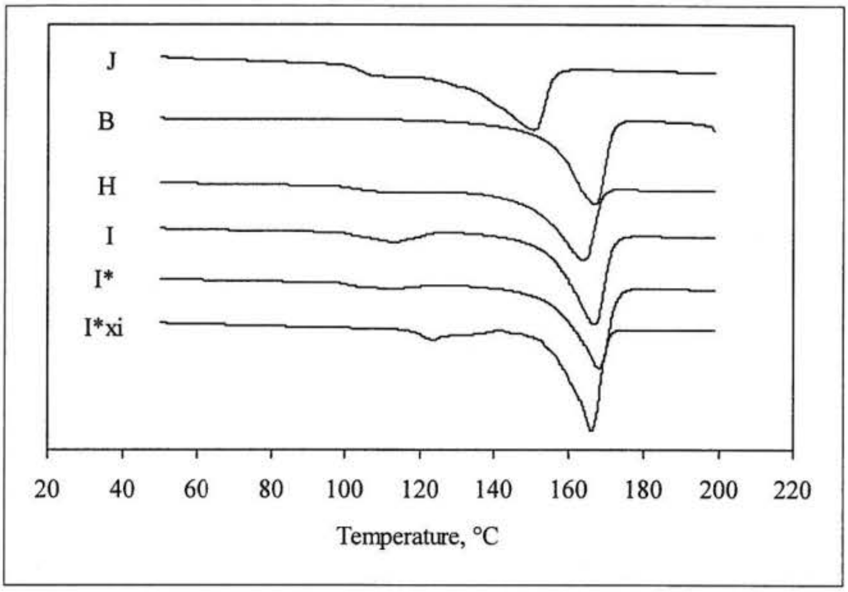

Figure 3.4: DSC scans of the random copolymer J, the polypropylene sample B, and the three block copolymers H, I and I* and the xylene insoluble fraction I^*_{xi} above room temperature. A heating rate of 10°C was used.

In the DSC scan (Figure 3.4) of sample H with 8% ethylene the two melting peaks are not completely separated and the melting peak of polyethylene is flatter than for the other block copolymers. This can be caused by the broader molecular weight distribution and the lower ethylene content compared with sample I and I* which have 15% ethylene.

The xylene insoluble fraction, I^*_{xi} contains the crystallisable fraction of sample I* and exhibits sharper melting endotherms than sample I* as a result of the absence of ethylene-propylene rubber.

Sample I^*_{xs} that consists of the ethylene-propylene rubber does not show any melting around 110°C or 168°C and hence contains no crystalline polyethylene or polypropylene.

	PP		PE	
sample name	percentage crystallinity (%)	melting temperature (°C)	percentage crystallinity (%)	melting temperature (°C)
B	38.3	165.4	0	-
J	29.2	150.7	-	-
H	29.3	164.0	2.5	108.8
I	32.3	166.9	2.8	113.4
I*	28.8	168.4	1.5	109.7
I^*_{xi}	30.2	166.2	3.06	123.7

Table 3.3: An overview of the percentage crystallinity and the melting point of polypropylene and ethylene-polypropylene copolymer samples determined with DSC (Figure 3.4). The melting temperature was deduced from the maximum in the melting transition. The percentage crystallinity was determined by comparing the area of the melting peak with the melting heat of 100% crystalline polypropylene (209J/g)[21] and polyethylene (277J/g)[24]. For the random it was not possible to determine the percentage crystallinity for polypropylene and polyethylene separately.

The degrees of crystallinity were determined and the results are summarised in Table 3.3. It is clear from this table that the copolymers have a lower percentage crystallinity than the homopolymer B. In copolymers the ethylene is distributed among the polypropylene chains and can be considered as imperfections in the polypropylene crystal lattice. Hence the ethylene reduces the percentage of crystalline polypropylene. The random copolymer with only three percent of ethylene has about the same percentage crystallinity as the block copolymers with up to 15 percent of ethylene. This means that in random copolymers the ethylene is randomly distributed in the polypropylene chains and reduces more efficiently the crystallinity compared with the block copolymers. The difference between the heterophasic copolymers will be discussed later in terms of their sequence distribution (chapter 5).

3.4.3. The effect of annealing on the crystallinity

The influence of the annealing of a copolymer was studied with DSC to compare the crystallinity and melting temperature with the solid-state NMR results (chapter 5). For polypropylene the effect of annealing was already studied in detail with X-ray scattering[25], DSC[26] and NMR[6,27] while for the ethylene-propylene copolymers the effect on the solid-state NMR results has never been discussed. The quenched copolymer films were heated at different temperatures as is described in the experimental part (chapter 9) and DSC scans were run for every sample. The results are collected in Table 3.4. The melting temperature of the bulk polypropylene increases from 167°C for the quenched sample to a maximum of 172.3°C for the sample annealed at 168°C. Besides the melting temperature the thermal pretreatment has also an influence on the percentage crystallinity (Table 3.4). The percentage crystallinity also finds its maximum at an annealing temperature of 168°C. This indicates that the most perfect α-crystalline form is found at that temperature. This is also visible in the wide-angle x-ray diffractogram of Figure 3.2 which represents smaller peaks for the best annealed copolymer sample I-168 than for other samples. Comparable results were found in the literature for polypropylene samples.[25,26]

	Polypropylene		Polyethylene
annealing temperature (°C)	Melting temperature (°C)	Percentage crystallinity (%)	Melting temperature (°C)
-	167.0	30.0	109.1
120	167.5	31.9	109.3 and 123.0
123	167.4	32.1	119.1 and 123.3
126	167.7	31.3	117.4 and 128.6
140	167.4	35.0	118.5
160	167.0	38.7	117.2
165	167.7	42.3	116.6
168	172.3	42.6	116.9
170	170.1	41.8	116.6
172	170.1	41.9	115.9

Table 3.4: The influence of the annealing temperature on the crystallinity and melting temperature of polypropylene and polyethylene of the ethylene-propylene block copolymer I as was measured with DSC. A heating rate of 10°C/min was used. The melting temperature was determined from the maximum in the melting transition. The percentage crystallinity is calculated by comparing the area of the melting peak with the melting heat of 100% crystalline polypropylene (209J/g)[21] and polyethylene (277J/g)[24].

Concerning the melting of polyethylene in ethylene-propylene copolymers the most remarkable temperatures in their DSC scans are found for the samples annealed at 120 to 126°C (Table 3.4). In that temperature range two melting peaks were seen: the high melting peak agrees with the melting of linear polyethylene.[28] The low melting peak is also found at other annealing temperatures and this melting point is caused by a less perfect crystallisation. The propylene in the copolymer chain can also be conceived as a defect in the polyethylene crystal and such a chain can be compared with branched polyethylene which has a lower melting point than linear polyethylene.

3.5. Glass transition temperature

The glass transition temperature of the homopolymer B, the random copolymer J, and the block copolymer I* and its xylene-soluble fraction I^*_{xs} were measured with a modulated differential scanning calorimeter and the results are shown in Figure 3.5.

For the polypropylene sample B the glass transition is found around -1.9°C. This is a weak transition because polypropylene is a semi-crystalline polymer.

The true ethylene-propylene copolymer sample, I^*_{xs} is completely amorphous and exhibits a strong transition at -54.8°C. For a real copolymer the glass transition temperatures can be calculated with the following equation:

$$\frac{1}{T_g} = \frac{F_1}{T_{g1}} + \frac{F_2}{T_{g2}} \qquad (3.2)$$

with T_{g1} and T_{g2} the glass transition temperature of respectively polyethylene and polypropylene. The weight fractions are represented by F_1 and F_2.
From the literature it is known that T_g of polypropylene ranges between -15°C and 0°C. The T_g (-1.9°C) of sample B lies between this range. For polyethylene glass transition temperature between -120°C and -105°C are found.[29] Taking for T_{g1} -105°C and for F_1 41.1% (chapter 4 Table 4.5) a glass transition temperature of -56.5°C is calculated with equation 3.2 for sample I^*_{xs}. This is in agreement with the experimental value of -54.8°C. It means that sample I^*_{xs} is a homogeneous mixture of ethylene and propylene.

For the ethylene-propylene block copolymer I* the same T_g is found as for the true ethylene-propylene copolymer, I^*_{xs}. This indicates that the copolymer I* exhibits a local T_g of the true ethylene-propylene copolymer domains. In fact, one should also expect a T_g of the amorphous polypropylene around -2°C, but this is not visible. This transition is also weak for the polypropylene sample B. Sample I* is also semi-crystalline and on top contains 25% true copolymer. Thus the T_g of the amorphous polypropylene of sample I* is too weak to be seen with DSC. From the literature it is known that such a commercial ethylene-propylene copolymer exhibits a glass transition temperature of amorphous polypropylene around 0°C and of polyethylene at -105°C, when measured with DMA.[30,31] It was not possible to detect the glass transition temperature of polyethylene with MDSC because transitions can be measured with the modulated DSC starting from -100°C.

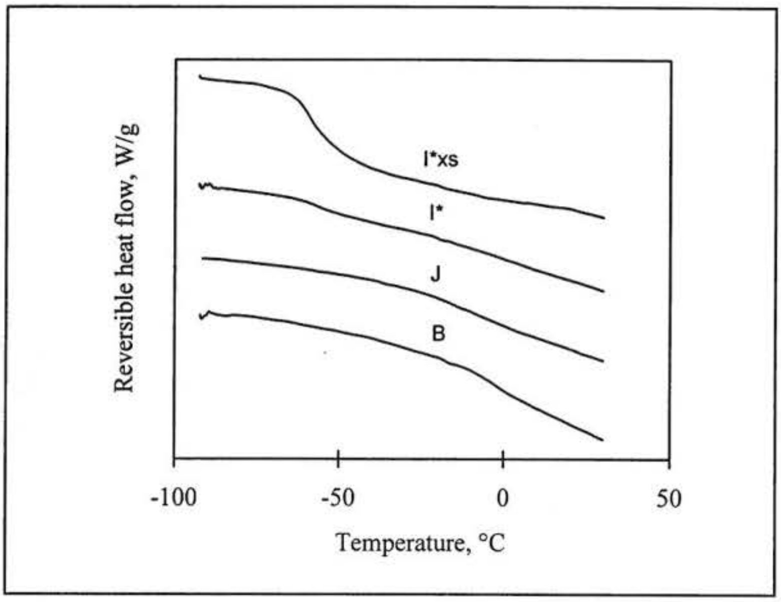

Figure 3.5: The glass transition of the polypropylene sample B, the random copolymer J, the block copolymer I* and its xylene-soluble fraction I^*_{xs} measured with modulated DSC. A heating rate of 2.5°C/min was used. The period of modulation was 60s and the temperature amplitude of modulation was 1.00°C.

The random copolymer J doesn't have a transition around -54°C of true ethylene-propylene copolymer, but it has one T_g at -14.9°C. This implies that the ethylene in the random copolymer reduces the global glass transition temperature of pure polypropylene. The random copolymer doesn't have such a big ethylene-propylene copolymer domains with their own T_g as for the block copolymers.

From these results it can be concluded that the polypropylene sample B and the random copolymer J are at room temperature just above their glass transition temperature and at this temperature the mobility of the amorphous chains will still be restricted. On the other hand, the true ethylene-propylene copolymer domains in the block copolymers are more than 50°C above T_g and will have a higher mobility compared with the random copolymer J. This will have an influence on the macroscopic properties and the solid-state NMR results.

3.6. Mechanical testing

For the mechanical tests injection moulded specimens were used. The results are shown in Table 3.5.

The flex modulus of pure polypropylene fluctuates between 1200 and 1700 MPa, while for the block copolymers it is mostly lower than 1200 MPa. This can be explained in terms of the lower crystallinity of the copolymers compared with the homopolymer. For polypropylene the empirical equation presented by Flory[32] can be obtained: $P = A + B/M$ where P stands for mechanical properties, A and B are constants and M is the molecular weight. B is a positive value for the elasticity, which means that the flexural modulus decreases with increasing molecular weight.[33] Such a simple equation for predicting the mechanical properties from the molecular weight cannot be applied for copolymers because the ethylene content as well as the sequence distribution have also an influence the macroscopic properties. The same can be said about the tensile properties. It can also be remarked here that samples I and I* which have about the same ethylene content and molecular weight, have a totally different impact strength. So further research is needed to get a better understanding of the macroscopic properties.

	H	I	I*
Charpy impact test (kJ/m^2)	30.5(2.6)	15.1(1.6)	100
Break	not complete	complete	not broken
Izod impact test (kJ/m^2)	not broken	15(2)	not broken
Flex modulus (N/m^2)	1032	1000	877
Tensile strength at yield (MPa)	25.7(0.1)	20.6(0.1)	18.6(0.1)
Elongation at yield(%)	14.13(0.32)	5.58(0.14)	6.0(0.2)
Modulus (MPa)	1087(14)	1054(26)	970(18)

Table 3.5: The results of the mechanical tests on the ethylene-propylene heterophasic copolymers. The standard deviation of the results are given between brackets. For the impact tests not broken means that a maximum pressure of 100kJ/m^2 was not enough to break the sample. The test methods are based on ISO norms.

3.7. Conclusions

In this chapter the polymer samples were characterised. The polypropylene as well as the copolymer samples have an α-crystalline form for polypropylene and the block copolymers only contains a few percentage of crystalline polyethylene. The percentage crystallinity and the melting temperatures of polypropylene and the copolymers depend on the thermal history.

The glass transition temperature of polypropylene is just below 0°C, while for the random copolymer in which the ethylene is randomly distributed T_g is reduced to -15°C. On the other hand, block copolymers are formed as multiphase structures comprised of polypropylene in which ethylene-propylene copolymer domains are dispersed.They have more than one glass transition temperature: a T_g of polypropylene and another transition around -54°C of the ethylene-propylene copolymer domains. This lower glass transition temperature of the copolymers compared with polypropylene improves the impact strength at room temperature. A simple correlation between the mechanical properties and other properties, like percentage crystallinity and molecular weight does not exist for the copolymers because the properties are also influenced by the ethylene content and the distribution of the ethylene in the polypropylene chains. This sequence distribution of the ethylene-propylene random and block copolymers is discussed in the next chapter.

3.8. References

1. Bauer, M.; Renmbold, M.; marti, E.; Schneider, H.A.; Mülhaupt, R.; Macromolecules, 197 (1996), 61.

2. Mani, R.; Singh, R.P.; Sivaram, S.; J. Macromol. Sci., Part A: Pure and Appl. Chem., 31(4) (1994), 413.

3. Zaharescu, T.; Giurginca, M.; Mihalcea, I.; Polym. Deg. Stab., 48 (1995), 151.

4. Zaharescu, T.; J. Mater. Sci. Lett., 14 (1995), 925.

5. Bunn, A.; Cudby, M.E.A.; Harris, R.K.; Packer, K.J.; Say, B.J.; Polymer, 23 (1982), 694.

6. Caldas, V.; Morin, F.G.; Brown, G.R.; Magn. Res. Chem., 32 (1994), 72.

7. Simonazzi, T.; Pure and Appl. Chem., 56(5) (1984), 625.

8. Fractionation was done according to the Himont wordwide test method.

9. Corradini, P.; Natta, G.; Ganis, P.; Temussi, P.A.; J. Polym. Sci.: Part C, 16 (1967), 2477.

10. Bunn, A.; Cudby, E.A.; Harris, R.K.; Packer, K.J.; Say, B.J.; J.C.S. Chem. Commun., (1981), 15.

11. Bovey, F.A.; "Nuclear magnetic Resonance Spectroscopy", Academic Press, California, 1987.

12. Sozzani, P.; Simonutti, R.; Comotti, A.; Magn. Res. Chem., 32 (1994), 45.

13. Jelinski, L.W.; Chemtech, 8(A2) (1986), 1.

14. Tonelli, A.E.; "NMR Spectroscopy and Polymer Microstructure: the conformational connection", VCH Publishers, USA, 1989.

15. Turner-Jones, A.; Aizlewood, J.M.; Bechett, D.R.; Macromol. Chem.. 75 (1964), 134.

16. Turner-Jones, A.; Cobbold, A.J.; J. Polym. Sci., Polym. Lett., 6 (1968), 539.

17. Meille, S.V.; Brüchner, S.; Porzio, W.; Macromolecules, 23 (1990), 4114.

18. Brückner, S.; Meille, S.V.; Sozzani, P.; Torri, G.; Makromol. Chem., Rapid Commun., 11 (1990), 55.

19. Mezghani, K.; Phillips, P.J.; Polymer, 36(12) (1995), 2407.

20. Turner-Jones, A.; Polymer, 12 (1971), 487.

21. Gomez, M.A.; Tantaka, H.; Tonelli, A.E.; Polymer, 28 (1987), 2227.

22. Thomann, R.; Wang, C.; Kressler, J.; Mülhaupt, R.; Macromolecules, 29(26) (1996), 8425.

23.Hosoda, S.; Nomura, H.; Gotoh, Y.; Kihara, H.; Polymer, 31 (1990), 1999.

24. Wunderlich, B.; Dole, M.; J. Polym. Sci., 24 (1957), 201.

25. Pluta, M.; Kryszewski, M.; Acta Polymerica, 37(11/12) (1986), 726.

26. Vittoria, V.;Polymer, 32(5) (1991), 856.

27. Tanaka, H.; Korogi, F.; Eur. Polym. J., 24(8) (1988), 759.

28. Billmeyer Jr., F.W.; "Textbook of Polymer Science", John Woley & Sons, Singapore, 1994.

29. Brydson, J.A.; "Plastics Materials", the Butterworth Group, London, 1975.

30. Sun, Z.; Yu, F.; Qi, Y.; Polymer, 32(6) (1991), 1059.

31. Karger-Kocsis, J.; Kiss, L.; Polym. Eng. Sci., 27(4) (1987), 254.

32. Flory, P.J.; J. Amer. Chem. Soc., 87 (1939), 2048.

33. Ogawa, T.; J. Appl. Polym. Sci., 44 (1992), 1869.

4. LIQUID-STATE NMR: A SEQUENCE ANALYSIS

4.1. Introduction

Liquid-state NMR is a powerful tool for the characterisation of polymers, both in a qualitative and in a quantitative way. For copolymers the molecular components can be discovered and the manner in which they are linked together can be determined. A lot of research concerning the sequence distribution of ethylene substituted polymers is already done.[1-5] Knowledge of the sequence distribution is important because it forms the link between the polymerisation process and its conditions and the final product with certain properties.

In this chapter the sequence distribution of the ethylene-propylene copolymers is discussed and compared with the distribution of the xylene soluble and xylene insoluble fraction. Finally, a correlation with the macroscopic properties is given.

4.2. Chemical shift assignment

Figure 4.1 shows the ^{13}C liquid-state NMR spectrum of an ethylene-propylene copolymer, which contains head-to-tail polypropylene with an isotacticity of more than 95%. To assign the signals the terminology of Carman et al.[6] is used: methylene (secondary) carbons are indicated by the letter S, methine (tertiary) carbons by the letter T and methyl (primary) carbons by the letter P. The distance between the carbon under investigation and the neighbouring methine carbon is given by a Greek letter (α, β, γ and δ). This terminology is illustrated in Figure 4.2. The Greek letter δ indicates that the carbon atom and the neighbouring methine carbon are at least separated by three carbon atoms. Many investigators[7-11] assigned the signals up to pentads, but for the sequence analysis that is used only dyads and triads have to be known.

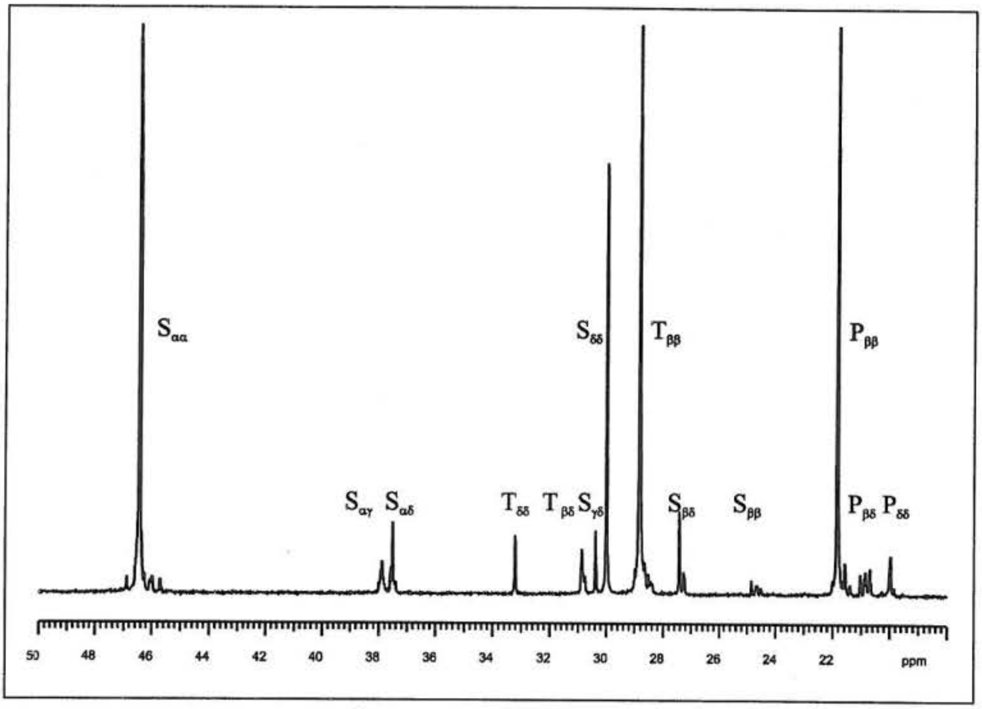

Figure 4.1: A quantitative 100MHz ^{13}C NMR spectrum of the ethylene-propylene copolymer I* with 15% ethylene. The polymer was dissolved in 1,2,4-trichlorobenzene and measured at 120°C. The experimental conditions are described in section 9.1.1. The sequences are shown. The terminology of Carman et al. is used.

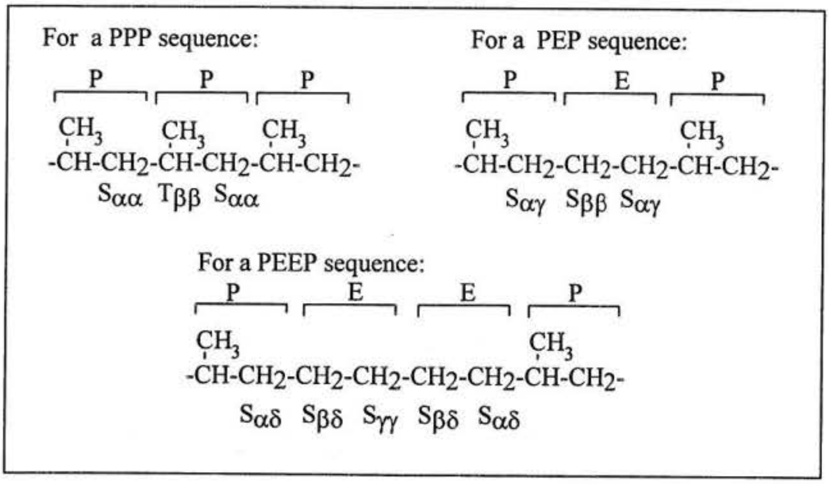

Figure 4.2: An explanation of the terminology of Carman et al.[6] for ethylene-propylene copolymers.

4.3. Sequence analysis

The sequence analysis of ethylene-propylene copolymers has been the subject of many NMR studies.[8,9,12] Therefore the intensities of the signals in the spectrum can be combined in different ways to obtain sequence information of the copolymers. In this study the equations of Kakugo et al.[12] were used. The equations for the determination of the triad distribution, the monomer distribution, the average sequence length and the weight percentage ethylene and propylene are given here.

The triad distribution indicates the percentage of a certain triad (e.g. EEE) to the sum total of the triads (EEE + EEP + PEP + EPE + PPE + PPP).

$$EEE = \tfrac{1}{2} S_{\delta\delta} + \tfrac{1}{4} S_{\gamma\delta} = \tfrac{1}{2} I_g + \tfrac{1}{4} I_h \quad (4.1)$$

$$PEE = S_{\alpha\delta} = S_{\beta\delta} = I_l = I_e \quad (4.2)$$

$$PEP = S_{\beta\beta} = \tfrac{1}{2} S_{\alpha\gamma} = I_d = \tfrac{1}{2} I_m \quad (4.3)$$

$$EPE = T_{\delta\delta} = Ik \quad (4.4)$$

$$PPE = T_{\beta\delta} = I_j \quad (4.5)$$

$$PPP = T_{\beta\beta} = I_f \quad (4.6)$$

To obtain the triad distribution the results of equation 4.1 to 4.6 have to be divided by the sum total of the triads and multiplied by 100.

The monomer distribution can be defined as the number of moles of a monomer in a sequence length divided by the total mole fraction of the monomer in the polymer. A distinction can be made between a sequence length of one, two or three to more monomer units long. This is given for ethylene by E_1, E_2 and $E_{n\geq3}$ and for propylene by P_1, P_2 and $P_{n\geq3}$.

$$E_1 = S_{\beta\beta}/E' = \tfrac{1}{2}S_{\alpha\gamma}/E' = (I_d + \tfrac{1}{2}I_m)/2E' \quad (4.7)$$

$$E_2 = 2S_{\gamma\gamma}/E' = (S_{\beta\delta} - S_{\gamma\delta})/E' = (I_e - I_h)/E' \quad (4.8)$$

$$E_{n\geq3} = 100 - E_1 - E_2 \quad (4.9)$$

$$P_1 = T_{\delta\delta}/P' = P_{\delta\delta}/P' = I_k/P' \quad (4.10)$$

$$P_2 = 2I_n/P' \quad (4.11)$$

$$P_{n\geq3} = 100 - P_1 - P_2 \quad (4.12)$$

with E' and P' an amount which is proportional with respectively the total ethylene and propylene content:

$$E' = \tfrac{1}{2}(S_{\delta\delta}+S_{\beta\delta}+S_{\alpha\gamma} + \tfrac{1}{2}(S_{\gamma\delta}+S_{\beta\delta}+S_{\alpha\delta})) \quad (4.13)$$

$$= \tfrac{1}{2}(I_g+I_e+I_m+ \tfrac{1}{2}(I_h+I_e+I_l))$$

$$P' = S_{\alpha\alpha} + \tfrac{1}{2}(S_{\alpha\gamma}+S_{\alpha\delta}) = I_o + \tfrac{1}{2}(I_m+I_l) \quad (4.14)$$

From these equations also the moles percentage of ethylene and propylene can be calculated:

$$E(\text{mol\% of ethylene}) = 100 * E'/(E'+P') \quad (4.15)$$

$$P(\text{mol\% of propylene}) = 100 * P'/(E'+P') \quad (4.16)$$

The weight percentage of ethylene and propylene is then given by:

$$E(\text{weight\%}) = 100 * 2* E(\text{mol\%})/(2*E(\text{mol\%}) + 3 * P(\text{mol\%})) \quad (4.17)$$

$$P(\text{weight\%}) = 100 - E(\text{weight\%}) \quad (4.18)$$

The average sequence of ethylene (propylene) is given by the moles percentage of ethylene (propylene) divided by the total number of ethylene (propylene) sequences:

$$\text{aver. seq.}(E) = (PEP + PEE + EEE)/(PEP + 0.5*PEE) \quad (4.19)$$

$$\text{aver. seq.}(P) = (EPE + EPP + PPP)/(EPE + 0.5* EPP) \quad (4.20)$$

The sequence of the different samples was analysed with these equations. Moreover the fractionated samples, i.e. the xylene-solubles and the xylene-insolubles were also investigated.

For the determination of the sequence distribution of a copolymer, quantitative spectra are required. Special attention has to be paid to get reproducible and reliable quantitative spectra and sequence results.

4.3.1. Quantitative ^{13}C liquid-state NMR spectra

For the determination of the sequence distribution of a copolymer, quantitative spectra are needed. To establish conditions for such an analysis a knowledge of the ^{13}C spin relaxation parameters and the Nuclear Overhauser Effect (NOE) for the carbons investigated is essential. Quantitative measurements ask for complete relaxation of the different carbon atoms to obtain reliable results. This means that a repetition time of 4-5 times the longest spin-lattice relaxation time has to be respected between two pulses.[13] Alternatively, shorter delay times combined with pulses less than 90° can be useful if the relaxation times of the distinct carbons are similar. Too short repetition times result in preferential saturation of some carbon atoms and in wrong integrated intensities. In polyolefins the T_1 relaxation time increases with the temperature. At 120°C the T_1 relaxation time of the backbone of branched polyethylene ranges between 0.9 and 1.6 s,[14,15] while for methyl carbons this is longer: for polypropylene a T_1 of 2.23s is found. So a 60° pulse in combination with a preparation time of 8s was used for the measurements.

In addition to the relaxation time the Nuclear Overhauser Enhancement is an important factor for quantitative analysis. This effect arises from the direct magnetic coupling between nuclei and an increase in the intensity of the resonances is observed if the transitions of other nuclei nearby are irradiated. Scalar decoupling removes the splittings introduced by indirect spin-spin coupling. Generally, to obtain quantitative spectra decoupling is only gated on during data acquisition because the Nuclear Overhauser Effect is not always the same for all the carbons of interest for polymers with a low mobility in solution.[16,17] This pulse sequence has the advantage that the NOE does not have the time to build up, while the splitting of the signals due to scalar coupling can be removed. A fully decoupled spectrum can only be used if the Nuclear Overhauser Enhancement is complete. This is the case for polypropylene[18] and for branched polyethylene[13]. The NOE is influenced by the correlation time of the atoms as is shown in Figure 4.3. Under "extreme narrowing" conditions, where T_1 equals T_2, all carbons have a purely dipolar relaxation mechanism and the NOE is complete. If the relaxation mechanism is dominated by the dipole-dipole relaxation between directly bonded ^{13}C and ^{1}H atoms, the number of bonded protons is irrelevant, and the same enhancement is seen for the carbon nuclei of methine, methylene and methyl groups in polypropylene. This suggests a condition of "extreme narrowing". One can run decoupled spectra to remove the scalar C-H coupling and it reduces the time required to obtain a spectrum due to the maximum Nuclear Overhauser Enhancement of the carbons of ethylene-propylene copolymers.

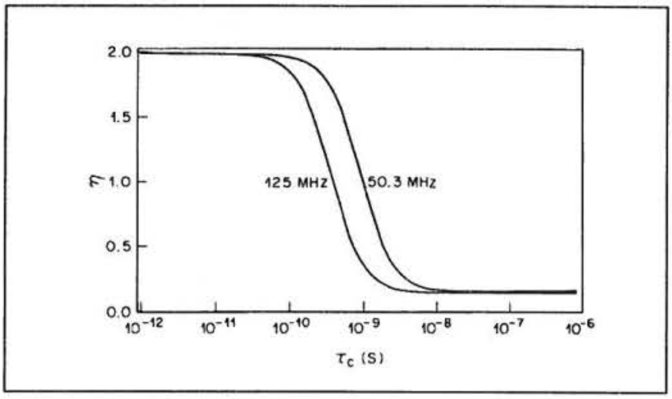

Figure 4.3: Nuclear Overhauser Enhancement factor η for a carbon-13 nucleus, produced by irradiation of neighbouring protons, as a function of the correlation time, τ_c. The NOE is given for carbon frequencies of 50.3 MHz and 125 MHz.

4.3.2. Reproducibility

With quantitative spectra of ethylene-propylene copolymers the sequence distribution can be determined and the results of the sequence analysis have to be reproducible.

The reproducibility test can be divided into three topics: the influence of the integration of the signals, the influence of the NMR measurement (one solution measured three times) and the influence of the sample preparation (three different solutions of one sample).

4.3.2.1. The influence of integration of the signals

First of all, the influence of the integration was tested for the random ethylene-propylene copolymer J with the lowest percentage of ethylene ($3\%_w$) and for a block copolymer I* with 15% ethylene. The results are given in Table 4.1. The influence seems to be small, but it has to noted here that well-defined integration regions are needed. This is certainly true for copolymers with low ethylene content like sample J. The integration regions are given below:

I_a (19.8-20.45ppm)
I_b (20.45-21.2ppm)
I_c (21.2-22.5ppm)
I_d (24.4-25.0ppm)
I_e (27.0-27.6ppm)
I_f (28.2-29.6ppm)
I_g (29.6-30.2ppm)
I_h (30.2-30.5ppm)
I_i (30.5-30.85ppm)
I_j (30.85-31.3ppm)
I_k (33.3ppm)
I_l (37.2-37.8ppm)
I_m (37.8-38.4ppm)
I_n (45.77ppm)
I_o ($S_{\alpha\alpha}$:45-48ppm)

	Integration influence		Different solutions of a sample	
	J	I^*	H	I*
E(wt%)	3.32(.03)	14.57(.04)	8.5(.7)	15.5(.9)
aver.seq.(E)	1.31(.05)	3.79(.01)	4.2(.1)	3.9(.1)
aver.seq.(P)	23.3(.4)	14.79(.09)	26(2)	13.3(.8)
EEE (%)	0.72(.02)	11.71(.03)	7.8(.5)	12.5(.7)
PEE+EEP (%)	0.90(.06)	6.24(.01)	3.2(.5)	6.4(.3)
PEP (%)	3.21(.02)	2.23(.01)	1.32(.06)	2.1(.2)
EPE (%)	0.42(.07)	3.28(.03)	1.9(.1)	3.2(.2)
PPE+EPP (%)	7.33(.02)	4.3(.1)	2.8(.1)	5.4(.3)
PPP (%)	87.41(.02)	72.21(.09)	83(1)	70(1)
E_1 (%)	65.2(.4)	10.92(.05)	10.8(.8)	10(1)
E_2 (%)	10.7(.1)	10.8(.5)	10.9(.9)	12(1)
$E_{n\geq3}$ (%)	24.1(.4)	78.3(.5)	78.9(.6)	78.2(.5)
P_1 (%)	0.44(.07)	4.09(.04)	2.2(.2)	4.2(.2)
P_2 (%)	0.9(.1)	3.7(.3)	1.8(.7)	3.58(.02)
$P_{n\geq3}$ (%)	98.65(.03)	92.2(.3)	96.3(.9)	92.6(.4)

Table 4.1: The influence of the integration of the random copolymer J and the block copolymer I* are given. In the latest columns the averages and standard deviations of the sequence analyses of the samples H and I* are given: three different solutions of each sample were measured. Equations 4.1 - 4.20 were used for the analysis. E(wt%) indicates the ethylene weight percentage and aver.seq. is the average sequence length.

4.3.2.2. The influence of a NMR experiment

	H	I*	J
E(wt%)	9.2(.4)	14.5(.2)	3.1(.2)
aver.seq.(E)	4.3(.1)	3.82(.05)	1.21(.07)
aver.seq.(P)	26.1(.9)	13.39(.02)	23.2(.4)
EEE (%)	8.3(.4)	11.7(.1)	0.5(.3)
PEE+EEP (%)	3.59(.01)	6.12(.07)	0.8(.2)
PEP (%)	1.3(.1)	2.17(.03)	3.26(.05)
EPE (%)	1.99(.03)	3.16(.04)	0.5(.1)
PPE+EPP (%)	2.8(.5)	5.6(.1)	7.4(.3)
PPP (%)	81.9(.9)	71.21(.04)	87.6(.3)
E_1 (%)	9.9(.7)	10.9(.2)	70(5)
E_2 (%)	11.7(.8)	11.5(.3)	9(4)
$E_{n\geq3}$ (%)	78.4(.6)	77.7(.5)	21(5)
P_1 (%)	2.28(.05)	4.00(.05)	0.5(.1)
P_2 (%)	2.5(.4)	3.6(.2)	1.0(.1)
$P_{n\geq3}$ (%)	95.2(.4)	93(1)	98.4(.3)

Table 4.2: Averages and standard deviation of the sequence analyses of the sample H, I* and J: the influence of an NMR measurement (one solution measured three times). Equations 4.1 - 4.20 were used for the analysis. E(wt%) indicates the ethylene weight percentage and aver.seq. is the average sequence length.

The second topic was the influence of the NMR measurement. Two block copolymers with different ethylene content (H:8% and I*: 15% of ethylene) and the random copolymer J were measured three times (Table 4.2). For the block copolymers the standard deviations are small (less than 1). For the random copolymer J the standard deviation is higher for the monomer distributions of ethylene. It seems that the uncertainty on the monomer distribution depends on the total ethylene content: a lower ethylene content causes a bigger standard deviation on the monomer distribution. So especially for samples with a low percentage of ethylene attention must be paid to tuning, locking and shimming to run reproducible NMR experiments.

4.3.2.3. The influence of the solution

Finally, different solutions of a sample were measured. From both samples, H and I*, three solutions were made and from each solution a NMR spectrum was recorded. This is shown in Table 4.1. Again, the standard deviation of the ethylene monomer distribution is generally higher than for the other data. For the liquid-state NMR measurements only three or four pellets were used for a measurements. Hence, small difference in the content of pellets can cause differences in content of the different solutions. Moreover, the homogeneity of the solution is an important parameter. Before the NMR measurement the homogeneity can be checked against light.

4.3.2.4. Conclusions

In order to get reproducible results, care has to be taken of the sample preparation to get an homogeneous solution. Careful tuning, locking and shimming is required to reduce the standard deviation. For the integration well-defined integration regions are needed.

4.3.3. Micro-structure of some ethylene-propylene copolymers

The sequence distribution of three block copolymers H, I and I* and one random copolymer J was determined. Different solutions of a sample were measured and the average of the sequence analysis is given in Table 4.3.

From these results it became clear that in the random copolymer J the ethylene is distributed in short sequences for about 70% (E_1), while for the block copolymers 70% of the ethylene belongs to a sequence of three or more ethylene units ($E_{n\geq3}$). The average sequence length of ethylene in sample J is 1.3; while in the block copolymers it is four to five units.

In the block copolymers (H, I, I*) the average sequence length of propylene is related to the total ethylene content: higher amounts of ethylene or lower amounts of propylene reduce the average propylene sequence length.

	H	I	I*	J
E(wt%)	8.5(.7)	14(2)	15.5(.9)	3.4 (.3)
aver.seq.(E)	4.2(.1)	5.0(.5)	3.9(.1)	1.2(.1)
aver.seq.(P)	26(2)	19(3)	13.3(.8)	24.2(.5)
EEE (%)	7.8(.5)	13(2)	12.5(.7)	0.8(.3)
PEE+EEP (%)	3.2(.6)	5.0(6)	6.4(.3)	1(.2)
PEP (%)	1.32(.01)	1.34(.06)	2.1(.2)	4.0(.6)
EPE (%)	1.9(.1)	2.6(.4)	3.2(.2)	0.7(.2)
PPE+EPP (%)	2.8(.1)	3.5(.2)	5.4(.3)	7.5(.3)
PPP (%)	83(1)	75(4)	70(1)	86(1)
E_1 (%)	10.8(.8)	7(1)	10(1)	71(5)
E_2 (%)	10.9(.9)	5(1)	12(1)	11(4)
$E_{n\geq3}$ (%)	78.9(.6)	88(3)	78.2(.5)	18(6)
P_1 (%)	2.2(.2)	3.4(.7)	4.2(.2)	0.6(.3)
P_2 (%)	1.8(.7)	1.9(.2)	3.58(.02)	1.2(.1)
$P_{n\geq3}$ (%)	96.3(.9)	94.7(.5)	92.6(.4)	98.1(.4)

Table 4.3: An overview of the sequence distribution of the block copolymer samples H, I and I* and the random copolymer J. The standard deviation is given between brackets. Equations 4.1 - 4.20 were used for the analysis. E(wt%) indicates the ethylene weight percentage and aver.seq. is the average sequence length.

The triad EEE seems to increase with the ethylene content. There is also a correlation with the percentage crystalline polyethylene, that was measured with DSC (section 3.4.). Ethylene runs of seven or more units long are needed to give crystalline polyethylene. With this sequence analysis only the dyad and triad distribution can be determined, nevertheless the EEE triad can give us an idea of the crystallinity. The sample J with only three percent of ethylene has an EEE triad of 0.8%. From this information it is clear that the percentage crystalline polyethylene must be very small or negligible. On the other hand, the sample I and I* with about 14 to 15% ethylene and an EEE triad of 13% give in the DSC spectrum a clear signal around 110°C, the melting temperature of polyethylene (Figure 3.4).

For these samples I and I* the ethylene content is more or less the same (14-15%), while there is a difference in the sequence. Comparing the monomer distribution, the triads and the average sequence length of ethylene and propylene, it seems that in sample I* compared with I the ethylene and propylene are more divided in short sequences. Short ethylene sequences in a long crystalline polypropylene chain can be considered as a defect in the crystal and reduce the percentage crystallinity. This explains the lower percentage crystallinity of sample I* compared with sample I. Furthermore, it is the short sequences of propylene and ethylene which cause improved properties of the ethylene-propylene copolymers over the pure polypropylene homopolymer. Sample I*, which has shorter ethylene and propylene sequences than sample I, has also a better impact strength (section 3.6). The sample H has also better properties compared with the sample I, although the total amount of ethylene is less. From Table 4.3 it can be seen that the ethylene of sample H is more divided in short sequences compared with sample I. The monomer distribution of ethylene is the same for sample I* and H, although the total ethylene content of sample I* is twice the content of sample H. Moreover, it is known from previous chapter that sample H has a lower impact strength than I* but a better strength than I. It has to be noted here that care have to be taken by comparing sample H with I and I* because sample H has a higher molecular weight compared with the two other samples. It is known that the molecular weight has also an influence on the macroscopic properties.

Conclusions:

From the liquid-state NMR results of the different samples it can be concluded that the *total ethylene content as well as the sequence distribution* are important parameters for the macroscopic properties. A higher percentage of short sequences of ethylene and propylene improves the impact strength and reduces the crystallinity.

4.3.4. Micro-structure of the fractionated samples

To get a better feeling of the sequences of the copolymers, the fractionated samples (chapter 3.3) were measured with liquid-state NMR. Sequence analyses of the xylene-insoluble, the amorphous and the xylene-soluble fractions was analysed.

Concerning the NMR spectra of the two fractions it has to be noticed that the solvents used for fractionation, i.e. o-xylene and acetone, can also give signals in the ^{13}C NMR spectrum. The chemical shift values are given in Table 4.4. Both o-xylene and acetone have signals between 19 and 50 ppm, the frequency area of the ethylene-propylene copolymers. This implies that the solvents have to be evaporated completely before liquid-state NMR experiments can be done.

The ^{13}C NMR spectra of the xylene soluble and the xylene insoluble fraction are given in Figure 4.4 and Figure 4.5.

o-xylene	1 and 2	3 and 6	4 and 5	7 and 8
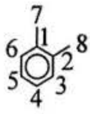	136.4	129.6	125.8	19.7
acetone	$\underline{C}H_3$	$\underline{C}=O$	-	-
	30.7	206.1	-	-

Table 4.4: Chemical shift values (ppm) of the solvents used for extraction.

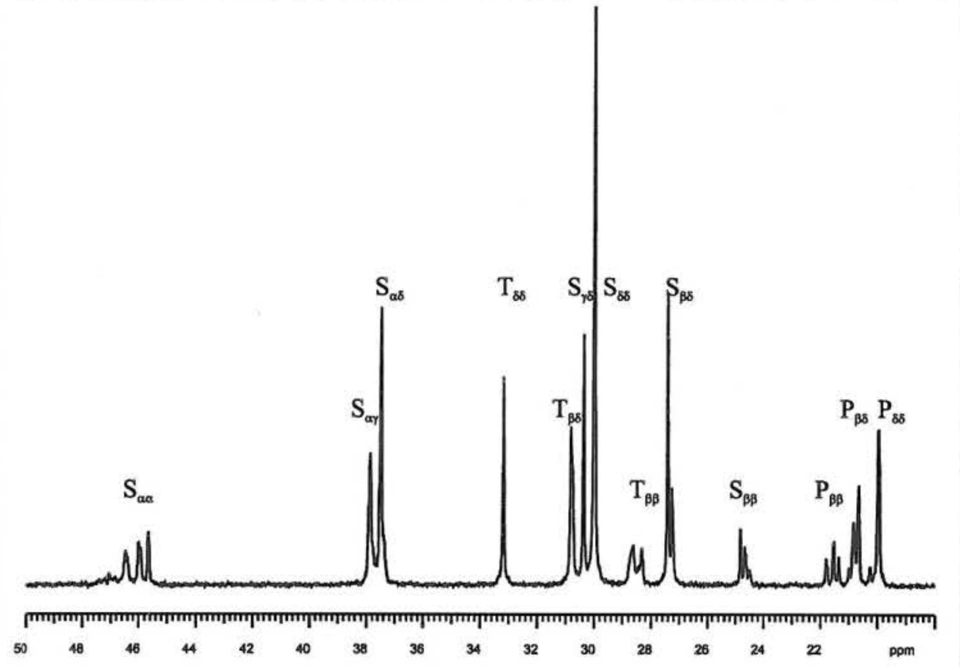

Figure 4.4: The quantitative 100MHz ^{13}C liquid-state NMR spectrum of the xylene soluble fraction I^*_{xs} dissolved in 1,2,4-trichlorobenzene and measured at 120°C. The experimental conditions are described in section 9.1.1.

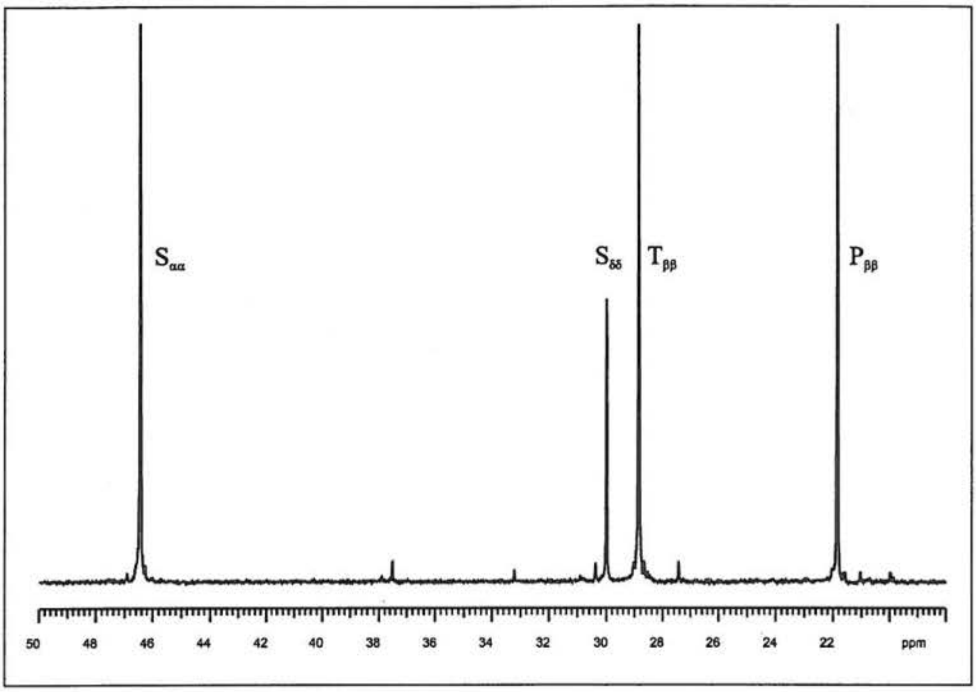

Figure 4.5: The quantitative 100MHz ^{13}C liquid-state NMR spectrum of the xylene insoluble fraction I^*_{xi} dissolved in 1,2,4-trichlorobenzene and measured at 120°C. The experimental conditions are described in section 9.1.1.

Comparing these spectra with those of the total sample (Figure 4.1) the signals of isotactic polypropylene - at 46.7 ppm for methylene, at 29.1 ppm for methine and at 21.8 ppm for methyl carbons - as well as long sequences of ethylene (30ppm) are dominant in the spectrum of the xylene insolubles. All the other signals of the total sample I* dominates in the spectrum of the xylene solubles. By integrating the spectra, the total ethylene content as well as the triads, the monomer and the sequence distribution can be calculated. The results are given in Table 4.5 for the xylene soluble fraction and in Table 4.6 for the xylene insoluble fraction.

4.3.4.1. The xylene soluble fraction

A comparison of the xylene soluble fraction of the different samples gives the following results: The weight percentage of ethylene in sample J_{xs} is lower than for the xylene solubles of the block copolymers. Also the triads EEE, PEE and EPE are lower, while the triad PPP is remarkably higher for J_{xs} compared with that fraction of the block copolymers. The total sample J has also only 3% ethylene and the ethylene is divided in short sequences as is known from section 4.3.3. Moreover, the random copolymer J has a small xylene soluble fraction of 7.7%. All this indicates that in the random copolymer the small amount of ethylene is randomly distributed or divided over many polypropylene sequences. Therefore real ethylene-propylene rubber can't be extracted from the sample J as is the case for the block copolymers. For the heterophasic block copolymers, H, I and I*, their xylene soluble fraction contains 40 to 50 percent ethylene and the monomer distribution of ethylene is comparable with that of propylene. Compared with the total sample (Table 4.3) the average sequence length of ethylene and surely of propylene is smaller for the xylene soluble fraction. These short sequences which can't crystallise are an indication for the crystallinity of 0% that was found for these fractions (section 3.4).

	H_{xs}	I_{xs}	I^*_{xs}	J_{xs}
E(wt%)	37.3	49.6	41.1	14.1
aver.seq.(E)	2.7	3.0	2.5	1.5
aver.seq.(P)	2.9	2.0	2.3	3.0
EEE (%)	19.5	26.5	19.1	3.1
PEE+EEP (%)	16.2	23.5	20.6	6.4
PEP (%)	7.9	7.5	9.5	9.7
EPE (%)	9.9	11.9	11.1	4.1
PPE+EPP (%)	18.5	19.0	22.8	22.6
PPP (%)	27.9	11.6	16.9	54.2
E_1 (%)	17.9	13.1	19.2	54.5
E_2 (%)	14.0	14.2	17.4	20.2
$E_{n\geq3}$ (%)	68.1	72.7	63.4	25.3
P_1 (%)	20.0	30.7	23.3	5.7
P_2 (%)	9.1	19.3	15.3	11.7
$P_{n\geq3}$ (%)	70.9	50.0	61.3	82.6

Table 4.5: Sequence analysis of the xylene soluble fraction of the samples. Equations 4.1 - 4.20 were used for the analysis. E(wt%) indicates the ethylene weight percentage and aver.seq. is the average sequence length.

Comparing the fractions of the three block copolymers, sample I_{xs} contains the longest average sequence length of ethylene, followed by sample H_{xs}. For it is also the total sample I that contains more long sequences of ethylene.

Knowing the differences in sequence between the fractions, it is possible to interpret the difference in the size of the fractions (section 3.3) in an exact way. Among the block copolymers, sample I* has the highest xylene soluble fraction or the highest fraction of true ethylene-propylene copolymer. As the true copolymer improves the impact strength of the bulk polypropylene, sample I* has the best impact strength (section 3.6).

4.3.4.2. The amorphous xylene soluble fraction

The fractionation of the xylene soluble fraction with acetone gives the oil fraction (low molecular weight fraction) and the amorphous fraction that contains the true ethylene-propylene copolymer. The sequence analysis of the amorphous fractions gives more or less the same results as the xylene soluble fractions. This means that the oil or low molecular weight fraction contains propylene as well as ethylene units.

4.3.4.3. The xylene insoluble fractions

The results of the sequence analysis of the xylene insoluble fraction are given in Table 4.6. The xylene insoluble fraction of the random copolymer J has less ethylene than those of the block copolymers. Besides sample J has in the xylene insoluble fraction remarkably much ethylene in a PEP sequence, while the block copolymers have their ethylene more in long sequences (EEE). Comparable results were found for the total sample, but now the difference is more pronounced.

The sample I_{xi} has its ethylene more in long sequences ($E_{n\geq3}$) compared with the two other block copolymer fractions, I^*_{xi} and H_{xi}. This causes a longer average sequence of propylene for sample I. The same results were found for the total samples.

Samples I^*_{xi} and H_{xi} have analogous results for the monomer distribution of propylene but their total ethylene content differ. It seems that the ethylene content in these fractions changes with the ethylene content of the total samples. Besides, the EEE triad changes with the total ethylene content.

	H_{xi}	I_{xi}	I^*_{xi}	J_{xi}
E(wt%)	5.0	9.5	10.0	2.6
aver.seq.(E)	5.3	8.8	8.3	1.1
aver.seq.(P)	51.7	91.4	59.3	32.8
EEE (%)	5.4	11.5	11.7	0.1
PEE+EEP (%)	1.2	2.5	2.2	0.7
PEP (%)	0.8	0.4	0.7	2.9
EPE (%)	1.0	0.8	1.1	0.0
PPE+EPP (%)	1.5	0.3	0.7	6.6
PPP (%)	90.1	84.6	83.7	89.8
E_1 (%)	10.5	2.7	4.5	75.7
E_2 (%)	4.4	1.8	8.5	13.2
$E_{n\geq3}$ (%)	85.1	95.5	86.9	11.1
P_1 (%)	1.1	0.9	1.3	0.0
P_2 (%)	1.7	0.6	2.0	1.8
$P_{n\geq3}$ (%)	97.2	98.5	96.7	98.2

Table 4.6: Sequence analyses of the xylene insoluble fraction of the different samples. Equations 4.1 - 4.20 were used for the analysis. E(wt%) indicates the ethylene weight percentage and aver.seq. is the average sequence length.

4.3.4.4. A comparison between the xylene insolubles and the xylene soluble fraction

By comparing the xylene soluble fraction (Table 4.5) with the xylene insolubles (Table 4.6) of the four samples, the weight percentage of ethylene is the highest for the xylene soluble fraction. On the other hand, when the amount of the two fractions is taken into account it is possible to calculate how the ethylene of the total sample is divided among the two fractions. The percentages are given in Table 4.7. Again, the results of the random copolymer distinguish from these of the block copolymers: the ethylene of sample J could not be extracted from the long polypropylene chains because the ethylene is distributed as short sequences among long polypropylene chains. The quantity of ethylene in such a chains is not sufficient to make them totally amorphous and soluble in xylene.

$\frac{E(wt\%)_A * F_A}{E(wt\%)_A F_A + E(wt\%)_B F_B}$	xylene insolubles (%)	xylene solubles (%)
H	43	57
I	49	51
I*	44	56
J	69	31

Table 4.7: The percentages of ethylene of the total sample found in a certain fraction. The results are given for the three block copolymers H, I and I* and the random copolymer J.

Among the block copolymer fractions, sample I* and H are alike with about 57% of ethylene for the xylene soluble fraction. Also their sequence distributions resemble, although the total amount of ethylene of sample H is smaller than for sample I*. Sample I contains more ethylene in its xylene insoluble fraction than sample I* and H. This agrees with the fact that sample I has longer ethylene sequences, which can crystallise and for that reason are not soluble in xylene.

Comparing the triad distribution of the xylene insolubles with the xylene soluble fraction (Table 4.5 and Table 4.6), it can be concluded the xylene insoluble fraction consists of presumably long propylene chains, while the xylene soluble fraction contains more short sequences of ethylene and propylene. Only long sequences of propylene and ethylene can crystallise and for that reason are insoluble in o-xylene.

4.4. Conclusions

A sequence analysis was done for the random (J) and block copolymers (H, I, I*) as well as for the fractions of the samples. The xylene insoluble fraction consists of long sequences ethylene and propylene, while the xylene soluble fraction mainly contains short sequences of ethylene and propylene. The amorphous fraction is the same as the xylene soluble fraction but without the oil or low molecular weight fraction and has more or less the same sequence distribution as the xylene soluble.

A clear difference is found between random and block copolymers. The random copolymer which is a true ethylene-propylene copolymer has its ethylene for more than 70% in a PEP sequence (E_1). On the other hand, in the block copolymers ethylene-propylene rubber particles are dispersed in a bulk polypropylene matrix and more than 70% of the ethylene is found in sequences of three or more ethylene units long ($E_{n\geq3}$). Moreover, the xylene soluble fraction of the random copolymer contains much less ethylene compared with the fractions of the block copolymers. The sequence distribution of ethylene and propylene in the xylene soluble fraction of the block copolymers resemble each other more or less, while for the fraction of the random copolymer there are much more long propylene sequences compared with long ethylene sequences. Thus for the random copolymer it is not possible to extract true ethylene-propylene copolymer like it is possible with the block copolymers. Yet, the percentage of the xylene soluble fraction is still used in industry as a parameter for the macroscopic properties. On has to be careful with the interpretation of the xylene soluble fractions because the fraction of a random copolymer does not contain the same polymer fraction as that of a block copolymer. Thus, the xylene soluble fractions of random and block copolymers may not be compared with each other. Moreover, there are also small differences between xylene soluble fractions of the block copolymers. Thus, a knowledge of only the amount of fraction can be misleading.

A comparison of the sequence of the block copolymers gave the following results:
The ethylene content as well as the sequence distribution of the copolymers are important with regard to their impact strength. The impact strength is better for samples with a high ethylene content and with the ethylene incorporated into short ethylene sequences. Samples that contain less ethylene but with the ethylene divided into short sequences have a better impact strength than samples with more ethylene that is incorporated in longer ethylene sequences. It has to be remarked here that the molecular weight and its distribution have also an influence on the macroscopic properties. Both parameters (molecular weight, the ethylene content and their distribution) affect the mechanical properties.

Finally, it can be concluded that the total ethylene content as well as the sequence distribution have to be known to get a better understanding of the macroscopic properties.

4.5. References

1.Doi, Y.; Ohnishi, R.; Soga, K.; Makromol. Chem., Rapid Commun., 4 (1983), 169.

2.Di Martino, S.; Kelchtermans, M.; J. Appl. Polym. Sci.; 56 (1995), 1781.

3. Aoki, A.; Polym. Commun.; 31 (1990), 130.

4. Higashi, F.; Kubota, K.; Sekizuka, M.; Goto, M.; J. Polym. Sci.: Polym. Lett. Edn.,18 (1980), 389.

5. Asakura, T.; Demura, M.; Nishiyama, Y.; Macromolecules, 24 (1991), 2334.

6. Carman, C.J.; Harrington, R.A.; Wilkes, C.E.; Macromolecules, 10(3) (1977), 536.

7. Cheng, H.N.; Macromolecules, 17 (1984), 1950.

8. Ray, G.J.; Johnson, P.E.; Knox, J.R.; Macromolecules, 10(4) (1977), 773.

9. Randall, J.C.; Hsieh, E.T.; Macromolecules, 15 (1982), 1584.

10. Zambelli, A.; Locatelli, P.; Provasoli, A.; Ferro, D.R.; Zambelli, Macromolecules, 13 (1980), 267.

11. Hayashi, T.; Inoue, Y.; Chûjô, R.; Asakura, T.; Polymer, 29 (1988), 138.

12. Kakugo, M.; Naito, Y.; Mizunuma, K.; Miyatake, T.; Macromolecules, 15 (1982), 1150.

13. Axelson, D.E.; Mandelkern, L.; Levy. G.C.; Macromolecules, 10(3) (1977), 557.

14. Inoue, Y.; Nishioka, A.; CHûjô, R.; Die Makromolekulare Chemie, 168 (1973), 163.

15. Randall, J.C.; J. Polym. Sci.: Polym. Phys. Edn., 14 (1976), 1693.

16. Bovey, F.A.; "Nuclear magnetic Resonance Spectroscopy", Academic Press, San Diego, California, 1988.

17. Schaefer, J.; Natusch, D.F.S.; Macromolecules, 5(4) (1972), 416.

18. De Pooter, M.; Smith, P.B.; Dohrer, K.K.; Bennett, K.F.; Meadows, M.D.; J. Appl. Polym. Sci., 42 (1991), 399.

5. HIGH RESOLUTION ^{13}C SOLID-STATE NMR

5.1. Introduction

The study of polymers in an aggregation state in which they are mostly used; i.e. the solid state can give information about the morphology of the polymer. With solid-state NMR it is possible to investigate the mobility of the polymer chains, molecular domains, crystallinity,...

With an industrial NMR (^{1}H wideline NMR) one composite decay curve can be obtained and this curve contains the information of the mobility of all proton atoms of the polymer. For the ethylene-propylene copolymers the relaxation of the bulk polypropylene and the ethylene-propylene rubber is summed up in one relaxation decay. So the analysis of such decay curve and the interpretation can be very complex. Complexity can be reduced by ^{13}C CP/MAS solid-state NMR, by which the relaxation of each chemical shift selective signal in the ^{13}C NMR spectrum can be determined. This means that in commercial ethylene-propylene copolymers the relaxation of the bulk polypropylene and the true ethylene-propylene copolymer can be determined separately and this can be useful for understanding the results of an industrial NMR.

To get a better understanding of the spectrum of the ethylene-propylene copolymers, a polypropylene sample was used as a reference. The xylene soluble and xylene insoluble fractions were also used for comparison yielding the relaxation of the ethylene-propylene rubber and the bulk polypropylene separately and to study the influence of each other on the relaxation times in the total sample.

In the literature a lot of articles describe the relaxation behaviour of polypropylene,[1-7] while only little information is available about ethylene-propylene copolymers.[8-11] Attention will be focused here on the ^{13}C solid-state NMR spectrum and on some relaxation times.

5.2. The MAS and CP/MAS spectra of polypropylene and ethylene-propylene random and block copolymers.

Figure 5.1 shows a quantitative MAS spectrum of an ethylene-propylene heterophasic copolymer at room temperature. It is obvious that a chemical shift assignment of the complex MAS spectrum simply can't be copied from the liquid-state spectrum (Figure 4.1). The differences in chemical shift can be caused by changes in bond angles, conformations and chain packing. Moreover the temperature plays an important role on the line width and the chemical shift of the chemically distinct carbons. In order to get a better understanding of the spectrum of the copolymer, a polypropylene homopolymer and the xylene soluble fraction (true ethylene-propylene copolymer) of the heterophasic copolymer were taken for comparison and the influence of the temperature on these spectra was studied. The influence of the thermal history of the copolymers on their spectrum will also be discussed. By making use of the different relaxation parameters of the phases in the polymer, it is possible to emphasise the mobile or the rigid phase of the polymer in its solid-state NMR spectrum.

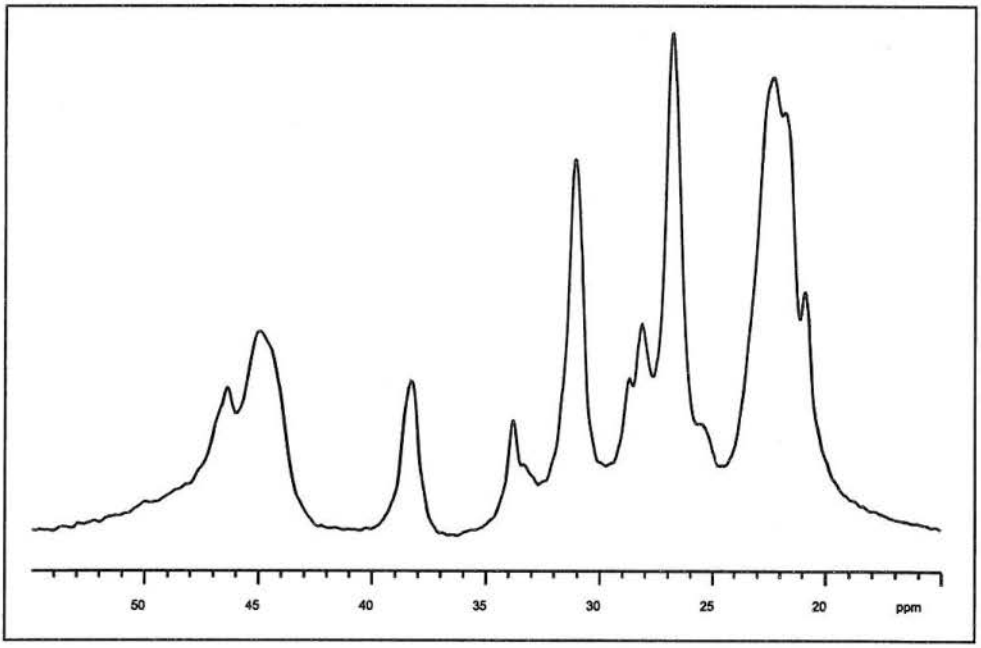

Figure 5.1: A quantitative ^{13}C DD/MAS spectrum of the block copolymer I* at room temperature. A preparation time of 120s was used.

5.2.1. The influence of the temperature on the ^{13}C MAS spectrum and a chemical shift assignment

5.2.1.1. The influence of the temperature on the ^{13}C MAS spectrum of polypropylene

Figure 5.2 shows the quantitative MAS spectra of the polypropylene sample B measured at temperatures between 30 and 90°C. The methylene, methine and methyl signal have a chemical shift around respectively 45-47ppm, 27-29ppm and 20-23ppm. Comparable spectra as a function of the temperature were found by Saito et al.[9] but he studied a polypropylene sample which was purified by Soxhlet extraction (with toluene) to remove low molecular weight compounds and the atactic polypropylene. Our polypropylene sample was not fractionated with the aim to use it as a reference for the copolymers which couldn't be fractionated to remove the low molecular weight without removing any ethylene-propylene copolymer.

In Figure 5.2 at higher temperature a second signal appears for the methine and methylene group associated with a decrease in bandwidth. The downfield signals have their chemical shift at high temperature very close to those of the isotactic sequence in solution-state NMR. That is why this resonance can be assigned to the mobile methylene and methine component. The upfield signals are associated with a more rigid phase.[9] For the methyl carbons one can not distinguish between mobile and rigid CH_3 carbons. This can be explained by the fast rotation around its C_3 axis which is present in the mobile (amorphous) as well as the rigid (crystalline) domains. For the chemical shift assignment one has to be careful with the use of words as 'amorphous' and 'crystalline' because at lower temperatures the signal at 44.9ppm does not only shows methylene carbons of the crystalline domain but also of the amorphous domain. At room temperature the mobility of the atoms in the amorphous domain is restricted since it is only 20°C above the glass transition temperature. Between the crystalline and amorphous domain a transition region should be considered, where the crystalline form is less perfect and the mobility of the segments is less restricted than in the crystalline domain above room temperature. At temperatures close to the glass transition temperature, the segments in the transition region will act more like the crystalline domain and they will give a signal with comparable chemical shift. At higher temperatures the segments in the amorphous domain have a higher mobility and influence the segmental motion in the transition region. At these temperatures the amorphous and transition regions contribute both to the mobile signals. So 'mobile' and 'rigid' CH_2 and CH signals would be more accurate although 'crystalline' and 'amorphous' are commonly used.[9,12]

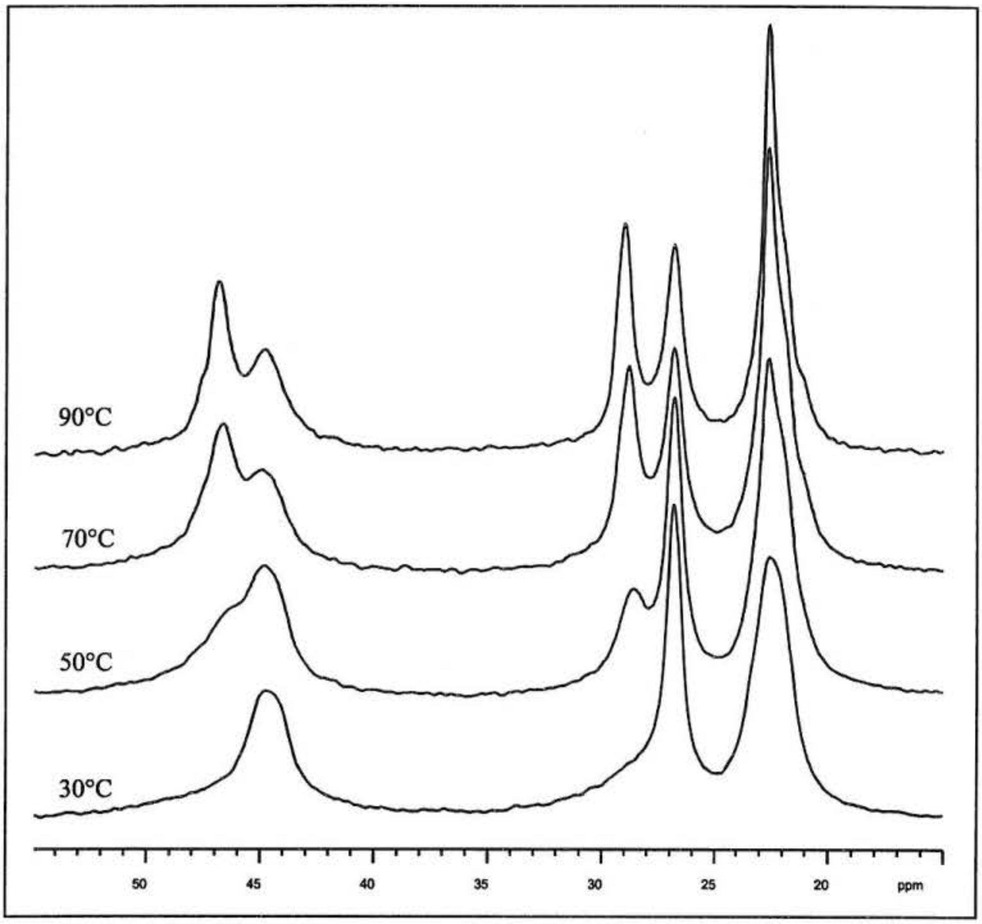

Figure 5.2: The quantitative 100MHz ^{13}C DD/MAS spectra of the polypropylene sample B as a function of the temperature. At 30°C a preparation time of 120s is used and at 90°C a time of 100s, depending on the T_{1C} relaxation times (section 5.3.3.).

To study the line width as a function of the temperature, a deconvolution of the signals is needed because of overlap. As is mentioned in the article of Saito et al.[9] the methylene signal can be divided into three components: the crystalline, the transition region and the amorphous region. According to Saito et al. the transition region has a chemical shift that is lying in between the two chemical shifts of the α-crystalline form. For the analysis he used a highly crystalline polypropylene sample which showed a splitting of the methylene and methyl signal due to the α-crystalline form. Our sample, on the other hand, was not annealed at such high temperatures and does not show the splitting of the signals. From WAXS measurements (section 3.4.2) it is known that sample B has a α crystalline form although it is less perfect than the sample used by Saito et al. This implies that the difference between the crystalline and the transition region becomes less and a separation with deconvolution is impossible. Transition regions are small and consist of segments with a wide range of mobilities. Their mobility varies from that of the mobile amorphous chains to the mobility of the rigid crystalline chains. Is it therefore realistic to present the transition region as a signal separated from the crystalline and the amorphous region? For our sample it is better to use two components for the methylene signal: a mobile component around 47ppm and a rigid component around 45ppm. By using this deconvolution, the line width and the peak position of the different signals can be analysed. The line width of the signals is given in Figure 5.3 as a function of the temperature.

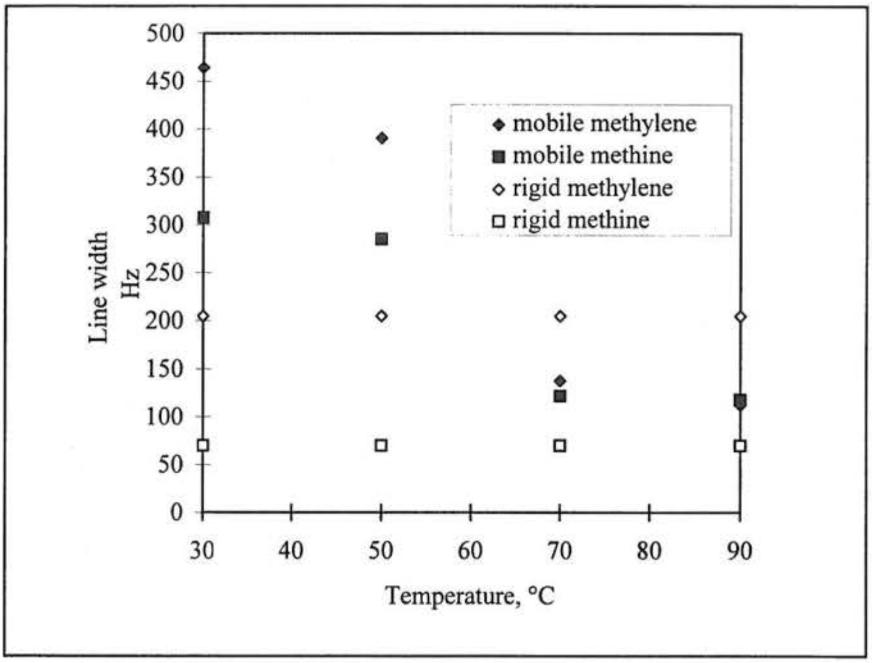

Figure 5.3: The line width of the mobile and rigid methylene and methine signal of the quantitative ^{13}C DD/MAS spectrum of the polypropylene sample B as a function of the temperature (Figure 5.2).

The line width of the mobile component reduces and this is an indication for the glass transition temperature. To produce sufficiently narrow ^{13}C lines for backbone segmental motions in amorphous polymers, the temperature has to be increased to 50°C or more above the glass transition temperature.[13] The dipolar interactions between carbons and protons and the chemical shift anisotropy are averaged out by molecular motions and the line width is reduced compared with spectra near the glass transition temperature. On the other hand, the line width of the rigid component stays constant over the temperature range. This component mainly consists of crystalline polypropylene, of which the mobility stays constant up to the melting temperature.

As is shown in Table 5.1 the chemical shift differences between the mobile and rigid components increase with the temperature. It is the mobile component that shifts downfield because the higher mobility of the amorphous polymer chains at higher temperatures cause less gauche interactions. Eventually near the melting temperature the amorphous carbons will reach the chemical shift of the signals of the liquid-state spectrum.

Temperature (°C)	$\Delta\delta_{CH2}$ (ppm)	$\Delta\delta_{CH}$ (ppm)
30	-	-
50	1.69	1.87
70	2.09	2.03
90	2.12	2.2

Table 5.1: Chemical shift difference ($\Delta\delta$) between the mobile and the rigid signal of the MAS spectrum (Figure 5.2) of polypropylene sample B as a function of the temperature.

5.2.1.2. The influence of the temperature on the solid-state spectrum of true ethylene-propylene copolymer

The MAS spectrum of the ethylene-propylene copolymer sample I^*_{xs} as function of the temperature is given in Figure 5.4. A rough chemical shift assignment was already given by Ziegler et al.[14] for a polypropylene homopolymer blended with ethylene-propylene copolymer. For the true ethylene-propylene copolymer I^*_{xs} without large signals of polypropylene a more detailed chemical shift assignment was possible (Figure 5.4) by comparing the high temperature spectra with the liquid-state NMR spectrum (Figure 4.4). At 90°C the signals of the different sequences are resolved in the MAS spectrum and the spectrum becomes liquid-like. At low temperature the signals overlap. The line width decreases with increasing temperature and this is shown for two separated signals in Table 5.2. The line width of the signals is smaller for the copolymer than for the homopolymer (Figure 5.3). This can be caused by the lower glass transition temperature of the copolymer (section 3.5) whereby the polymer chains have a higher mobility. Line broadening due to incomplete motional narrowing has become less important.

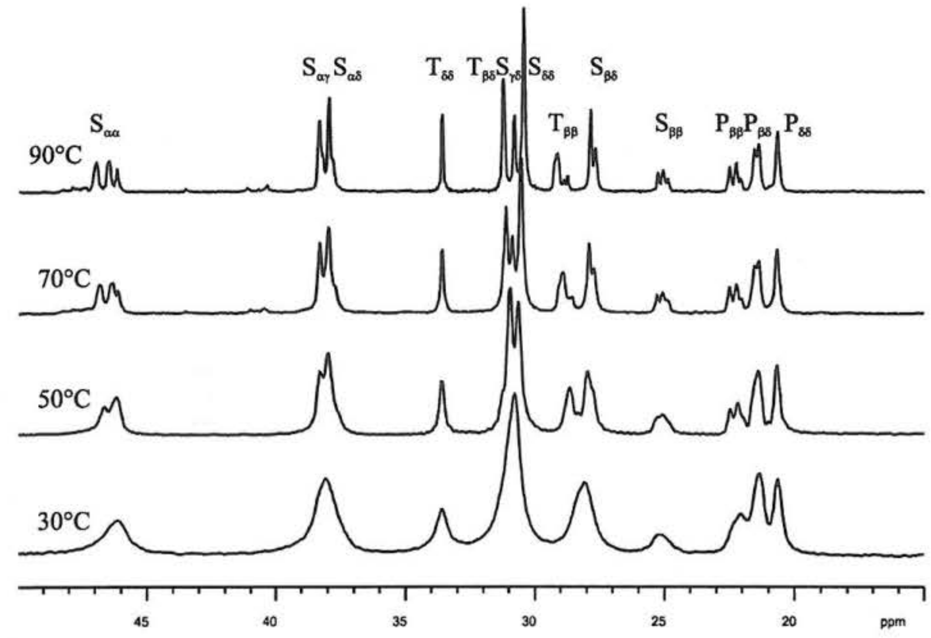

Figure 5.4: Quantitative ^{13}C DD/MAS spectra of the ethylene-propylene copolymer I^*_{xs} measured at temperatures between 30 and 90°C. A preparation time of 5s was used at all temperatures. A detailed chemical shift assignment is given.

Chemical shift (ppm)	Assignment	Line width (Hz)			
		30°C	50°C	70°C	90°C
20.8	$P_{\delta\delta}$	40.1	36.3	15.4	13.2
33.1	$T_{\delta\delta}$	67.7	41.4	13.9	10.2

Table 5.2: The influence of the temperature on the line width (Hz) of two signals in the ^{13}C MAS NMR spectrum of an ethylene-polypropylene copolymer, I^*_{xs} (Figure 5.4).

5.2.1.3. The influence of the temperature on the solid-state NMR spectrum of ethylene-propylene heterophasic copolymers and an accurate chemical shift assignment.

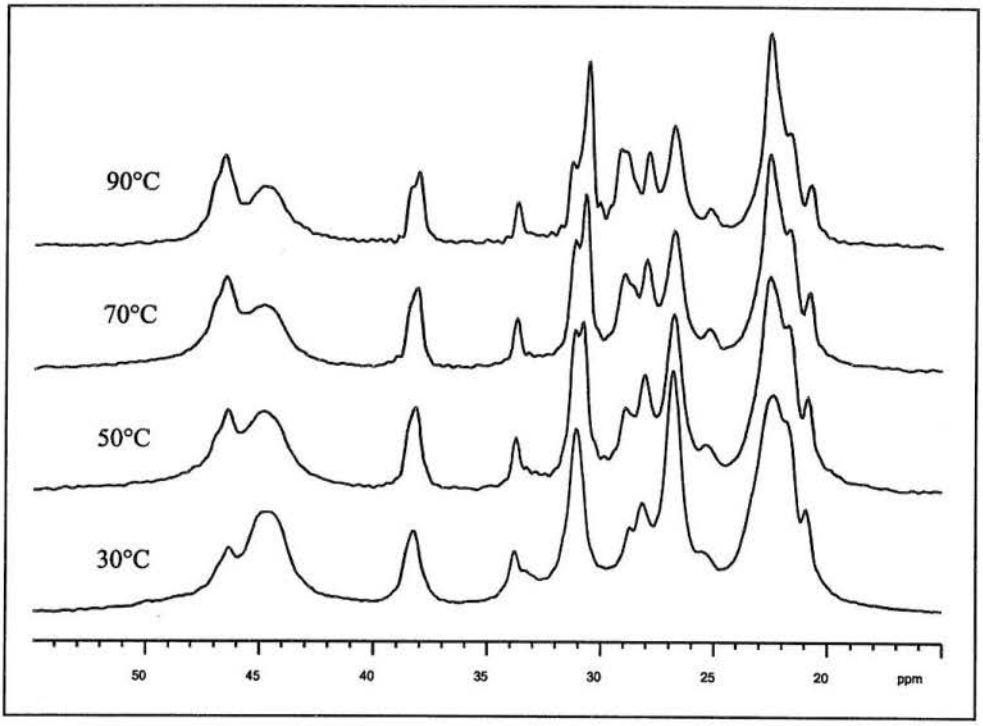

Figure 5.5: The 100MHz ^{13}C DD/MAS spectra of the ethylene-propylene heterophasic copolymer I* as a function of the temperature. At 30°C a preparation time of 120s was used and at 90°C a time of 100s.

The quantitative ^{13}C MAS spectrum of an ethylene-propylene heterophasic copolymer is given in Figure 5.5. These spectra are a superposition of the spectrum of the true ethylene-propylene copolymer and the polypropylene spectrum with different signals for the mobile and rigid methylene and methine carbons. In addition, the copolymer also shows a different signal for crystalline and amorphous polyethylene. The crystalline polyethylene has an all-trans conformation while the amorphous regions are more or less composed of equal amounts of gauche and trans bonds and therefore be subject to γ-gauche shielding.[15-17] Some signals shift downfield, like $S_{\alpha\alpha,\ \mathrm{mobile}}$ (PPPPP), $S_{\alpha\alpha,\ \mathrm{mobile}}$ (EPPE) (PPPE + EPPP) and $T_{\beta\beta,\ \mathrm{mobile}}$ as a function of the temperature. This can again be explained by the γ-gauche effect. The crystalline isotactic polypropylene chain adopts a ...(gt)(gt)(gt)... conformation[15] which induces an upfield shift for the signal of crystalline polypropylene compared to the signal of the amorphous polypropylene. An accurate chemical shift assignment of the solid-state spectra of ethylene-polypropylene block copolymers is given in Table 5.3. It has to be noted that a different chemical shift is found for the methylene carbon ($S_{\alpha\alpha,a}$) of a long mobile propylene sequence PPPPP at 46.7ppm and for the methylene carbon of the sequence EPPE and PPPE at 46.0ppm. The methylene signal of the PPPPP sequence is shown in Figure 5.5 as a shoulder on the other signal at 46.0ppm.

Chemical shift (ppm)	assignment		description
46.7^*	$\underline{S_{\alpha\alpha,a}}$	PPPP	polypropylene, mobile (amorphous)
46.0	$S_{\alpha\alpha}$	PPPE, EPPE	
44.9	$\underline{S_{\alpha\alpha,c}}$	PPPP	polypropylene, rigid (crystalline)
38.6	$S_{\alpha\gamma}$	PEP.+.PEP	
38.2	$S_{\alpha\delta}$	$PEE_{n\geq1}+E_{n\geq1}EP$	
33.8	$S_{\delta\delta,c}$	$(EEE)_{n\geq1}$	polyethylene, rigid (crystalline)
33.1	$T_{\delta\delta}$	EPE	
31.3	$T_{\beta\delta}+S_{\gamma\gamma}$	PPE+PEEP	
31.3	$S_{\gamma\delta}$	$PEEE_{n\geq1}$	
30.7	$S_{\delta\delta,a}$	$(EEE)_{n\geq1}$	polyethylene, mobile (amorphous)
29^*	$\underline{T_{\beta\beta,a}}$	PPP	polypropylene, mobile(amorphous)
28.0	$S_{\beta\delta}$	$PEE_{n\geq1}$	
26.8	$\underline{T_{\beta\beta,c}}$	PPP	polypropylene, rigid (crystalline)
25.2	$S_{\beta\beta}$	PEP	
22.6	$\underline{P_{\beta\beta}}$	PPP	polypropylene, rigid and mobile
21.7	$P_{\beta\delta}$	PPE	
20.8	$P_{\delta\delta}$	EPE	

Table 5.3: An accurate chemical shift assignment of an ethylene-propylene heterophasic copolymer. The underlined signals are also found for polypropylene. *: these signals are temperature dependant and can only be seen clearly above 50°C.

A comparison of the line width of the different signals as a function of the temperature has become more complex than for the homopolymer and the true ethylene-propylene copolymer because of the overlap of the signals. For some signals the results are given in Table 5.4.

Chemical shift (ppm)	assignment	30°C	50°C	70°C	90°C
20.8	$P_{\delta\delta}$	52	45	35	32
21.7	$P_{\beta\beta}$	158	120	96	79
44.9	PPPP, rigid	205	209	209	200
46.0	PPPE+EPPE	97	103	52	56
46.7	PPPP, mobile	409	400	160	132

Table 5.4: The line width (Hz) of the signals of the ethylene-propylene heterophasic copolymer I* in a 100MHz ^{13}C DD/MAS spectrum as a function of the temperature (Figure 5.5).

The line width of the signal of the mobile or amorphous domain decreases as the measuring temperature increases. This is comparable with polypropylene and the ethylene-propylene copolymer. The line width of the rigid methylene signal at 44.9ppm stays constant over the whole temperature range as was found for polypropylene. The mobile methylene signal at 47ppm shows the same reduction in the line width. This indicates that the ethylene-propylene copolymer domains in ethylene-propylene heterophasic copolymers do not affect the chain mobility of the polypropylene part. The same information was found with the T_g measurements: a separated glass transition temperature was detected for the ethylene-propylene domains and for the bulk polypropylene.

The copolymer signals behave like the true ethylene-propylene copolymer although the signals at 90°C are broader. This can be explained by the restriction of the mobility of the chains due to the immobilisation of the homopolymer matrix.

5.2.1.4. Conclusions

It can be concluded that the spectrum of an ethylene-propylene copolymer is a superposition of the spectrum of polypropylene and that of true ethylene-propylene copolymer. The methylene and methine signals of the bulk polypropylene split in two signals at temperatures above 50°C and this results in a rigid and mobile signal. The line width of the signals of the amorphous polypropylene and the true ethylene-propylene copolymer decreases with the temperature while the line width of the crystalline domain doesn't change between 20 and 90°C.

5.2.2. Selectivity of the MAS and CP/MAS spectrum with regard to the mobile and rigid phase in an ethylene-propylene copolymer.

In order to separate the signals of the rigid and mobile phase of the polymer, MAS as well as CP/MAS spectra can be useful if attention is paid to specific relaxation parameters.

5.2.2.1. Selectivity of the ^{13}C MAS spectrum of ethylene-propylene copolymers

The carbon-13 signal in a normal MAS experiment is generated directly after the 90° pulse, like in liquid-state NMR. The selectivity of such a MAS spectrum is based on differences in the longitudinal relaxation time, T_{1C}. The carbon-13 spins which have T_{1C} values shorter than the waiting time between two pulses in a MAS experiment, can be seen in the MAS spectrum. In general, in a MAS experiment with a short delay time signals from amorphous or non-crystalline regions in polymers are emphasised due to their short T_{1C} time.[19] The T_{1c} relaxation times in rigid crystalline solids can be very long and preparation times of more than 100s can be needed to show the signals of the rigid phase.[20,21] Such a long preparation time was used for the spectra shown in previous section 5.2.1.

The T_{1C} relaxation times of the copolymers are discussed in detail in section 5.3.3 and from these results it is known that a MAS spectrum with a preparation time of 3 seconds suppresses the rigid component of the copolymer. The MAS spectra of ethylene-propylene block and random copolymers, measured at room temperature with a preparation time of 3 seconds, are shown in Figure 5.6. Because the T_{1C} relaxation time of the mobile polypropylene carbons and the ethylene-propylene rubber signals are all less than 1 second, both are seen in the MAS spectrum. The methyl signal is very intense in comparison with the other signals because the methyl group has a high mobility even in the crystalline domain. A separation between methyl groups of the rigid and mobile domains is hence not possible. Differences in the MAS spectrum of the ethylene-propylene copolymers can be found: First of all, the spectrum seems to be influenced by the total ethylene content. The random copolymer J, with only three percent ethylene shows less intense signals of the short sequences of ethylene and propylene compared with the block copolymers. Secondly, the ration of the intensity of the signals is also in agreement with the xylene soluble fraction. The intensity of the methylene signals of the PPPE and EPPE sequences (46.0ppm) to that of a

PPPP sequence (44.9ppm) is higher for the copolymers with a higher xylene soluble fraction (Chapter 3.3), like sample I*.

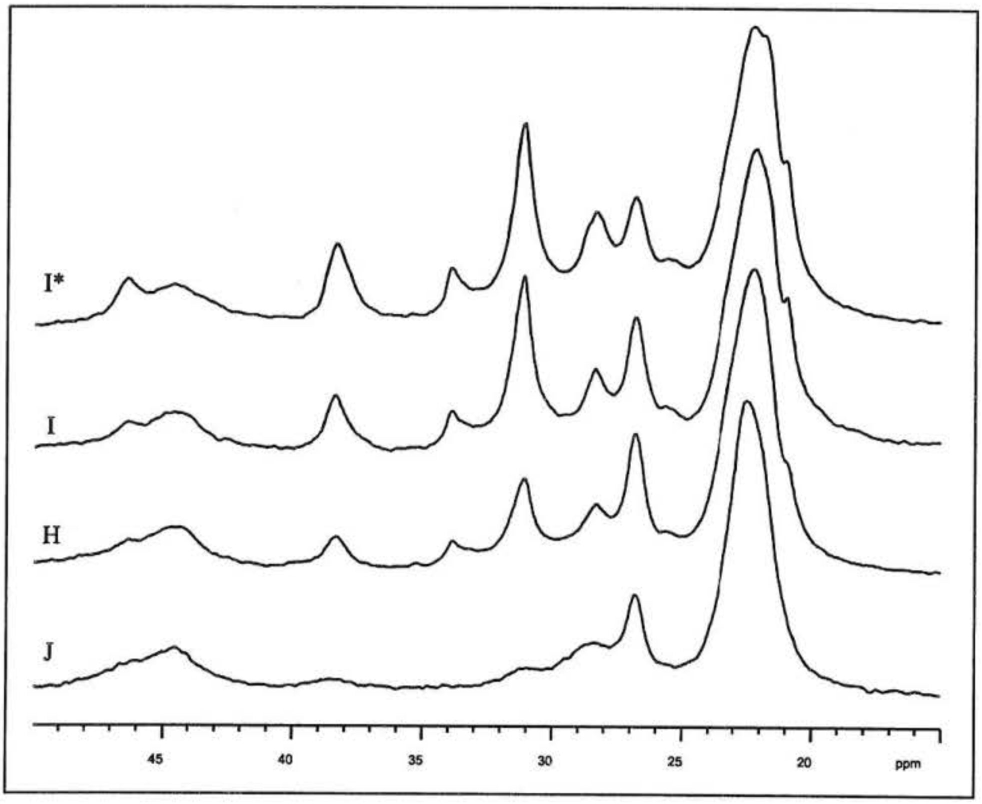

Figure 5.6: 100MHz ^{13}C DD/MAS spectra of the ethylene-propylene block (H, I, I*) and random (J) copolymers, measured at room temperature. A preparation time of 3 seconds was used.

It is important to know the mobile fraction of the sample with respect to the mechanical properties. With the short-delay MAS spectra it is possible to make a distinction between mobile and rigid methylene and methine carbons however not between methyl carbons of the rigid and mobile domain. Thus T_{1C} is not a phase property for these ethylene-propylene specimens.

The mobility of the polymer chains is analysed by relaxation times which in general are determined by CP/MAS experiments rather than by MAS spectra. CP/MAS spectra, which mostly emphasise the rigid component, has gain importance.

5.2.2.2. The influence of the length of the contact time on CP/MAS spectra

The intensity of a signal in a ^{13}C CP/MAS spectrum is influenced by the length of the contact time. During the contact time there is an increase in carbon magnetisation by polarisation transfer from the protons ($1/T_{CH}$) and at the same time a depletion of the carbon and proton magnetisation by proton spin-lattice relaxation processes ($1/T_{1\rho H}$) with rates depending on the mobility of the atoms in the sample. The increase in magnetisation, determined by the T_{CH} cross polarisation time, is mainly dependant on the strength of the C-H dipolar interaction. This means that a rigid region will transfer the magnetisation from proton to carbon more easily than mobile regions. This implies that rigid regions will have shorter T_{CH} times than more mobile regions. Cross polarisation is a heteronuclear diffusion process of magnetisation. The optimal contact time will be different for domains with different mobilities. To find this optimal contact time one generally makes use of a contact time study, in which CP/MAS spectra with varying contact times are recorded. For the polypropylene homopolymer sample B a contact time of 1ms is optimal at room temperature, while for the ethylene-propylene rubber sample, I^*_{xs} a contact time of 2ms gives the most intense signals. This means that only a small difference in optimal contact time is found between the bulk polypropylene and the ethylene-propylene rubber in copolymer I* at room temperature and this difference cannot be used to emphasise the mobile or the rigid phase.

When the temperature is elevated to 90°C, the mobility of the ethylene-propylene rubber is increased and this high mobility averages the static dipolar interactions necessary for the magnetisation transfer. The less efficient dipole-dipole interactions or heteronuclear spin diffusion causes a slower increase in magnetisation of the carbon atoms during cross polarisation. The optimum contact time of the ethylene-propylene rubber is *13ms* at 90°C instead of *2ms* at room temperature. This means that there is an important increase in molecular mobility. Measuring the ethylene-propylene block copolymer I* with a contact time of 13ms at 90°C emphasises the mobile part of the polymer (Figure 5.7). This is quite remarkable because in general the CP/MAS spectra are used to promote the rigid component and to reduce the mobile one. Short contact times of a few microseconds favour the rigid crystalline polypropylene as was found for the polypropylene homopolymer sample B. For this sample, the optimal contact time for the rigid crystalline fraction did not change with the temperature. In the temperature range of 20 to 90°C the mobility of the atoms of the crystalline lattice does not change until the melting temperature. Measuring the polypropylene sample with a contact time of 13ms the intensity of the mobile component has increased compared with the short contact time spectrum. The difference in optimal contact time for the rigid polypropylene and the ethylene-propylene copolymer at high temperature is very interesting in regard to the measurement of the relaxation times of the signals of the copolymer. From the liquid-state spectra, it is known that the signals of the ethylene-propylene copolymer part are small in comparison with the bulk polypropylene. Thanks to the long optimum contact time at 90°C it is possible to emphasise the mobile ethylene-propylene copolymer and to reduce the large signals of the bulk polypropylene in the ethylene-propylene block copolymers. In this way the relaxation times of the ethylene-propylene rubber in the ethylene-propylene heterophasic copolymer can be determined more accurately.

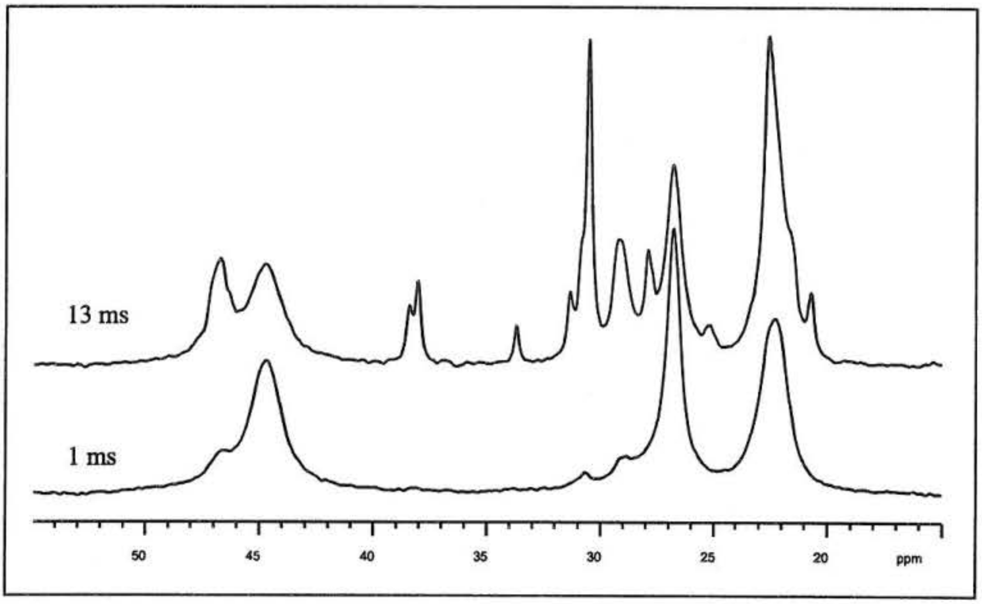

Figure 5.7: The 100MHz ^{13}C CP/MAS NMR spectrum of sample I* at 90°C with a contact time of 1ms and of 13ms. A preparation time of 4ms was used.

5.2.3. The influence of the thermal pretreatment of the samples on the solid-state NMR spectrum

The thermal history of a polymer sample can have a important influence on its solid-state NMR spectrum because the percentage crystallinity and the crystalline form depends on the thermal pretreatment which has an effect on the NMR spectrum.

For the study of the ethylene-propylene heterophasic copolymers, a polypropylene sample was used as a reference.

5.2.3.1. The influence of the annealing temperature on the spectrum of polypropylene

Isotactic polypropylene is a polymorphic polymer. The predominant and most stable form is the α-monoclinic crystalline form. The ^{13}C high-resolution NMR spectrum of the α-crystalline form of polypropylene shows a splitting of the CH_2 and the CH_3 signal due to inequivalent local sites, A and B produced by pairing of helices of opposite handedness (Figure 3.3). The ratio of the intensities of the downfield to the upfield signal is about 2:1 for both carbon types.[22] Caldas et al.[12] also found a splitting of the methine signal although the signals are less resolved compared with the methylene and methyl signal. The splitting of the signals of our polypropylene sample A can be seen in Figure 5.8. This figure shows the CP/MAS spectra of a polypropylene film quenched in ice-water and annealed at different temperatures as was already described in section 3.4.

To compare the spectra of the samples with a different thermal pretreatment a deconvolution of the spectrum was performed. The amorphous signal is very broad at room temperature (Figure 5.3) and in a CP/MAS spectrum with a contact time of five milliseconds this signal must be weak because of the fast $T_{1\rho H}$ relaxation and the slow increase in magnetisation as will be discussed later. Eventually, two components were used to describe the methylene signal. For the methine signal only one component was used because the two signals, due to the α-crystalline form, are less resolved. Two components were needed for the best annealed samples. For the methyl signal at least two components had to be used because of the two signals of the crystalline form. It seemed that two components were not enough to describe the methyl signal exactly. The downfield signal is composed of two signals at 22.8 and at 23.4ppm which gives a better deconvolution. The signal at 23.4ppm was described by Caldas et al.[12] as an intermediate environment which is formed during the initial stages of crystal reorganisation and disappears when the final crystalline state is attained.

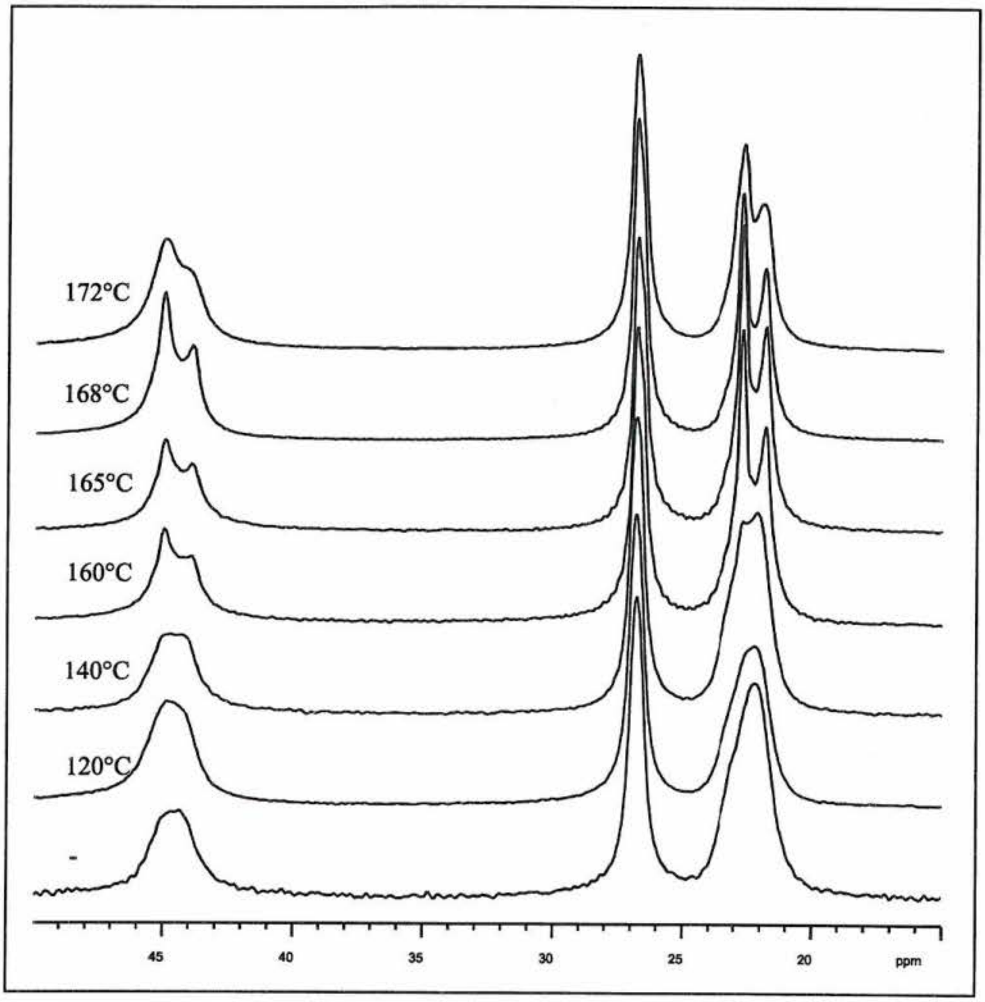

Figure 5.8: 100MHz ^{13}C CP/MAS NMR spectra at room temperature utilising a cross-polarisation time of 5ms for the quench-cooled iPP samples A annealed at various temperatures for 1 hour: 172, 168, 165, 160, 140, 120°C and no annealing. A preparation time of 4s is used.

A deconvolution of the samples annealed at different temperatures showed that the line width, the peak position and the ratio of the signals were influenced by the annealing temperature. The effect of the annealing temperature on the line width is shown for the downfield methylene and the midfield methyl signals in Figure 5.9.

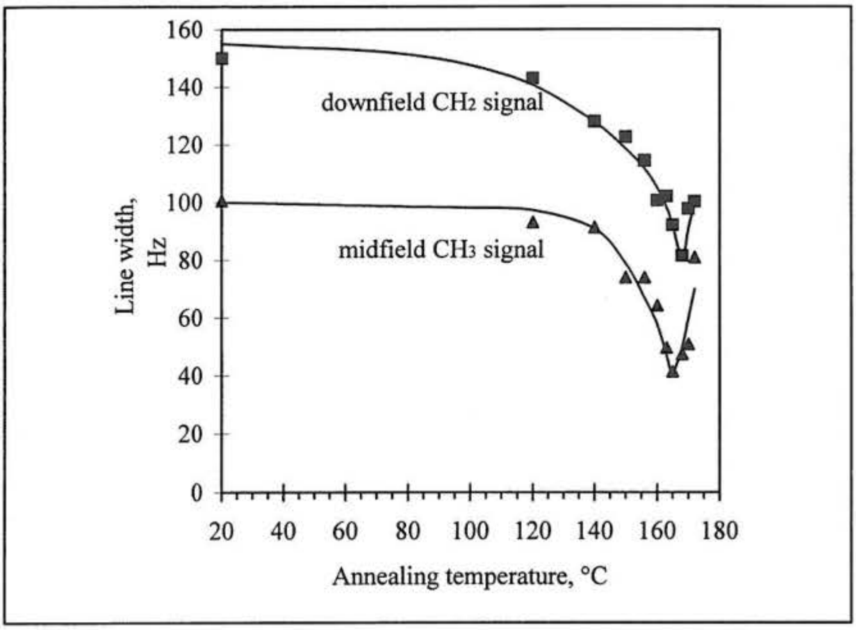

Figure 5.9: The line width of the downfield methylene and midfield methyl signals of the ^{13}C CP/MAS spectra of the polypropylene sample A after annealing at different temperatures (Figure 5.8). The influence on the upfield signal was less: for the methylene signal the line width changed from 113Hz to 94Hz and the line width of the methyl signal between 99 and 65Hz.

At elevated annealing temperatures the line width of the peaks decreases as a function of the annealing temperature and the minimum is reached at 165°C for the methyl signal and at 168°C for the methylene signal. This means that around that temperature the polymer chains get just enough energy to organise themselves as good as possible in the α-crystalline form which is the most stable crystalline form of polypropylene. At lower temperatures the polymer chains have less kinetic energy to organise themselves which implicates a less perfect crystalline form and broader signals. At temperatures higher than 168°C, the polymer starts to melt which causes a distribution of distances between the helices after cooling down to room temperature. The effect on the line width is less pronounced for the upfield signal of methylene and methyl carbons. This can be explained by the fact that the downfield signals represent carbon atoms at that site of the helix (A site) that is only 0.528nm separated from an helix axis of opposite handedness (Figure 3.3). The upfield signal represents carbon atoms at that site of the helix (B site) that is 0.614nm apart from other helices. When the crystalline lattice is less perfect the interhelical separation is larger, surely for the A site. For quenched samples, the splitting can even be absent. It has been suggested that the morphology of quenched samples is composed of an α-monoclinic phase where inequivalent distances within the unit cell do not exist. This explanation requires that the inter-helical distances in the unit cell are larger than in the stable α-monoclinic crystal.[22] When the crystalline lattice has a high perfection the interhelical distances will be inequivalent and at the A site it will reach the smallest separation of 0.528nm.

The chemical shift difference between the two splitted signals of the α-crystalline form also depends on the annealing temperature (Table 5.5). The chemical shift difference of the midfield to upfield signal ranges from 0.42 ppm for non-annealed samples to 0.86 ppm for the best annealed samples around 168°C. It is the low field signal that shifts downfield.

annealed at (°C)	chemical shift difference (ppm)	ratio of the α-form
-	0.42	0.90
120	0.52	0.81
140	0.71	0.85
150	0.75	0.84
156	0.75	0.84
158	0.78	0.82
160	0.81	0.81
165	0.82	0.93
168	0.86	1.00
170	0.79	0.81
172	0.73	0.80

Table 5.5: The chemical shift difference and the ratio of the areas of the two signals of the ^{13}C CP/MAS spectrum (Figure 5.8: at room temperature) of the α-form of the methyl signal of the polypropylene sample A annealed at different temperature. Comparable results were found for the methylene signal.

In addition to the chemical shift and the line width, also the area of the two signals of the α-form change with the annealing temperature. Consider the area of the methyl signal: the midfield signal increases with increasing annealing temperature (Table 5.5). At an annealing temperature of 120°C the ratio of the midfield to the upfield peak equals 0.81 while for the sample annealed at 168°C the ratio is 1.00. Again, it can be concluded that an annealing temperature of 168°C gave the most perfect crystalline form. It has to be noted here that in theory, this ratio equals two. Two explanations can be found: The α-crystals are not perfect in our samples due to molecular weight distribution and polymer chain ends. Another possibility is that the amorphous part of the sample has a chemical shift of around 21.9ppm which overlaps with the upfield signal of the α-form. For the calculation of the ratio a too high area was maybe taken for the upfield signal

5.2.3.2. The influence of the annealing temperature on the spectrum of ethylene-propylene copolymers.

Ethylene-propylene block copolymer are composed of a propylene matrix with domains of 'real' ethylene-propylene copolymers. Annealing the polymer at different temperatures can have an influence on the crystallisable polypropylene and on the crystallisable polyethylene. The spectra of the copolymer I annealed at different temperature are given in Figure 5.10.

Annealing the copolymer has the same influence on the bulk polypropylene as for pure polypropylene (Figure 5.8): the line width of the signals of the bulk polypropylene also shows a minimum at 168°C (Table 5.6). Concerning the peak position and the ratio of the crystalline form, the same results were found for the copolymer as for the pure polypropylene. Small differences can exist due to the amorphous ethylene-propylene rubber signals which overlap with the polypropylene signals. The true ethylene-propylene rubber seems to have no influence on that annealing temperature.

With differential scanning calorimetry the melting point and the percentage crystallinity were determined as was discussed in chapter 3.4. For the crystalline polypropylene the highest melting temperature and crystallinity was also found around 168°C.

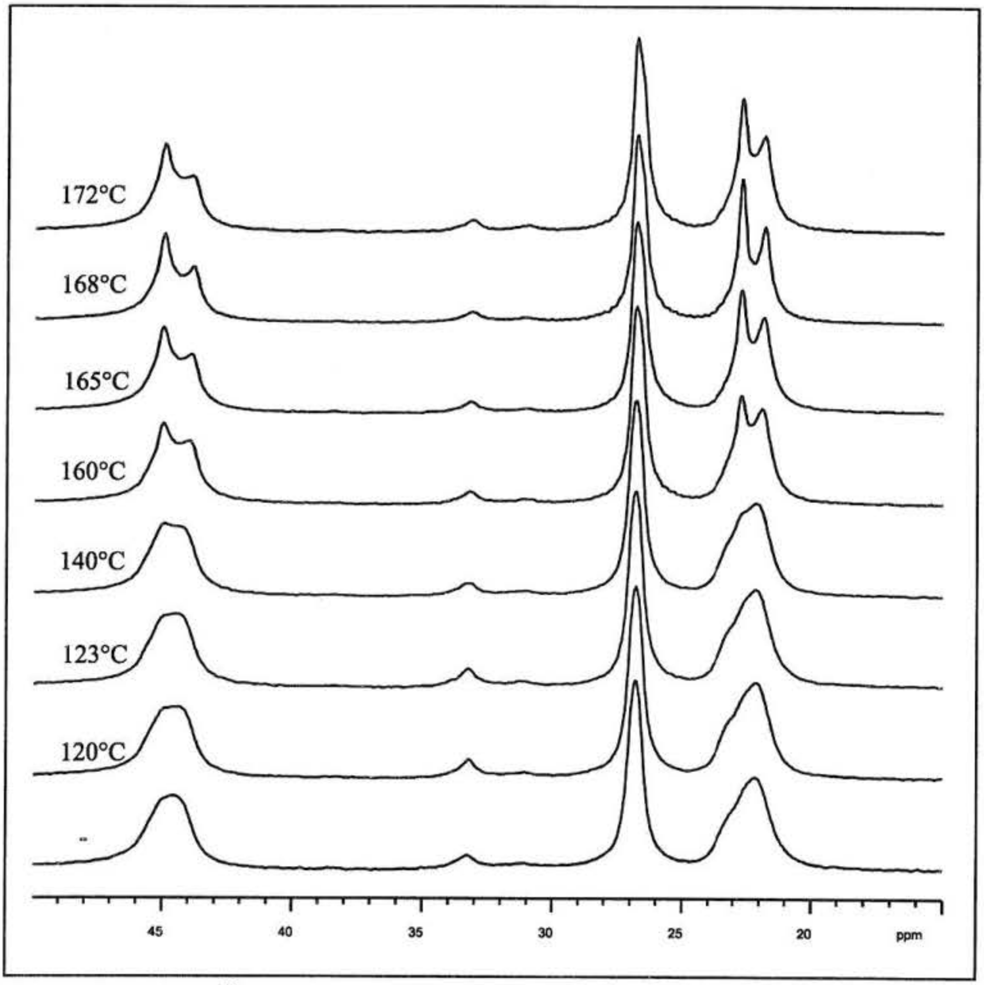

Figure 5.10: 100MHz ^{13}C CP/MAS NMR spectra at room temperature utilising a cross-polarisation time of 5ms for the quench-cooled ethylene-propylene block copolymer I annealed at various temperatures for 1 hour: 172, 168, 165, 160, 140, 123, 120°C and no annealing. A preparation time of 4s was used.

The signal of crystalline polyethylene at 33 ppm in Figure 5.10 does not change remarkably with the annealing temperature but the signal of crystalline polyethylene falls together with the $T_{\delta\delta}$ (EPE) signal which cannot be separated with deconvolution. An EPE sequence cannot crystallise because of its heterogeneity. This implies that its line width stays unaffected by the annealing temperature. Moreover, the percentage crystalline polyethylene amounts to only a few percentages. From the DSC results the maximum in the melting point of polyethylene is around 120-126°C and in Figure 5.10 the signal around 33ppm seems to be a little bit smaller.

Annealing temperature (°C)	$CH_{2,downfield}$	$CH_{2,upfield}$	$CH_{3,midfield}$	$CH_{3,upfield}$
-	162	101	105	132
120	154	95	114	119
123	160	89	106	125
126	149	83	116	116
140	154	77	122	97
160	124	71	84	77
165	113	70	61	71
168	98	67	49	61
170	108	69	55	66
172	111	74	67	69

Table 5.6: The line width (Hz) of the signals of the CP/MAS spectrum at room temperature of copolymer I annealed at different temperatures (Figure 5.10).

5.2.3.3. Conclusions

Annealing of ethylene-propylene copolymers has the same influence on the polypropylene signal of the ethylene-propylene heterophasic copolymers as for pure polypropylene. The effect of annealing is visible in the CP/MAS spectrum by differences in the line width and the peak position. The optimum annealing temperature for the bulk polypropylene in ethylene-propylene copolymers is found around 168°C, as was found for the pure polypropylene sample. This means that the ethylene-propylene rubber has no influence on the annealing of the bulk polypropylene. These results, obtained from NMR are in agreement with the maximum in percentage crystallinity and melting temperature measured with DSC (chapter 3.4).

5.2.4. Conclusions

It can be concluded that the MAS and CP/MAS NMR spectra are influenced by the measuring temperature as well as by the annealing temperature of the sample.

Annealing of ethylene-propylene copolymers causes a splitting of the methylene and methyl signals of the bulk polypropylene due to the α crystalline form. The splitting diminishes when the annealing temperature deviates more from the optimal temperature of 168°C. For the relaxation measurements which will be discussed later (section 5.3), an annealing temperature of 100°C was chosen to avoid crystallisation during the high temperature measurements.

Measurements at higher temperature give a splitting of the methylene and methine signal due to mobile and rigid carbon atoms. This makes higher temperature measurements more interesting because the relaxation times of the mobile and rigid carbon atoms can be separately determined.

For the CP/MAS spectra the length of the contact time can be used to emphasise the signals of the rigid or the mobile phase. Short contact times (around 1ms) at 90°C suppresses the mobile phase while this phase is emphasised at contact times around 13ms. This improves the determination of the relaxation times of the ethylene-propylene rubber, which normally has small signals in comparison with the bulk polypropylene.

5.3. A study of the relaxation times at different temperatures

5.3.1. A $T_{1\rho H}$ relaxation study

The $T_{1\rho H}$ relaxation is sensitive to motions in the kHz range. This makes the $T_{1\rho H}$ relaxation more interesting for polymers than T_{1H} (which is determined by motions in the MHz region) because many important motional processes in polymers have characteristic frequencies in the kHz region. $T_{1\rho H}$ can be measured together with the T_{CH} time in a contact time study in which the length of the contact time is varied, as was carried out by N. Vereycken[23] on a 200MHz NMR. Only one $T_{1\rho H}$ and T_{CH} time were found while in the literature at least two $T_{1\rho H}$ times were detected.[12,24,25] $T_{1\rho H}$ can also be determined with a spin lock experiment (section 2.3.3.1), but in that case a fixed duration of the contact time has to be chosen. From the contact time study it is known that a contact time of 400µs gave the most intense signals. The spin lattice relaxation times in the rotating frame of a homopolymer and some copolymers were measured with the spin lock experiment (section 2.3.3.1).

5.3.1.1. Choice of the $T_{1\rho H}$ equation[26]

In a spin lock experiment there is $T_{1\rho H}$ relaxation during the spin lock time t and during the contact time or cross polarisation time (CP). The form of the relaxation decay curve is well understood and can be described as an exponential or a sum of exponential components (equation 2.25):[27,28]

$$M(t) = \sum_i M^i{}_0 * \exp\left(-\frac{t + CP}{T^i{}_{1\rho H}}\right) \qquad (5.1)$$

An analysis based on two components resulted in the best fit. The short relaxation time of 1 or 2ms can be assigned to the mobile phase while the long component of about 10ms can be ascribed to the rigid phase.[12,24] To get quantitative results the contact time has to be four to five times the longest T_{CH} time. The T_{CH} time is different for rigid and mobile phases. So the maximum intensity of 400µs found with the contact time study can be too short for the mobile phase to reach its optimal intensity.

5.3.1.2. Determination of the T_{CH} time

The T_{CH} relaxation time can be more accurately determined by the cross depolarisation experiment described in paragraph 2.3.3.2. In this experiment the magnetisation changes from a positive into a negative value. To fit the decay the equation 2.26 can be used if the magnetisation at the beginning M_0, differs from the magnetisation at the end, M_∞:

$$M(t) = -M_\infty + (M_\infty + M_0) * \exp\left(\frac{-t}{T_{CH}}\right) \tag{5.2}$$

Taking $m_1 = \frac{M_\infty}{M_0}$, equation 5.2 can be written as follows:

$$M(t) = M_0 * \left((m_1 + 1) * \exp\left(\frac{-t}{T_{CH}}\right) - m_1\right) \tag{5.3}$$

The Gaussian function can be written in the same way:

$$M(t) = M_0 * \left((m_1 + 1) * \exp\left(-0.5 * \left(\frac{t}{T_{CH}}\right)^2\right) - m_1\right) \tag{5.4}$$

Two component fittings can be done by a combination of two exponentials, two Gaussian functions or an exponential and a Gaussian function with typical M_0 and T_{CH} values for each component. On ground of the criteria for the goodness of fit, a combination of an exponential and a Gaussian function gave the best fit:

$$M(t) = M'_0 * \left((m_1 + 1) * \exp\left(\frac{-t}{T'_{CH}}\right) - m_1\right) + M''_0 * \left((m_1 + 1) * \exp\left(-0.5 * \left(\frac{t}{T''_{CH}}\right)^2\right) - m_1\right) \tag{5.5}$$

with the short relaxation time for the Gaussian function and the long time for the exponential one. The longest T_{CH} time that was found for the copolymers was close to 200µs. This implies that a contact time of 400µs, used in this pulse sequence, is too short for quantitative results because it has to be at least 4 à 5 times the longest T_{CH} time. Corrections for the slow increase in magnetisation during the contact time can be added to equation 5.5, i.e. $(1-\exp(-CP/T_{CH}))$ with CP as the contact time. During the contact time and the variable time t the magnetisation can decrease by the $T_{1\rho H}$ relaxation, which can be described by the equation:

exp(-(t + CP)/$T_{1\rho H}$). Eventually, the equation 5.5 can be written as:

$$
\begin{aligned}
M(t) = {} & M'_0 * \exp\left(-\frac{t+400}{T'_{1\rho H}}\right) * \left(\left(m_1+1\right) * \exp\left(\frac{-t}{T'_{CH}}\right) - m_1\right) * \left(1-\exp\left(-\frac{400}{T'_{CH}}\right)\right) \\
& + M''_0 * \exp\left(-\frac{t+400}{T''_{1\rho H}}\right) * \left(\left(m_1+1\right) * \exp\left(-0.5 * \left(\frac{t}{T''_{CH}}\right)^2\right) - m_1\right) * \left(1-\exp\left(-\frac{400}{T''_{CH}}\right)\right)
\end{aligned}
\qquad (5.6)
$$

The T_{CH} relaxation times of the polypropylene sample and the ethylene-propylene copolymers were determined with equation 5.6. The $T_{1\rho H}$ values determined with the spin lock experiment and analysed with equation 5.1 of section 5.3.1.1 were used in equation 5.6. The rigid phase with strong dipole-dipole interactions exhibits a Gaussian curve with a short T_{CH} time and has a long $T_{1\rho H}$ relaxation time. More mobile carbon atoms take longer to cross polarise than immobilised carbons because molecular motion attenuates the interdipolar interactions. Its decrease in magnetisation is faster compared with the rigid phase.

An overview of the cross depolarisation times is given in Table 5.7 for the polypropylene sample B, the ethylene-propylene block copolymer H and the random copolymer J. The cross depolarisation times are different for the chemically distinct carbons because the dipole-dipole interaction depends on the number of directly bonded protons. This explains the shorter values for methylene carbon atoms compared with methine carbons. For the methyl carbons the dipolar interaction is reduced by the reorientation of the methyl group. For all signals only small differences were found between the samples. So the choice of minimal contact time will be determined by the methyl group (largest T_{CH}).

Finally, it can be concluded that the contact time, which has to be at least four times the longest contact time, must be 1500μs or more to get quantitative results.

signal	sample	M'_0 (%)	T'_{CH} (μs) exponential	M''_0 (%)	T''_{CH} (μs) Gaussian
CH_2	B	51(2)	141(12)	49(2)	18.8(.4)
	H	51(2)	156(17)	49(2)	13.9(.3)
	J	54(1)	153(11)	46(1)	13.1(.3)
CH	B	65(1)	178(10)	35(1)	26.7(.5)
	H	66(1)	194(8)	34.1(.7)	19.1(.2)
	J	68(3)	178(17)	32(1)	18.2(.6)
CH_3	B	88(7)	340(39)	12.2(.9)	45(2)
	H	87(4)	287(21)	13.0(.9)	29(1)
	J	89(6)	364(40)	10.9(.7)	30(1)
$T_{\delta\delta}$, $S_{\delta\delta}$, $T_{\beta\gamma}$, $S_{\gamma\gamma}$, $S_{\gamma\delta}$	H	53(4)	157(27)	47(4)	22.1(.8)
	J	55(7)	190(77)	45(6)	25(2)

Table 5.7: Cross depolarisation times, T_{CH} of the quenched polypropylene sample B, the ethylene-propylene block copolymer H and the random copolymer J, measured at room temperature on the 200MHz NMR. The cross depolarisation experiment (section 2.3.3.2) was used with a contact time of 400μs. The cross depolarisation time (t_2) was varied between 0 and 1000μs. For the $T_{1\rho H}$ values I refer to reference 23. For the analysis equation 5.6 was used. The standard deviation is given between brackets.

5.3.1.3. The influence of the cross polarisation time on the $T_{1\rho H}$ relaxation

From the cross depolarisation experiment it is known that the contact time has to be at least 1.5ms to get quantitative results on the 200MHz NMR spectrometer. The increase in magnetisation during the contact time depends mainly on the effective strength of the dipolar interactions and on the Hartmann-Hahn match. The results at 200MHz can give an idea of the contact time needed on a 400MHz NMR. Measurements on a 400MHz NMR are more interesting because of the higher resolution. The influence of the length of the contact time on the $T_{1\rho H}$ was tested on a 400MHz NMR for a polypropylene sample and the results are collected in Table 5.8.

contact time (ms)		M'_0 (%)	$T'_{1\rho H}$ (ms)	M''_0 (%)	$T''_{1\rho H}$ (ms)
1	CH_2	40(1)	3.8(.6)	60(2)	26(1)
	CH	42(2)	3.9(.4)	58(3)	25(1)
	CH_3	42(2)	3.6(.4)	58(3)	26(1)
2	CH_2	30(9)	2.1(.6)	70(6)	20.9(.4)
	CH	30(2)	4.1(.5)	70(3)	22.1(.5)
	CH_3	35(2)	3.4(.4)	65(2)	23.2(.6)
3	CH_2	28(4)	5(1)	72(7)	24(1)
	CH	32(3)	4.0(.6)	68(3)	22.7(.6)
	CH_3	37(1)	5.1(.5)	63(3)	25.3(.7)

Table 5.8: $T_{1\rho H}$ relaxation times and their fractions of the quenched polypropylene sample B as a function of the contact time in a spin lock experiment (section 2.3.3.1). $T_{1\rho H}$ was measured at room temperature on a 400MHz NMR spectrometer. A contact time (CP) of 1ms was chosen and the spin lock time was varied between 0.5 and 37ms. Equation 5.1 was obtained for the analysis. The standard deviation is given between brackets.

It seems that the relaxation times and the fractions fluctuate less between the methylene, methine and methyl carbons when the contact time is short. This can be explained as follows: the component with the short $T_{1\rho H}$ relaxation time is already partly relaxed during the contact time so that a fraction of the original signal is lost during that time. For a contact time of respectively 1, 2 and 3 ms there is directly after the contact time only 72, 57 and 44% visible of the original intensity of the mobile component (with short $T_{1\rho H}$). Figure 5.11 shows the increase and depletion of the magnetisation of a mobile and rigid component during the contact time. It seems that the total signal at 1ms consists for 35% of the mobile component while this is respectively 30 and 25% for a contact time of respectively 2 and 3 ms. Thus, for longer contact times it becomes more difficult to determine the relaxation time and its fraction accurately. In fact, the maximum in intensity of the mobile component is not found after 4 times the longest T_{CH} time but at a shorter contact time of 800μs as a result of the fast $T_{1\rho H}$ relaxation. This indicates that the contact time must be close to the maximum of 800μs to have the highest intensity of the less intense component, i.e. the mobile component.

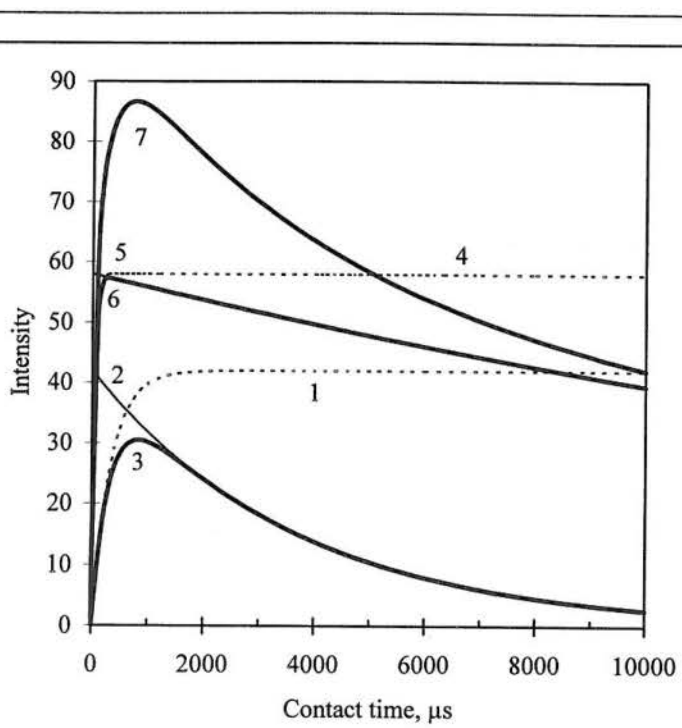

Figure 5.11: Increase and depletion of the intensity of the two components of the methyl signal of a polypropylene sample B as a function of the contact time. For the mobile component a T_{CH} time of 340μs and a $T_{1\rho H}$ time of 3.6ms was taken while a T_{CH} time of 45μs and a $T_{1\rho H}$ time of 26ms characterise the rigid component. Equation 2.4 was used for the analysis. Legend: the increase (1), the relaxation (2) of the mobile component; 3: the change of magnetisation of the mobile component during the contact time. The increase (4) and the relaxation (5) of the rigid component; 6: the change of the magnetisation of the rigid component during the contact time. 7: the change of magnetisation of the sum of the rigid and mobile component.

Eventually, from Table 5.8 a contact time of 1ms was chosen for the $T_{1\rho H}$ relaxation time measurements to obtain accurate relaxation times although it is known the fractions are not reliable.

5.3.1.4. The $T_{1\rho H}$ behaviour of polypropylene and ethylene-propylene copolymers

5.3.1.4.1. The $T_{1\rho H}$ relaxation of polypropylene

The $T_{1\rho H}$ data of the polypropylene sample B are given in Table 5.9. For the measurements at 20°C the relaxation times were determined by integration of the signals. At 20°C two relaxation times were found: the short relaxation time around 5 ms can be ascribed as the mobile or amorphous component while the long time of 38ms can be assigned as the rigid or crystalline component. For the high temperature measurement, a contact time of 1ms and of 13ms was used for the determination of the spin lattice relaxation time in the rotating frame. In both cases a deconvolution and an integration of the signals was performed. In all cases a long time of around 27ms was found. For the short $T_{1\rho H}$ time a contact time of 13ms gave the best agreement between the results from integration and deconvolution and these results were used in the table.

		M'_0 (%)	$T'_{1\rho H}$ (ms)	M''_0 (%)	$T''_{1\rho H}$ (ms)
20°C	CH_2	32.0(.9)	5.3(.3)	68(1)	39.1(.7)
	CH	34.0(.9)	5.2(.3)	66(1)	38.1(.6)
	CH_3	37(1)	4.4(.3)	63(1)	37.8(.8)
90°C	CH_{2a}		15(1)		
	CH_{2c}				25.4(.6)
	CH_a		15(1)		
	CH_c				27.3(.5)
	CH_3				27.1(.4)

Table 5.9: The $T_{1\rho H}$ times of the polypropylene sample B measured at 20 and 90°C with the spin lock experiment described in section 2.3.3.1. For the measurement at 20°C a contact time of 1ms was used. A contact time of 1 and of 13ms was taken for the high temperature measurements. At 20°C and 90°C the spin lock time was varied between 0.5 and 60ms. Equation 5.1 was used for the analyses. The standard deviation is given between brackets.

The fact that two components were found indicates that in the time scale of milliseconds the relaxation cannot be averaged out over the whole sample by spin diffusion. The relaxation is averaged out in certain domains as can be seen by the similar relaxation times between chemically distinct carbons. This result confirms the fact that $T_{1\rho H}$ is a phase property. The maximum spin diffusive path length or the length over which spin diffusion takes place in a certain time t can be determined by the equation $L = \sqrt{6Dt}$ with D the spin diffusion coefficient and t the characteristic time for diffusion. A typical value for D in solids is $10^{-16}m^2/s$.[29-31] The maximum diffusive path length, measured from a $T_{1\rho H}$ time of 38.3ms yields 4.8nm. This means that the size of the crystalline domain must be at least 4.8nm.

As a function of the temperature the short or mobile $T_{1\rho H}$ component increases while the rigid or long component decreases (Table 5.9). As was reported for polypropylene by McBrierty et al.[32] and for polyethylene by McCall, et al.[33] there are three $T_{1\rho H}$ minima, which depends on motions in the kHz range. $T_{1\rho H}$ relaxation can be ascribed at low temperature (<0°C) to rotation of methyl groups about their threefold axis. Above 0°C the relaxation of the rigid component is dominated by the α relaxation process while the mobile component is dominated by the β relaxation or glass transition process and the higher temperature α relaxation process. The relaxation of the rigid component of polypropylene sample B is determined by the α relaxation process and in the temperature range of 20 to 90°C it is located on the right side of the $T_{1\rho H}$ minimum versus correlation time for molecular motions. The mobile component is located on the left side of its $T_{1\rho H}$ minimum and is determined by the α and β relaxation process.

5.3.1.4.2. The $T_{1\rho H}$ behaviour of the true ethylene-propylene copolymer

The relaxation times of the xylene-soluble fraction I^*_{xs} are given in Table 5.10. Only one relaxation time was found for every carbon atom for a sample which is completely amorphous. Spin diffusion is not sufficiently strong so that different relaxation times are found for chemically distinct carbons. This can be caused by the high mobility of the rubbery material. The relaxation time increases remarkably with the temperature and relaxation times up to 95ms were found at 90°C. This indicates that the relaxation time of the ethylene-propylene rubber is very sensitive to the temperature and that the mobility of the polymer chains are strongly affected by the temperature.

For completely amorphous polymers the relaxation can be dominated below the glass transition temperature by methyl reorientation and at higher temperature by the β relaxation or glass transition as was found for natural rubber.[33] All this indicates that the ethylene-propylene rubber is located on the left side of the $T_{1\rho H}$ minimum which is dominated by the β relaxation process.

At 20°C the relaxation times of sample I^*_{xs} are shorter compared to the short relaxation time of the polypropylene sample B while at high temperature the relaxation time is much longer. This clearly indicates the higher mobility of the ethylene-propylene rubber compared to the amorphous polypropylene. It is a result of the lower glass transition temperature of the ethylene-propylene rubber compared to polypropylene (section 3.5).

	$T_{1\rho H}$ (ms) at 20°C		$T_{1\rho H}$ (ms) 90°C
$S_{\alpha\alpha}$	2.4(.1)	$S_{\alpha\alpha}$	55(3)
$S_{\alpha\gamma}$,$S_{\alpha\delta}$	2.64(.07)	$S_{\alpha\gamma}$,$S_{\alpha\delta}$	70(2)
$T_{\delta\delta}$	2.6(.2)	$T_{\delta\delta}$	95(4)
$T_{\beta\delta}$,$S_{\beta\delta}$,$S_{\delta\delta}$	2.86(.06)	$T_{\beta\delta}$	65(2)
		$S_{\beta\delta}$	65(2)
		$S_{\delta\delta}$	65(2)
$T_{\beta\beta}$ ($S_{\beta\delta}$)	2.5(.1)	$T_{\beta\beta}$	80(6)
		$S_{\beta\delta}$	67(2)
$S_{\beta\beta}$	2(1)	$S_{\beta\beta}$	85(4)
$P_{\beta\beta}$,$P_{\beta\delta}$,$P_{\delta\delta}$	6.5(.3)	$P_{\beta\beta}$,$P_{\beta\delta}$,$P_{\delta\delta}$	94(9)

Table 5.10: The $T_{1\rho H}$ relaxation times of the xylene soluble fraction, I^*_{xs} measured at 20°C (CP=2ms and the spin lock time was varied between 0.5 and 25ms) and 90°C (CP=13ms and the spin lock time was varied between 1 and 90ms) with the spin lock experiment described in section 2.3.3.1. Equation 5.1 was used for the analysis. The standard deviation is given between brackets.

5.3.1.4.3. The $T_{1\rho H}$ behaviour of ethylene-propylene block copolymers

For the ethylene-propylene heterophasic copolymer, I* the relaxation data are shown in Table 5.11. Integration was used for the analysis of most of the signals at 20°C. For the $T_{\delta\delta}$, $S_{\delta\delta,k}$,.. and the $T_{\beta\delta}$, $S_{\delta\delta,a}$, ... signals deconvolution was used because these small signals overlap with the very intense methine signal, $T_{\beta\beta}$. At a temperature of 90°C the mobile methine and methylene signal could be integrated separately when a contact time of 13ms was used. For the methyl signal this was not possible as was also found for the polypropylene sample B. This resulted in one $T_{1\rho H}$ relaxation time of the methyl signal (Table 5.11).

		M'_0 (%)	$T'_{1\rho H}$ (ms)	M''_0 (%)	$T''_{1\rho H}$ (ms)
20°C	$\underline{S_{\alpha\alpha}}$	37(2)	5.8(.6)	63(2)	37(1)
	$S_{\alpha\gamma}$,$S_{\alpha\delta}$		1.95(.4)		
	$T_{\delta\delta}$,$S_{\delta\delta,k}$	53(8)	4.0(.8)	47(5)	27(2)
	$T_{\beta\delta}$, $S_{\delta\delta,a}$, $S_{\gamma\delta}$		2.8(.2)		
	$\underline{T_{\beta\beta}}$($S_{\beta\delta}$, $S_{\beta\beta}$)	30(1)	5.0(.4)	70(1)	35(1)
	$\underline{P_{\beta\beta}}$, $P_{\beta\delta}$, $P_{\delta\delta}$	35(2)	4.5(.4)	65(2)	35(1)
90°C	$\underline{S_{\alpha\alpha,a}}$		18(2)		
	$\underline{S_{\alpha\alpha,c}}$				26(1)
	$S_{\alpha\gamma}$,$S_{\alpha\delta}$		60(2)		
	$T_{\delta\delta}$, $S_{\delta\delta,c}$		100(4)		
	$T_{\beta\delta}$, $S_{\delta\delta,a}$, $S_{\gamma\delta}$		42(2)		
	$\underline{T_{\beta\beta,a}}$		16.3(.9)		
	$\underline{T_{\beta\beta,c}}$ ($S_{\beta\beta}$,$S_{\beta\delta}$)				27.5(.4)
	$\underline{P_{\beta\beta}}$, $P_{\beta\delta}$, $P_{\delta\delta}$				21(2)[a]

Table 5.11: The proton spin lattice relaxation times in the rotating frame of the ethylene-propylene heterophasic copolymer, I* measured at 20°C (CP=1ms and the spin lock time is varied between 0.5 and 60ms) and at 90°C (CP=13ms to determine the mobile component and CP=1ms to determine the rigid component, the spin lock time is varied between 1 and 90ms) on a 400MHz NMR spectrometer. Equation 5.1 was used for the analysis. The standard deviation is given between brackets. The underlined signals contain the carbon atoms of a long polypropylene chain. [a] One averaged relaxation time was found for the methyl signal, because the relaxation times resemble each other too much.

The $T_{1\rho H}$ relaxation behaviour of the bulk polypropylene ($S_{\alpha\alpha}$, $T_{\beta\beta}$ and $P_{\beta\beta}$) in sample I* is similar to that of the polypropylene sample B (Table 5.9): two components were found for the methylene, methine and methyl signal and the relaxation times in the domains are averaged out by spin diffusion. The crystalline domains must be at least 4.6nm as can be determined by the maximum diffusive path length. The rigid component decreases with the temperature and the mobile component increases with it. The short sequences of ethylene and propylene in sample I* have one strongly increased relaxation time as was also found for sample I^*_{xs}. The relaxation times of the copolymer sequences are not averaged out over the copolymer domain by spin diffusion.

It can be concluded that the relaxation of the copolymer can be divided in two parts: the relaxation of the bulk polypropylene and that of true ethylene-propylene rubber. The $T_{1\rho H}$ relaxation times of the bulk polypropylene and the ethylene-propylene rubber are not influenced by each other. This indicates that the domains must be too large to be averaged out by spin diffusion and that the ethylene-propylene rubber domains have a too high mobility.

		M'_0 (%)	$T'_{1\rho H}$ (ms)	M''_0 (%)	$T''_{1\rho H}$ (ms)
20°C	$\underline{S_{\alpha\alpha}}$	35(2)	5.7(.5)	65(3)	36(1)
	$T_{\delta\delta}$, $S_{\delta\delta,c}$	50(3)	4.3(.5)	50(3)	28(1)
	$T_{\beta\delta}$, $S_{\delta\delta,a}$, $S_{\gamma\delta}$		3.1(.4)		
	$\underline{T_{\beta\beta}}$ ($S_{\beta\delta}$, $S_{\beta\beta}$)	35.6(.9)	4.7(.3)	64(1)	34.4(.6)
	$\underline{P_{\beta\beta}}$, $P_{\beta\delta}$, $P_{\delta\delta}$	38(2)	3.5(.3)	62(2)	33.5(.7)
90°C	$\underline{S_{\alpha\alpha,a}}$		15.2(.4)		
	$\underline{S_{\alpha\alpha,c}}$				20.5(.3)
	$T_{\beta\delta}$,$S_{\delta\delta}$,$T_{\delta\delta}$,…		52(2)		
	$\underline{T_{\beta\beta,a}}$		16(1)		
	$\underline{T_{\beta\beta,c}}$				20.6(.4)
	$\underline{P_{\beta\beta}}$, $P_{\beta\delta}$, $P_{\delta\delta}$		17.2(.5)		

Table 5.12: The $T_{1\rho H}$ relaxation behaviour of the xylene insoluble fraction, I^*_{xi} at two temperatures: 20°C (CP=2ms and the spin lock time was varied between 0.5 and 60ms) and 90°C (CP=13ms and the spin lock time was varied between 1 and 90ms). The underlined signals are those of long sequences of polypropylene. Equation 5.1 was used for the analysis. The standard deviation is given between brackets. For the methyl signal at 90°C one average relaxation time is found for the different domains, because the relaxation times lie to close to each other.

The difference between the sample I* and I^*_{xs} is that sample I* contains crystalline polypropylene and crystalline polyethylene. The signal at 33ppm in the spectrum of sample I* represents among other things the crystalline polyethylene. This explains the fact that in sample I^*_{xs} only one relaxation component is found for the signal at 33ppm while for the sample I* two components are needed for a good fit. These two components are also found for the *xylene insoluble fraction,* I^*_{xi} (Table 5.12). As is known from the thermal measurements, this sample also contains 1.5% crystalline polyethylene. This small amount of crystalline polyethylene causes small crystals and the edge of a crystal can be conceived as an imperfection. This can explain the smaller relaxation time of the crystalline polyethylene compared with that of crystalline polypropylene.

At 20°C two relaxation times were found for the signal $T_{\delta\delta}$, $S_{\delta\delta,c}$ of the xylene soluble fraction I^*_{xi} while at high temperature one component can describe the decay curve. At 90°C the crystalline polyethylene gets a higher mobility so that eventually the long sequences of ethylene have their signal at 30ppm as for amorphous polyethylene.

5.3.1.4.4. The $T_{1\rho H}$ behaviour of some ethylene-propylene copolymers

The $T_{1\rho H}$ relaxation of the different ethylene-propylene block copolymers H, I and I* were measured and it seemed that no clear difference was found between the relaxation times of the samples. This can be explained by the fact that the relaxation times depend on the sequence. The sequence determines the mobility which has an influence on the relaxation times. The only difference that was found was the relative intensity of the signals.

It should be expected for the random copolymer J that the same $T_{1\rho H}$ results were found for the mobile polypropylene signals and the copolymer signals because this sample is a homogeneous system as is known from the single glass transition temperature. At 20°C there is only a small difference between the $T_{1\rho H}$ values of amorphous polypropylene of sample B (Table 5.9) and the copolymer signals of sample I^*_{xs} (Table 5.10) so that it is difficult to see the change in $T_{1\rho H}$ for sample J. Moreover, sample J has at room temperature small copolymer signals which makes an accurate analysis difficult. On the other hand, at high temperature the $T_{1\rho H}$ relaxation times of the copolymer signals are very long. Spin lock times of 300ms or more are needed to determine these long relaxation times accurately. As this is practically not possible, measurements at lower temperatures (for example 60°C) give shorter relaxation times and shorter times can be easier detected. At higher temperature the advantage is that the copolymer signals can be emphasised and the disadvantage is that the $T_{1\rho H}$ relaxation times are too long to be detected. It should be expected that at temperatures between 20° and 90°C a compromise can be found between this advantage and disadvantage.

5.3.1.5. Conclusions

For polypropylene the relaxation is averaged out in certain domains by spin diffusion. Two $T_{1\rho H}$ relaxation times were found for polypropylene; the short or mobile $T_{1\rho H}$ relaxation time describes among others the relaxation of the amorphous polypropylene and the long or rigid relaxation time is ascribed to the crystalline polypropylene.

For ethylene-propylene copolymers the same results were found for the bulk polypropylene. For the true ethylene-propylene rubber domains one short relaxation time was found at room temperature and this relaxation time increases remarkably with the temperature. At 90°C relaxation times of 90ms were found, while for the amorphous polypropylene relaxation times were at most 18ms. This is an indication for the higher mobility of the ethylene-propylene rubber domains compared with the bulk polypropylene. In other words, this means that the ethylene-propylene copolymer has a lower glass transition temperature than the amorphous polypropylene, as was confirmed with DSC.

To compare different ethylene-propylene copolymers problems arise: at room temperature the copolymer signals have a low intensity compared with the polypropylene signals and the relaxation times cannot be determined accurately. Moreover, around 20°C the differences between the relaxation times of the mobile phases are too small, even the difference between the ethylene-propylene copolymer and the amorphous polypropylene is small. On the other hand, at 90°C the copolymer signals can be emphasised but the $T_{1\rho H}$ relaxation times are too long to measure them in a good way. It should be expected that these problems can be solved by measuring at temperatures between 20°C and 90°C, for example at 60°C.

5.3.2. T_{1H} relaxation time

The spin lattice relaxation time T_{1H} gives information about motions of the polymer in the MHz region. The relaxation is most efficient when the correlation frequencies of these motions are near the Larmor frequencies as was deduced from equation 2.10 of chapter 2. For polypropylene two minima were observed in the T_{1H} curve versus temperature. The low temperature minimum can be ascribed to rotations of the methyl group around its threefold axis. At these low temperatures below the glass transition temperature only the methyl group has motions in the MHz regions. Protons of the methine and methylene group undergo relaxation to the lattice by spin-spin coupling to the methyl group. This T_1 minimum is generally broad, which suggests that there is a variation in the degree of mutual hindrance among the methyl groups throughout the solid. The high temperature T_1 minimum occurs at temperatures well above the glass transition at which the amorphous polypropylene is rubbery. This minimum is associated with reorientation of segments of the main chain. This motion includes translation over short distances within the solid. It has to be noted here that the minimum depends on the frequency of the NMR spectrometer and the minimum is found at higher temperatures as the magnetic field is increased.[34-37]

To measure the spin lattice relaxation time the inversion recovery pulse sequence for protons, given in section 2.3.3.3 was used. For the measurements at room temperature a contact time of 1ms was used for the polypropylene sample and 2ms was taken for the ethylene-propylene copolymers. For the measurements at 90°C a short contact time of respectively 1ms and 13ms was used for respectively the rigid phase and the mobile phase as was determined in section 5.2.2.2. For the analysis of the integrated signals the following equation was used:

$$M(t) = M_\infty - (M_\infty - M_0) * \exp\left(-\frac{t}{T_{1H}}\right) \qquad (5.7)$$

with M_0 the magnetisation at time $t = 0$

M_∞ the magnetisation at time $t = \infty$ or the magnetisation at equilibrium.

5.3.2.1. T_{1H} measurements at room temperature

Table 5.13 gives the T_{1H} times for the polypropylene sample B and for the ethylene-propylene heterophasic copolymer I*, its xylene soluble fraction I^*_{xs} and its insoluble fraction I^*_{xi} at room temperature. For all the signals of the ^{13}C NMR spectrum one exponential component was used for the fitting. This means that no distinction between rigid and mobile or crystalline and amorphous phases can be made for the polypropylene sample and the ethylene-propylene copolymer, although it is known that they are semi-crystalline.

The methylene, methine and methyl signals of the *polypropylene sample B* exhibit the same relaxation time which is an indication for spin diffusion. The proton spins rapidly diffuse throughout the sample resulting in an averaged T_{1H} value. Such a single exponential process for the T_{1H} for polypropylene was generally found,[22,32,34,35] although Tanaka et al.[38] found two components by annealing the samples at high temperatures.

From the relaxation time the maximum diffusive path length can be determined and for sample B it yields 23nm. This means that the crystalline and amorphous domains must be smaller than 23nm.

20°C	B	I*	I^*_{xs}	I^*_{xi}
$\underline{S_{\alpha\alpha}}$	0.89(.01)	0.88(.02)	0.62(.05)	0.91(.01)
$S_{\alpha\gamma}$, $S_{\alpha\delta}$		0.6(.1)	0.52(.01)	
$T_{\delta\delta}$, $S_{\delta\delta c}$		0.74(.02)	0.52(.07)	0.89(.02)
$T_{\beta\delta}$, $S_{\delta\delta a}$, $S_{\gamma\delta}$		0.68(.01)	0.48(.01)	0.89(.02)
$\underline{T_{\beta\beta}}$ ($S_{\beta\delta}$, $S_{\beta\beta}$)	0.895(.005)	0.836(.009)	0.51(.08)	0.903(.006)
$\underline{P_{\beta\beta}}$, $P_{\beta\delta}$, $P_{\delta\delta}$	0.893(.008)	0.828(.009)	0.59(.02)	0.879(.007)

Table 5.13: The spin lattice relaxation times of the polypropylene sample B (CP=1ms), the ethylene-propylene heterophasic copolymer I* (CP=1ms), the xylene-soluble fraction I^*_{xs} (true ethylene-propylene copolymer) (CP=2ms) and the xylene-insoluble fraction I^*_{xi} (CP=1ms) measured with the inversion recovery method (section 2.3.3.3) at room temperature. The waiting time t was varied between 0.001 and 5s. Equation 5.7 was used for the analysis. The signals of polypropylene are underlined and the standard deviation is given between brackets.

For the *ethylene-propylene block copolymer sample I** not all the signals have the same relaxation time. This means that spin diffusion is not efficient over the whole sample as was also found with the $T_{1\rho H}$ relaxation measurements. The signals of long sequences of propylene, i.e. $S_{\alpha\alpha}$, $T_{\beta\beta}$ and $P_{\beta\beta}$, have the same T_{1H} time which is the same value as for the polypropylene sample B. This is an indication for spin diffusion in the bulk polypropylene of the block copolymer and the relaxation of the bulk polypropylene seems to be independent of the presence of true ethylene-propylene copolymer domains. The crystalline and amorphous polypropylene domains must also be smaller than 23nm. The relaxation times of the short sequences of ethylene and propylene in sample I* differ from those of the bulk polypropylene. This indicates that the domains must be too large to be averaged out by spin diffusion or that they have a too high mobility. Probably both will be true. The copolymer signals relax faster than the bulk polypropylene and the same short relaxation times are found for the *sample* I^*_{xs}, the sample that only contains short sequences of ethylene and propylene. In this sample the relaxation times of the signals differ from each other. Spin diffusion, which is a static magnetisation transfer process, is not efficient in such mobile domains of polymers above their glass transition temperature. The ethylene-propylene rubber sample I^*_{xs} relaxes faster than polypropylene because this mobile sample has more motions in the MHz region. The xylene *insoluble fraction* I^*_{xi} resembles the polypropylene homopolymer. In this sample the maximum diffusive path length is of the same size.

5.3.2.2. The T_{1H} behaviour at 90°C

Measurements were also done at higher temperature, the results are given in Table 5.14. Still, one component was used for the fitting. This indicates that spin diffusion is also efficient in the *polypropylene sample B* at high temperature although the amorphous polypropylene (which has a higher mobility at this temperature compared with 20°C) can reduce the diffusion. T_{1H} increases with the temperature for the polypropylene signals of the homopolymer as well as for the copolymer. For the true ethylene-propylene copolymer the relaxation times rather seem to decrease. This is not very clear though.

For the relaxation times of *the ethylene-propylene copolymer sample I** measured at 90°C (Table 5.14) on should expect that if sample I* is an homogeneous mixture of I^*_{xs} and I^*_{xi} that the T_{1H} relaxation time of the methylene signal $S_{\alpha\alpha}$ equals 0.79s. This was calculated with the equation:

$$\frac{1}{T_{1H}(I^*)} = \frac{F_{XS}}{T_{1H}(I^*_{xs})} + \frac{F_{XI}}{T_{1H}(I^*_{XI})} \qquad (5.8)$$

with F_{XS} and F_{XI} the xylene soluble and xylene insoluble fraction (Table 3.2).

As the relaxation time of the methylene signal of sample I* differs completely from 0.79s, it can be concluded that in sample I* the two fractions I^*_{xs} and I^*_{xi} are not homogeneous mixed. Thus, the block copolymer I* consist of a polypropylene matrix in which ethylene-propylene copolymers are dispersed. Even at 90°C the relaxation is not averaged out over the whole sample as was also found at room temperature.

90°C	B	I*	I^*_{xs}	I^*_{xi}
$\underline{S_{\alpha\alpha}}$	1.06(.02)	1.22(.02)	0.36(.01)	1.29(.02)
$S_{\alpha\gamma}$, $S_{\alpha\delta}$		0.66(.04)	0.44(.01)	
$T_{\delta\delta}$, $S_{\delta\delta c}$		0.6(.1)	0.51(.02)	
$T_{\beta\delta}$, $S_{\delta\delta a}$, $S_{\gamma\delta}$		0.87(.02)	0.533(.05)	0.9(.1)
$\underline{T_{\beta\beta a}}$	1.2(.2)	1.3(.03)	0.42(.02)	1.30(.04)
$S_{\beta\delta}$		0.81(.04)	0.49(.01)	
$\underline{T_{\beta\beta c}}$	1.1(.1)	1.23(.02)		1.26(.02)
$S_{\beta\beta}$		[a]	0.36(.02)	
$\underline{P_{\beta\beta}}$, $P_{\beta\delta}$, $P_{\delta\delta}$	1.05(.06)	1.26(.01)	0.51(.02)	1.28(.03)

Table 5.14: The spin lattice relaxation times of the polypropylene sample B (CP=1ms), the ethylene-propylene heterophasic copolymer I* (CP=13ms), the xylene-soluble fraction I^*_{xs} (true ethylene-propylene copolymer) (CP=13ms) and the xylene-insoluble fraction I^*_{xi} (CP=1ms) measured with the inversion recovery pulse sequence (section 2.3.3.3) at a temperature of 90°C. The waiting time was varied between 0.001 and 5s. Equation 5.7 was obtained for the analysis. The signals of polypropylene are underlined and the standard deviation is given between brackets. [a]$S_{\beta\beta}$ was integrated together with $T_{\beta\beta k}$

5.3.2.3. Conclusions

The spin lattice relaxation of polypropylene and ethylene-propylene block copolymers is affected by spin diffusion. This resulted for polypropylene in one T_{1H} relaxation time. For the block copolymers one relaxation time was found for the bulk polypropylene which was longer than the T_{1H} times of the copolymer signals.

The copolymer fraction is at room temperature more than 70° above its glass transition temperature and therefore it must be chiefly determined by the backbone motions, as was also found by Kontos et al.[39] who measured an ethylene-propylene copolymer with a 30MHz NMR spectrometer. On the other hand, polypropylene is only 20°C above its glass transition temperature and the methyl rotation will mainly determine the relaxation. This will be discussed more precisely in next chapter of the wideline measurements. These wideline measurements have the advantage that it is a much faster technique so that it is possible to measure the samples at more temperatures.

5.3.3. T_{1C} relaxation study

The T_{1C} relaxation time is determined by motions in the MHz region. In contrast with proton relaxation processes the carbon spin lattice relaxation is not a phase property since the transport of magnetisation through spin diffusion for ^{13}C nuclei is very slow as a result of the high degree of isotopic dilution. For the T_{1C} measurement the saturation recovery method (section 2.3.3.4) was preferred to the Torchia pulse sequence, which is also often used.[40-42]

In the latter pulse sequence cross polarisation is used which this emphasises the rigid phase. In this research more attention is paid to the mobile phase that improves the mechanical properties. The saturation recovery method makes use of the MAS spectra instead. The T_{1C} relaxation measured with the saturation recovery method is expected to be an exponential increasing function or a sum of them:

$$M(t) = \sum_i M^i{}_0 * \left(1 - \exp\frac{-(t + HSP)}{T^i{}_{1C}}\right) \qquad (5.9)$$

with HSP the length of the homogeneity spoiling pulse.

5.3.3.1. T_{1C} relaxation of polypropylene

The results for the polypropylene sample B, measured at room temperature and at 90°C, are shown in Table 5.15. For the methyl signal only one component satisfied while a two component fit was needed for the methylene and methine carbons. The chemically distinct carbons each display an individual relaxation time because spin diffusion is not effective. Polypropylene does not have long side chains; hence the two components of the methylene and methine can be ascribed to the rigid and mobile domains. This is a result of the very rapid relaxation of the carbon nuclei in the mobile amorphous phase above the glass transition temperature due to local chain motions. Any selectivity of the methyl signal with respect to the mobile and rigid components cannot be achieved because the methyl relaxation is dominated by the methyl C_3 reorientation. The fact that methine carbons have a higher relaxation rate than methylene carbons, in the mobile as well as in the rigid phase, indicates that the relaxation is influenced by dipolar interactions with methyl protons. Backbone motions are characterised by low frequencies and small amplitudes so that relaxation via direct C-H interaction has a minor effect. The higher relaxation times of the methylene and methine relative to the methyl carbons can be explained by the r^{-6} distance dependence of the dipolar relaxation.[43,44]

Increasing the temperature gives a higher relaxation time for the methyl carbons (Table 5.15) because the T_{1C} minimum versus correlation time is located for below 0°C. On the other hand, the relaxation rates for the methylene and methine carbons decrease. The higher molecular mobility of the chains at 90°C cause a higher spectral density in the MHz range. At 90°C the relaxation is less dominated by the methyl relaxation. So there must be two minima in the T_{1C} plot versus temperature: an important minimum due to the methyl reorientation, as was described by Lyerla et al.,[43,44] and a flatter minimum at a higher temperature due to backbone motions. The latter minimum will only be seen for methylene and methine carbons.

		M' (%)	T'_{1C} (s)	M"	$T"_{1C}$ (s)
20°C	CH_2	38(2)	1.6(.1)	62(2)	30(3)
	CH	37(2)	1.5(.1)	63(3)	18(1)
	CH_3		0.23(.01)		
90°C	CH_2	57(3)	0.17(.03)	43(3)	19(2)
	CH	48(3)	0.28(.02)	52(2)	16(2)
	CH_3		0.71(.05)		

Table 5.15: The carbon spin lattice relaxation time, T_{1C} of the polypropylene sample, B measured with the saturation recovery method (section 2.3.3.4). At 20°C the waiting time t is varies between 0.01 and 120s while at 90°C it is gradually changed from 0.0025 to 90s. Equation 5.9 was obtained for the analysis. The standard deviation is given between brackets.

5.3.3.2. T_{1C} relaxation of the true ethylene-propylene copolymer

For the xylene soluble fraction I^*_{xs}, the carbon spin lattice relaxation times as a function of the temperature are collected in Table 5.16. The relaxation could be described by one component. In comparison with the polypropylene sample, sample I^*_{xs} relaxes fast. This can be ascribed to the high mobility of the ethylene-propylene rubber which is already at room temperature more than 50°C above T_g. As a function of the temperature the methyl carbons have an increased relaxation time because the minimum of T_1 must be even lower than the T_{1C} minimum of polypropylene resulting from the higher mobility. For the methylene and methine carbons the influence of the temperature is less pronounced.

20°C	T_{1C} (s)	50°C	T_{1C} (s)	90°C	T_{1C} (s)
$S_{\alpha\alpha}$	0.30(.01)	$S_{\alpha\alpha}$	0.186(.005)	$S_{\alpha\alpha}$	0.24(.01)
$S_{\alpha\gamma}+ S_{\alpha\delta}$	0.23(.01)	$S_{\alpha\gamma}+ S_{\alpha\delta}$	0.239(.004)	$S_{\alpha\gamma}$	0.357(.008)
				$S_{\alpha\delta}$	0.449(.009)
$T_{\delta\delta}$	0.42(.01)	$T_{\delta\delta}$	0.41(.02)	$T_{\delta\delta}$	0.77(.05)
$T_{\beta\delta}+ S_{\gamma\delta}+ S_{\delta\delta}$	0.334(.004)	$T_{\beta\delta}$, $S_{\gamma\delta}$	0.346(.004)	$T_{\beta\delta}$	0.516(.008)
				$S_{\gamma\delta}$	0.63(.02)
		$S_{\delta\delta}$	0.454(.008)	$S_{\delta\delta}$	0.770(.009)
$T_{\beta\beta}+S_{\beta\delta}$	0.315(.008)	$T_{\beta\beta}$	0.349(.005)	$T_{\beta\beta}$	0.43(.02)
		$S_{\beta\delta}$	0.47(.01)	$S_{\beta\delta}$	0.52(.02)
$S_{\beta\beta}$	0.23(.02)	$S_{\beta\beta}$	0.20(.01)	$S_{\beta\beta}$	0.34(.02)
$P_{\beta\beta}+P_{\beta\delta}+P_{\delta\delta}$	0.51(.01)	$P_{\beta\beta}+P_{\beta\delta}+P_{\delta\delta}$	0.64(.01)	$P_{\beta\beta}$	0.89(.04)
				$P_{\beta\delta}$	1.07(.02)
				$P_{\delta\delta}$	1.17(.04)

Table 5.16: The carbon spin lattice relaxation time of the xylene soluble fraction (true ethylene-propylene copolymer), I^*_{xs} measured at different temperatures with the saturation recovery method (section 2.3.3.4). The waiting time t was gradually changed between 0.01 and 4s. For the analysis equation 5.9 was used. The standard deviation is given between brackets.

5.3.3.3. The T_{1C} relaxation of ethylene-propylene block copolymers

The T_{1C} results of the ethylene-propylene block copolymer I* at 90°C are shown in Table 5.17. The signals of the bulk polypropylene relax in the same way as was found for the pure polypropylene sample B. The ethylene-propylene rubber signals each exhibit one relaxation component like the xylene-soluble fraction, I^*_{xs}. Thus, it can be concluded that bulk polypropylene in ethylene-propylene block copolymers consists of two domains: the rigid and the mobile polypropylene. A distinction can be made between them with a T_{1C} study of the methylene and methine signal. But caution with the interpretation of the relaxation times is necessary because T_{1C} is also influenced by the methyl reorientation.

Anyway, the difference in relaxation time between rigid and mobile signals can be used to emphasise the mobile phase of the ethylene-propylene copolymer, as was shown in section 5.2.2.1.

	M' (%)	T'_{1C} (s)	M" (%)	T''_{1C} (s)
$\underline{S_{\alpha\alpha}}$	55(1)	0.23(.01)	45(1)	11.5(.8)
$S_{\alpha\gamma}$		0.33(.03)		
$S_{\alpha\delta}$		0.44(.03)		
$T_{\delta\delta}$, $S_{\delta\delta,c}$		0.71(.03)		
$T_{\beta\delta}$, $S_{\gamma\delta}$		0.52(.03)		
$S_{\delta\delta,a}$		0.55(.05)		
$\underline{T_{\beta\beta}}$	46(1)	0.35(.02)	54(1)	12.9(.7)
$S_{\beta\delta}$		0.51(.02)		
$S_{\beta\beta}$		0.34(.03)		
$\underline{P_{\beta\beta}}$		0.94(.03)		
$P_{\beta\delta}$		1.03(.06)		
$P_{\delta\delta}$		1.4(.1)		

Table 5.17: The carbon spin lattice relaxation times T_{1C} of the ethylene-propylene block copolymer I* measured at 90°C with the saturation recovery method (section 2.3.3.4). The waiting time t is varied between 0.02 and 90s. The methylene, methyl and methine signal were deconvoluated. The percentage of the mobile M' and rigid fraction M" were determined by using the peak integral of the methylene and methine signals of the deconvoluated spectrum with a waiting time of 90seconds. The signals of the bulk polypropylene are underlined. The standard deviation is given between brackets.

5.3.4. A T_{2H} study

T_{2H} relaxation is generally measured directly from the FID or after Fourier transformation from the relaxation of the signals of the proton spectrum as a function of the waiting time.[45,46] On the other hand, it can also be measured via cross polarisation as is described in section 2.3.3.5. The advantage is that a distinction can be made between the relaxation of the different domains in a polymer if their signals have a different chemical shift. This is interesting for the ethylene-propylene heterophasic copolymers because the difference in molecular mobility can be studied between the bulk polypropylene and the ethylene-propylene copolymer domains. These T_{2H} can be used to understand the T_{2H} times, obtained from FID analyses, in terms of the domains.

5.3.4.1. The T_{2H} relaxation behaviour of polypropylene

For the analysis of the spin spin relaxation decay curve, measured via cross polarisation, Gaussian and Lorentzian functions can be used.[37] The relaxation curve of the polypropylene sample B at 20°C was fitted with a Gaussian function while a combination of a Gaussian and a Lorentzian function was used for the high temperature measurements. The spin spin relaxation times of sample B are given in Table 5.18. A Gaussian function indicates that the relaxation is a distribution of relaxation times. This is typical for atoms of the crystalline domain which have restricted mobility so that the relaxation is not averaged out by molecular motions. At high temperature the short relaxation component represents the rigid phase with the crystalline polypropylene and the long relaxation time can be ascribed as the mobile component, which is representative for the amorphous phase. The mobility of the crystalline and amorphous phase must be more or less the same at room temperature while a difference is found between them at high temperature as is shown by the two relaxation times. At room temperature the polymer is already above its glass transition temperature, but it is only 20°C above T_g. The amorphous polymer chains must be at least 50°C above T_g to be a real rubber. This means that the mobility at 20°C is still restricted as is the case in the glassy state and no difference in molecular mobility can be found between the crystalline and amorphous phase with T_{2H} at room temperature.

		M' (%)	T'_{2H} (μs) Gauss	M'' (%)	T''_{2H} (μs) Lorentz
20°C	CH_2		8.3(.1)		
	CH		8.5(.1)		
	CH_3		8.4(.1)		
90°C	CH_2	78(3)	8.2(.2)	22(2)	44(7)
	CH	80(4)	7.9(.1)	20(4)	44(6)
	CH_3	81(3)	8.1(.3)	19(3)	46(6)

Table 5.18: T_{2H} relaxation of the polypropylene sample B, measured via cross polarisation (section 2.3.3.5) and at temperatures of 20 and 90°C. A contact time of 1ms was used. At 20°C the waiting time was varied between 1 and 20μs, while at 90°C the time was gradually changed between 1 and 110μs. The standard deviation is given between brackets.

5.3.4.2. The T_{2H} relaxation behaviour of ethylene-propylene copolymers

The spin spin relaxation times of the *ethylene-propylene block copolymer, I** and *its xylene soluble fraction I^*_{xs}* at room temperature are given in Table 5.19. As was found for the polypropylene sample B, the methylene, methine and methyl signals of the bulk polypropylene of sample I* are represented by a Gaussian function. Again, no distinction can be made between crystalline and amorphous polypropylene. The other signals of sample I* show a exponential T_{2H} relaxation as is found for the xylene soluble fraction, I^*_{xs}. This longer relaxation time compared with the amorphous polypropylene is again an indication for the fact that the mobility of the ethylene-propylene rubber must be higher than the amorphous phase in polypropylene. This is in agreement with its lower glass transition temperature compared with polypropylene.

	I^*		I^*_{xs}
	Gauss	Lorentz	Lorentz
$S_{\alpha\alpha}$	7.2(.1)		26(3)
$S_{\alpha\gamma}$,$S_{\alpha\delta}$		20(3)	26.7(.9)
$T_{\delta\delta}$,$S_{\delta\delta,c}$		20(2)	24.8(.7)
$T_{\beta\delta}$, $S_{\delta\delta,a}$, $S_{\gamma\delta}$		19.8(.8)	24.5(.4)
$T_{\beta\beta}$, $S_{\beta\delta}$, $S_{\beta\beta}$	7.4(.2)		23.7(.2)
$P_{\beta\beta}$, $P_{\beta\delta}$, $P_{\delta\delta}$	7.9(.1)		23.9(.1)

Table 5.19: The spin spin relaxation times of the ethylene-propylene heterophasic copolymer, I* and the xylene soluble fraction, I^*_{xs} at room temperature. The pulse sequence described in section 2.3.3.5 was used with a contact time of 2ms. For sample I* the waiting time was varied between 1 and 100μs. For sample I^*_{xs} the time was gradually changed between 1 and 200μs. The relaxation times are given in microseconds. The standard deviation is given between brackets.

5.3.5. Conclusions

With solid-state NMR it is possible to study the mobility of the polymer chains by determining the relaxation times.

The spin spin relaxation time T_{1H}, is sensitive to motions in the MHz region and is influenced by spin diffusion. No distinction can be made between mobile and rigid or amorphous and crystalline polypropylene. However, it is possible to make a difference between the bulk polypropylene and the ethylene-propylene copolymer domains. From this relaxation time it is known that the crystalline polypropylene domain must be smaller than 23nm.

In the $T_{1\rho H}$ relaxation spin diffusion is only effective over smaller domains compared with T_{1H} and a distinction can be made between the crystalline and amorphous domains. From this relaxation time it was concluded that the crystalline polypropylene domains must be at least 4.8nm. The $T_{1\rho H}$ relaxation is very sensitive to the temperature. For the ethylene-propylene rubber domains the relaxation time increases from a few microseconds at 20°C to almost 100ms at 90°C. This is an indication for the high mobility of the copolymer domains in the bulk polypropylene.

With the T_{1C} relaxation time a difference can be made between mobile and rigid methylene and methine signals in the MAS spectrum and this can be used to emphasise the mobile phases of the polymer.

T_{2H} is not influenced by spin diffusion as is the case for T_{1H} and $T_{1\rho H}$. The higher mobility of the ethylene-propylene rubber is reflected in longer relaxation times. At temperatures well above the glass transition temperature a distinction can be made between the rigid or crystalline and mobile or amorphous polypropylene.

5.4. $T_{1\rho H}$ relaxation time as a function of the annealing temperature and the annealing time.

The thermal history of the sample affects the relaxation rate and $T_{1\rho H}$ seemed to be the most sensitive for it among the different relaxation times. So, $T_{1\rho H}$ is used for studying the annealing of polypropylene and ethylene-propylene copolymers.

In section 3.4.3 the influence of annealing on the melting temperature and on the percentage crystallinity of a polypropylene and an ethylene-propylene copolymer sample was discussed.

In section 5.2.3 the influence on the CP/MAS spectra is discussed. On top, the thermal pretreatment has also an influence on the relaxation times. Tanaka et al.[38] has studied the effect of annealing on T_{1H} and T_{2H} relaxation times for a polypropylene sample. The spin lattice relaxation time seems to increase slowly. For the spin spin relaxation time it is only the largest time that is effected when the optimum annealing temperature is reached. The spin lattice relaxation time in the rotating frame is stronger effected by the thermal pretreatment.

Attention will be focused on the influence of annealing on the relaxation times of the crystalline polypropylene and polyethylene of ethylene-propylene block copolymers. First of all, the influence of the annealing on the relaxation times of a polypropylene sample is discussed for comparison.

5.4.1. The influence of the annealing temperature and annealing time on the $T_{1\rho H}$ relaxation time of polypropylene

The $T_{1\rho H}$ relaxation times were determined for the polypropylene samples annealed at different temperatures and the results are given in Table 5.20. For a $T_{1\rho H}$ study of this sample it isn't necessary to give the relaxation times of every signal of the sample because $T_{1\rho H}$ is a domain property, i.e. the same results were found for the methylene, methine and methyl signal (section 5.3.1.4.1).

Annealing temperature (°C)	M'_0 (%)	$T'_{1\rho H}$ (ms)	M''_0 (%)	$T''_{1\rho H}$ (ms)
-	38(2)	4.5(.4)	62(2)	32.3(.9)
120	34(1)	5.0(.3)	66(1)	44(1)
140	31(1)	5.9(.5)	69(2)	55(1)
160	28(1)	6.3(.6)	72(2)	79(3)
165	29.2(.2)	6.4(.4)	71(1)	87(2)
168	27(1)	7.0(.4)	73(1)	88(2)
170	30(1)	6.2(.5)	70(1)	82(2)
172	28(1)	5.9(.5)	72(2)	77(3)

Table 5.20: $T_{1\rho H}$ relaxation times of a film of the polypropylene sample A after annealing at different temperatures and measured at room temperature. The spin lock pulse sequence described in section 2.3.3.1 was used with a contact time of 1ms. The spin lock time was varied between 0.5 and 60ms. For the analysis equation 5.1 was obtained. The standard deviation is given between brackets.

The annealing temperature affects the relaxation time. The longest relaxation time which is related to the crystalline domain is influenced most. Annealing a polymer near the melting temperature affects the organisation in the crystalline domain and therefore, it has an important influence on the relaxation time. The maximum in the relaxation time is reached at 168°C as was also concluded from the analysis of the spectra (section 5.2.3). By increasing the annealing temperature up to the optimum annealing temperature of 168°C the polymer chains get more and more kinetic energy to organise themselves in a stable crystalline form. Above the optimum temperature melting of the polymer starts its influence. This means that at a temperature of 168°C an optimum equilibrium exists between melting and recrystallisation. At the best annealing temperature the crystalline lattice must be the most perfect which means that the interhelical distances are the smallest in comparison with other annealing temperatures. This implies that the polymer chains are more restricted and this has an influence on the relaxation times. From section 5.3.1.4.1 it is known that the rigid component is located on the right side of the $T_{1\rho H}$ minimum. Reducing the mobility of the polymer chains does increase the relaxation times. This explains the higher relaxation time for the sample annealed at 168°C compared with others.

The effect of the annealing on the percentage of the rigid component or the percentage crystallinity is less compared with the relaxation times. This implies that the perfection of the crystals and less the total percentage of the crystalline fraction change with the annealing process.

The spin lattice relaxation time in the rotating frame seems to be very sensitive to the annealing temperature. For that reason $T_{1\rho H}$ can be used to check the thermal pretreatment. For this annealing study the samples were annealed for one hour. To verify that an annealing time of one hour is enough to get an equilibrium, $T_{1\rho H}$ is used. The annealing time was varied for a sample with a low annealing temperature of 120°C. The results are shown in Figure 5.12. The mobile component is not affected by annealing while the rigid component which represents the crystalline domain increases. It seems that even for such low annealing temperature of 120°C the maximal relaxation time is reached after less than one hour. At higher annealing temperatures the annealing will go faster.

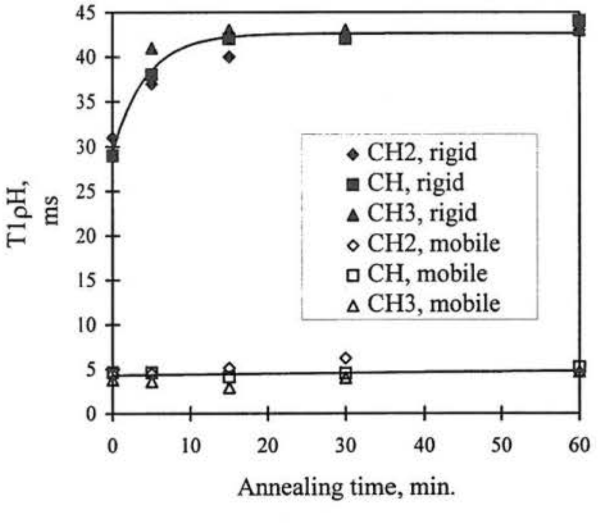

Figure 5.12: The $T_{1\rho H}$ relaxation times of the polypropylene sample A, annealed at 120°C, as a function of the annealing time. The rigid and mobile components are shown for the three carbon atoms of polypropylene. The spin lock pulse sequence described in section 2.3.3.1 with a contact time of 1ms was used. The spin lock time was varied between 0.5 and 60ms. The relaxation times were measured at room temperature.

5.4.2. The influence of the annealing temperature on the $T_{1\rho H}$ relaxation time of ethylene-propylene block copolymers

The effect of annealing on the $T_{1\rho H}$ relaxation of the copolymers was also analysed. It is not allowed to integrate all signals together in the NMR spectrum, as was done for the polypropylene sample, because the copolymers are composed of 'bulk' polypropylene and 'real' copolymer domains. All the signals have to be integrated separately and analysed separately for the determination of their $T_{1\rho H}$ relaxation.

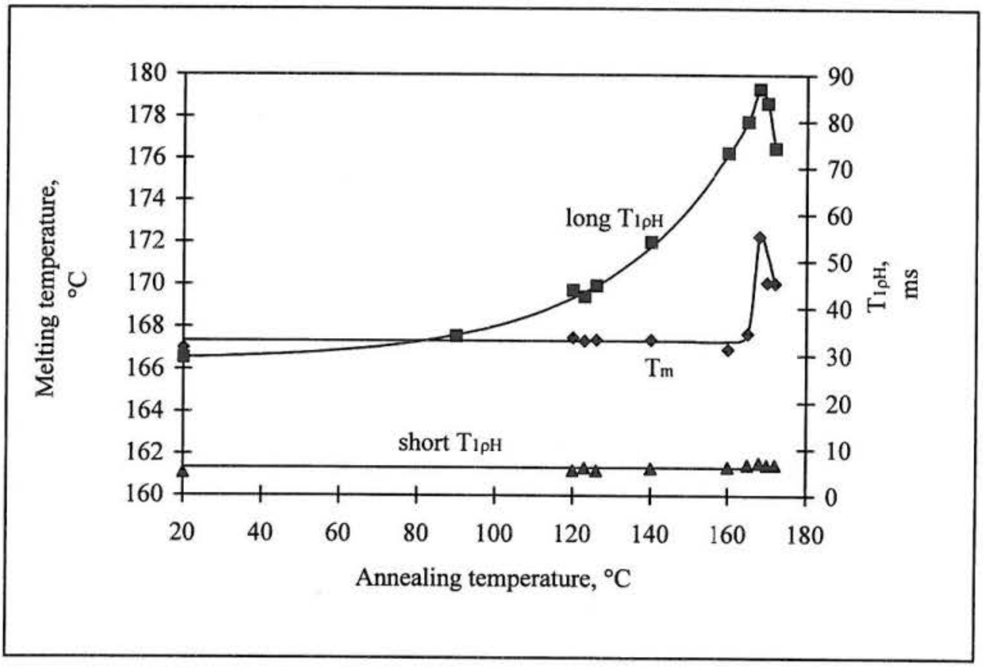

Figure 5.13: The $T_{1\rho H}$ relaxation times and the melting temperature (DSC: section 3.4) of the bulk polypropylene of the ethylene-propylene block copolymer, I as a function of the annealing temperature. For the determination of the $T_{1\rho H}$ relaxation times the spin lock pulse sequence described in section 2.3.3.1 was used with a cross polarisation time of 1ms. The relaxation times were measured at room temperature and the spin lock time was gradually changed between 0.5 and 60ms.

For the CH_2, the CH and the CH_3 signal of the bulk polypropylene in the copolymer, the same results were found as for the pure polypropylene sample: the long $T_{1\rho}(H)$ reaches its maximum near 168°C with a $T_{1\rho H}$ of 87 ms while the short relaxation time is less affected by the annealing temperature and fluctuates between 5 and 7ms. This indicates that the presence of the ethylene-propylene copolymer domains has less or no influence on the annealing of the bulk polypropylene. The results of the $T_{1\rho H}$ relaxation times as a function of the annealing temperature are shown in Figure 5.13. The melting temperature, determined with DSC, is also given. Both have their maximum value at 168°C. The melting temperature changes from 167°C to 172°C while the long relaxation time changes from 30 to 87ms. Thus the long relaxation time is more sensitive to the thermal pretreatment than the melting temperature.

Comparing the percentage crystallinity, determined with DSC and NMR as a function of the temperature (Figure 5.14), a great difference is found. To get a better understanding of the difference, the definition of the percentage crystallinity measured with the two techniques has to be defined. A crystallinity of 30%, measured with DSC, means that 30 percent of the total ethylene-propylene block copolymer is crystalline polypropylene. For the NMR results, the fraction of the rigid component (in a $T_{1\rho H}$ experiment) of the bulk polypropylene gives the percentage crystalline polypropylene to the total bulk polypropylene in a block copolymer. To determine the percentage crystallinity of the polypropylene in the total copolymer sample, the fraction of bulk polypropylene in the copolymer has to be known. This can be estimated from the quantitative liquid-state NMR spectrum (Table 4.3). The product of the fraction of the rigid component and the fraction bulk polypropylene is calculated and the results are shown in Figure 5.14. The too high percentage of the NMR result can also be explained in terms of the cross polarisation. In this $T_{1\rho H}$ experiment a contact time of 1ms was used as was previously defined to be the best for getting reliable $T_{1\rho H}$ relaxation times. During the contact time there is an increase in magnetisation which is faster for the crystalline than for the amorphous domain. If the contact time is shorter than 4 to 5 times the longest T_{CH} time, then the amorphous component can be underestimated. This results in a too high crystalline fraction. On top, the percentage crystallinity is determined from the fraction of the rigid component. As was already mentioned previously in this chapter, one has to be careful with the words crystalline and amorphous component because at room temperature the amorphous phase is just above the glass transition temperature and more acts like a glass with still restricted mobility. So the rigid component can contain that the rigid part of the amorphous phase and surely the interphase.

Concerning the influence of the annealing on the relaxation times of the crystalline polyethylene, the signal at 33ppm has to be observed (Table 5.21). For the signals at 33 ppm a maximum of the long $T_{1\rho H}$ relaxation time at 123°C is found. For the melting temperature the maximum is also found around that temperature. It has to be pointed out that it is not evident to see a maximum in the relaxation times because the sample contains only a few percentages of crystalline polyethylene.

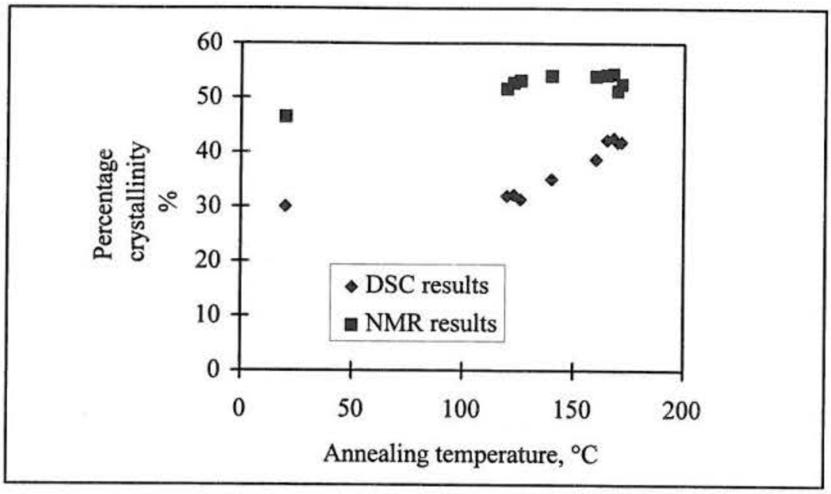

Figure 5.14: The percentage crystallinity of the ethylene-propylene block copolymer I, measured with DSC (section 3.4) and NMR as a function of the annealing temperature (Table 5.20). With NMR the fraction of the rigid component of the bulk polypropylene signals is multiplied by fraction of the signals of long sequences of polypropylene to the total signal intensity of the liquid-state spectrum.

Annealing temp. (°C)	Tm (°C)	M'_0 (%)	$T'_{1\rho H}$ (ms)	M''_0 (%)	$T''_{1\rho H}$ (ms)
20	109.1	65(5)	3.4(.3)	35(5)	16(1)
120	109.3/123	63(3)	3.1(.2)	37(2)	30(2)
123	119.1/123.3	54(3)	4.2(.4)	46(2)	36(2)
126	117.4/128.6	63(4)	4.2(.4)	37(3)	30(2)
140	118.5	52(4)	3.0(.4)	48(4)	18(1)
160	117.2	49(5)	2.6(.5)	51(5)	15(1)
165	116.6	55(5)	3.4(.6)	45(5)	16(2)
168	116.9	57(5)	3.7(.5)	43(5)	17(2)
170	116.6	56(4)	3.5(.2)	46(4)	17(2)
172	115.9	55(6)	3.5(.6)	45(5)	17(2)

Table 5.21: The melting temperature (section 3.4) of polyethylene and the $T_{1\rho H}$ relaxation of the signal at 33ppm ($S_{\delta\delta,c}$ and $T_{\delta\delta}$) for the ethylene-propylene block copolymer I annealed at different temperatures. The spin lock pulse sequence described in section 2.3.3.1 was used with a contact time of 1ms. The relaxation times were measured at room temperature and the spin lock time was varied between 0.5 and 60ms.

5.4.3. conclusions

It can be concluded that the crystalline polypropylene and polyethylene in ethylene-propylene block copolymers are both effected by the annealing temperature. The $T_{1\rho H}$ relaxation time is very sensitive to the annealing temperature and can be used as a control of the thermal pretreatment. The annealing temperature that gave the highest $T_{1\rho H}$ relaxation time gave also the maximum in melting temperature when measured with DSC.

5.5. The influence of the magnetic field

One final goal of the solid-state NMR results obtained from the 400MHz NMR is to get a better understanding of the results of a industrial low-field NMR, often a 10 or a 20 MHz NMR. The knowledge of the influence of the magnetic field is therefore necessary. As the relaxation times, measured with an industrial NMR, have to be determined from the free induction decay and not from a ^{13}C spectrum the CP/MAS results of the 400MHz were initially compared with CP/MAS results from a 200MHz NMR. Later in chapter 6, the relaxation times obtained from the FID will be discussed as a function of the magnetic field.

The relaxation times, T_1, T_2 and $T_{1\rho H}$ are influenced by the strength of the magnetic field as can be deduced from the equations 2.10, 2.11 and 2.12 of chapter 2. From this equation is it clear that $T_{1\rho H}$ also depends on the strength of the spin lock field B_1.

T_{1H}, T_{2H}, $T_{1\rho H}$ and T_{1C} were measured on a 200 MHz NMR spectrometer with a B_1 field of 40 kHz and on a 400 MHz with a B_1 field of 57 kHz. The results are given in Table 5.22. For the determination of the T_{1C} time on the 200 MHz NMR the methine and methyl signal couldn't be integrated separately and the same values are given in Table 5.22 for the methine and methyl signal. On the 400 MHz the signals could be analysed separately. This can be explained by the fact that a higher magnetic field gives a higher resolution. This high resolution was important for ethylene-propylene copolymer samples because the small signals of the short sequences of propylene and ethylene needed to be separately observed from the large signals of the bulk polypropylene. By the way, it is the presence of the short sequences of ethylene and of propylene that improves the properties of the bulk polypropylene. The disadvantage of a higher magnetic field is the chemical shift anisotropy which becomes more important and which causes a broadening of the signals. This can be excluded by increasing the spinning rate at the 'magic angle'. For a 200 MHz NMR spectrometer a spinning rate of

3.6 kHz satisfied. For the 400 MHz NMR measurements it seemed that the spinning side bands completely disappeared at a spinning rate of 6 kHz.

Concerning the relaxation times, the T_{1C}, T_{1H} and the $T_{1\rho H}$ relaxation times increase with the magnetic field (Table 5.22). A higher magnetic field causes a slower relaxation and the minimum in the plot of the relaxation time versus correlation time is shifted to a higher correlation time and the curve becomes more shallow. This means that the minimum is found at a higher temperature when the magnetic field is increased.[35,47] On the other hand, the T_{2H} relaxation time stays more or less the same as was expected from Figure 2.4 of chapter 2.
Thus, it can be concluded that a high magnetic field is interesting when a high resolution is required as for CP/MAS experiments. When the resolution is not important, as is the case for wideline measurements, a high magnetic field is not needed.

Relaxation	field strength	CH_2	CH	CH_3
T_{1H} (s)	200MHz	0.77(.07)	0.77(.08)	0.76(.06)
	400MHz	0.89(.01)	0.989(.005)	0.893(.008)
T_{2H} (μs)	200MHz	7.0(.2)	7.3(.3)	7.8(.2)
	400MHz	8.3(.1)	8.5(.2)	8.4(.1)
$T_{1\rho H}$ (ms)	200MHz/40kHz	2.2(.3)	1.4(.1)	1.0(.1)
		10.5(.9)	9.1(.4)	8.3(.3)
	400MHz/57kHz	5.3(.3)	5.2(.3)	4.4(.3)
		39.1(.7)	38.1(.6)	37.8(.8)
T_{1C} (s)	200MHz	0.6(.2)	0.34(.02)[a]	0.34.02)[a]
		18(3)	13(2)[a]	13(2)[a]
	400MHz	1.6(.1)	1.5(.1)	0.23(.01)
		30(3)	18(1)	-

Table 5.22: The T_{1H}, T_{2H}, $T_{1\rho H}$ and T_{1C} relaxation times of the polypropylene sample B measured with a 400 MHz (B_1=57kHz) and a 200MHz NMR (B_1=40kHz) spectrometer at room temperature. For the analysis and the pulse sequence : see sections 5.5.3.1, 5.3.2, 5.3.3. [a]The methine and methyl signal in the MAS spectrum couldn't be integrated separately on the 200 MHz NMR. The standard deviation is given between brackets.

5.6. Conclusions

In this chapter it is shown that the solid state of a polymer can be studied with solid-state NMR, like the mobility of the polymer chains, the rigid and mobile domains in the polymer,...

The mobility of ethylene-propylene copolymers is spread over a wide range of frequencies and the polymer can be divided in crystalline and amorphous polypropylene, true ethylene-propylene copolymer and polyethylene. In the ^{13}C solid-state NMR spectrum of an ethylene-propylene copolymer it is possible to assign the signals of the bulk polypropylene and those of the ethylene-propylene rubber. At temperatures above 50°C a distinction can be made in the spectrum between the signals of the crystalline and amorphous polypropylene. The relaxation times of the domains will be summarised here.

The *crystalline polypropylene* is immobile and is characterised by a short T_{2H} relaxation time of a few microseconds, a long T_{1C} of some tens of seconds and a $T_{1\rho H}$ relaxation time of some tens of microseconds. The crystalline polypropylene domain is very sensitive to the thermal pretreatment which is reflected in the long $T_{1\rho H}$ relaxation time. The relaxation time varies from 30ms for the non-annealed sample to 87ms for the best annealed sample. Annealed samples show a splitting of the methylene and methyl signal. Increasing the measuring temperature reduces the $T_{1\rho H}$ relaxation time, while the T_{2H} relaxation time stays constant.

From the $T_{1\rho H}$ and T_{1H} relaxation times it is known that the dimensions of the crystalline domains lie between 4.8 and 23nm.

The *amorphous polypropylene* has signals with more or less the same chemical shift as the crystalline polypropylene at room temperature. At higher temperatures the mobile methylene and methine signals shift downfield and a distinction can be made between mobile and rigid signals of the bulk polypropylene. At room temperature the amorphous polypropylene is only 20°C above its glass transition temperature and the mobility of the amorphous polypropylene chains is still restricted. This is reflected in the single T_{2H} relaxation time for polypropylene. At higher temperatures the T_{2H} relaxation time of the amorphous polypropylene deviates from the crystalline polypropylene. Moreover, a short T_{1C} and short $T_{1\rho H}$ are typical for this amorphous domain at room temperature. Compared with crystalline polypropylene the relaxation times of amorphous polypropylene are less influenced by the thermal history of the polymer. Concerning T_{1H}, spin diffusion dominates the relaxation and no distinction can be made between crystalline and amorphous polypropylene.

The *true ethylene-propylene copolymer domain* has small signals in the quantitative MAS and the CP/MAS spectrum at room temperature compared with the intense signals of the bulk polypropylene. At 90°C it is possible to emphasise the mobile or rigid part of the polymer by changing the contact time. A short contact time of 1ms suppresses the mobile domain while this phase is emphasised with a contact time of 13ms. This improved the analysis of the relaxation times of the ethylene-propylene copolymer domains. The $T_{1\rho H}$ relaxation times of the copolymer rubber are very sensitive to the temperature: the relaxation time increases from a few milliseconds at room temperature to almost 100ms at 90°C. The relaxation time of amorphous polypropylene increases from a few milliseconds to only 15ms. This indicates that the copolymer domain must have a higher mobility than the amorphous polypropylene. This is in agreement with the lower glass transition temperature of the true ethylene-propylene copolymer domains compared with the T_g of polypropylene. The higher mobility of the copolymer compared with the bulk polypropylene is also shown in their larger T_{2H} and the shorter T_{1C} relaxation times. The ethylene-propylene domains in the bulk polypropylene must be large because the ethylene-propylene domains relax independently from the bulk polypropylene. This is valid for $T_{1\rho H}$, T_{1H}, T_{1C} and T_{2H}.

Commercial ethylene-propylene copolymers also contain a small amount of *polyethylene*. The optimal annealing temperature can be detected with $T_{1\rho H}$ relaxation measurements.

Until now little or less attention is paid to the interphase between crystalline and amorphous polypropylene and between the bulk polypropylene and the ethylene-propylene copolymer because maximum two components were found with the relaxation measurements: the mobile or amorphous phase and the rigid or crystalline phase. With T_{1H} and $T_{1\rho H}$ the relaxation times are averaged out by spin diffusion and the local relaxation times, like those of the region between the crystalline and amorphous polypropylene, cannot be measured. In spin spin relaxation measurements spin diffusion is less efficient and the relaxation is not averaged out over domains. In the next chapter we will focus our attention on this parameter.

5.7. References

1. Auriemma, F.; Born, R.; spiess, H.W.; De Rosa, C.; Corradini, P.; Macromolecules, 28(20) (1995), 6902.

2. Bunn, A.; Cudby, E.A.; harris, R.K.; Packer, K.J.; Say, R.J.; J. Chem. Soc.: Chem. Commun., (1981), 15.

3. Loboda-Cackovic, J.; Cackovic, H.; Hosemann, R.; J. Macromol. Sci.: Phys., 16(1) (1979), 127.

4. Tanaka, H.; Inoue, Y.; Polym. Intern., 31 (1993), 9.

5. Nishioka, A.; Koike, Y.; Owaki, M.; naraba, T.; Kato, Y.; J. Phys. Soc. Japan, 15(3) (1960), 416.

6. Nakaoki, T.; Shuto, H.; Kitamaru, R.; Hayashi, H.; Rep. Preg. Polym. Phys. Japan, 38 (1995), 167.

7. Caldas, V.; Brown, G.R.; Nohr, R.S.; macDonald, J.G.; Raboin, L.E.; Polymer, 35(5) (1994), 899.

8. Marsh, G.; Edwards, J.; Mishra, M.; Amer. Chem. Soc.: Polym. Prepr., 35(1) (1994), 759.

9. Saito, S.; Moteki, Y.; Nakagawa, M.; Horii, F.; Kitamaru, R.; Macromolecules, 23 (1990), 3256.

10. Clayden, N.J.; Polymer, 33(15) (1992), 3145.

11. Clayden, N.J.; J. Polym. Sci.: Part B: Polym. Phys., 32 (1994), 2321.

12. Caldas, V.; Morin, F.G.; Brown, G.R.; Magn. Res. Chem.; 32 (1994), 72.

13. Komoroski, R.A.; "High resolution NMR spectroscopy of synthetic polymers in bulk", VCH, Florida, 1986.

14. Zeigler, R.C.; Macromol. Symp., 86 (1994), 213.

15. Cheng, J. Fone, M.; Reddy, V.N.; Schwartz, K.B.; Fisher, F.P.; Wunderlich, B.; J. Polym. Sci.: PartB: Polym. Phys., 32 (1994), 2683.

16. Dechter, J.J.; Komoroski, R.A.; Axelson, D.E.; mandelkern, L.; J. Polym. Sci.: Polym. Phys. Ed., 19 (1981), 631.

17. Kitamaru, R.; Horii, F.; Murayama, K.; Am. Chem. Soc., 19 (1986), 636.

18. Tonelli, A.E.; "NMR spectroscopy and polymer microstructure: the conformational connection", VCH, USA, 1989.

19. Yu, T.; Gyo, M.; Prog. Polym. Sci; 15 (1990), 825.

20. Kitamaru, R.; Horii, F.; Murayanma, K.; Polym. Bull., 7 (1982), 583.

21. Komoriski, R.A.; Maxfield, J.; Mandelkern, L.; Macromolecules, 10 (1977), 545.

22. Bunn, A.; Cudby, E.A.; Harris, R.K.; Packer, K.J.; Say, B.J.; Polymer, 23 (1982), 694.

23. Vereycken, N.; "Spectroscopische karakterisatie van ethyleen-propyleen copolymeren", PhD thesis, UIA, Antwerp, 1994.

24. Tanaka, H.; Eur. Polym. J., 27(7) (1991), 565.

25. Tanaka, H.; Fujiwara, Y.; Asano, T.; Polizzi, S.; Makromol. Chem., 194 (1993), 2279.

26. This study was done in corporation with PhD student N. Vereycken.

27. Dadayli, D.; Harris, R.K.; Kenwright, A.M.; Say, B.R.; Sünnetçioglu, M.M.; Polymer, 35(19) (1994), 4083.

28. Lecture of Packer, K.J.; DSM, The Nederlands, 8/4/1997.

29. Packer, K.J.; Poplett, I.J.F.; Taylor, M.J.; J. Chem. Soc., Faraday Trans. 1, 84(11) (1988), 3851.

30. Kenwright, A.M.; Kenneth, J.P.; Say, B.J.; J. Magn. Reson., 69 (1986), 426.

31. Ibbett, R.N.; "NMR Spectroscopy of Polymers", Chapman & Hall, London, 1993.

32. McBrierty, V.J.; Douglass, D.C.. Falcone, D.R.; J. Chem. Soc. Faraday Trans. 2, 68 (1972), 1051.

33. McCall, D.W.; Falcone, D.R.; Trans. Faraday Soc., 66 (1970), 262.

34. McDonald, M.P.; Ward, I.M.; Proc. Phys. Soc., 80 (1962), 1.

35. Slichter, W.P.; NMR basic Principles and progress, 4 (1961), 209.

36. McCall, D.W.; Acc. Chem. Res., 4 (1971), 223.

37. McCall, D.W.; Falcone, D.R.; Trans. Faraday Soc., 66 (1970), 262.

38. Tanaka, H.; Korogi, F.; Eur. Polym. J., 24(8) (1988), 759.

39. Kontos, E.G.; Slichter, W.P.; J. Polym. Sci., 61 (1962), 61.

40. Hoai, A.; Horii, F.; Kitamaru, R.; Fatou, J.F.; Bello, A.; Macromolecules, 23 (1990), 2913.

41. Tonelli, A.E.; Gomez, M.A.; Tanaka, H.; Cozine, M.H.; Abstr. Papers Am. Chem. Soc., 195 (1988), 47.

42. Axelson, D.E.; J. Polym. Sci.: Polym. Phys. Ed., 20 (1982), 1427.

43. Lyerla, J.R.; Yannoni, C.S.; J. Res. Develop., 27(4) (1983), 302.

44. Lyerla, J.R.; Yannoni, C.S.; Fyfe, C.A.; Acc. Chem. Res., 15 (1982), 208.

45. Tanaka, H.; Yoshinori, I.; Eur. Polym. J.; 29(4) (1993), 569.

46. McDonald, M.P.; Ward, I.M.; Proc. Phys. Soc., 80 (1962), 1249.

47. Nolle, A.W.; Billings, J.J.; J. Chem. Phys., 30(1) (1958), 84.

6. ^{1}H WIDELINE NMR

6.1. Introduction

In CP/MAS experiments the relaxation times of the different signals of the ^{13}C NMR spectrum can be studied, while with ^{1}H wideline NMR all the information of the polymer under investigation is collected in one FID. For semi-crystalline polymers like polyethylene and polypropylene which consist of only a crystalline and an amorphous domain a lot of wideline NMR results are available.[1-10] For the ethylene-propylene block copolymers no information can be found in the literature; probably because this polymer is more complex. The polymer consists of crystalline and amorphous polypropylene, polyethylene and ethylene-propylene copolymer. The relaxation decay of these parts of the sample are collected in one FID. Thanks to the CP/MAS results reported in previous chapter it was possible to get a better understanding of the wideline results.

As ^{1}H wideline measurements take up less time than the CP/MAS measurements, it was possible to measure the relaxation times in more detail as a function of the temperature. Different samples were measured and the influence of the magnetic field is also discussed.

6.2. The proton spin lattice relaxation time

T_{1H} was measured with the inversion recovery method (section 2.4.2.). For the analysis of the data, the same equation (eq.5.7) could be used as for the CP/MAS experiments. Both for the homopolymer as for the copolymer only one T_{1H} relaxation time was found at all temperatures. The results are given in Table 6.1. For the polypropylene sample B the same results at 20°C were found as with the CP/MAS measurements at room temperature (Table 5.13). For the copolymer this is not valid because the ^{13}C CP/MAS NMR measurements gave different relaxation times for the bulk polypropylene and the copolymer part. Thus, it can be concluded that it is not possible to make a distinction between the relaxation times of the bulk polypropylene and the true ethylene-propylene copolymer when measured directly via proton NMR. The first reason is that the short sequences of ethylene and propylene have relaxation times which differ only less than 0.2 seconds from those of the bulk polypropylene and secondly, their fraction is small.

As function of the temperature the T_{1H} relaxation time of the homopolymer B increases to a temperature of 60°C and above that temperature it starts to decrease. Based on results in literature,[11,12] the relaxation below 60°C is dominated by methyl reorientation, although relaxation due to backbone motions starts to become more and more important with increasing temperature. Eventually, above 60°C the relaxation via backbone motions seems to be the most important relaxation way. For the copolymer I* the relaxation time increases slightly with the temperature. Contrary, when measured via CP/MAS the relaxation time of the bulk polypropylene increases while that of the copolymer part stays more or less the same.

	20°C	40°C	60°C	80°C	100°C	120°C	140°C
B	0.86(.01)	1.07(.01)	1.17(.01)	1.13(.01)	1.02(.01)	1.01(.01)	1.06(.02)
I*	0.74(.01)	0.85(.02)	0.92(.02)	0.93(.01)	0.92(.01)	1.07(.02)	1.12(.01)

Table 6.1: T_{1H} relaxation times of the polypropylene sample B and the ethylene-propylene block copolymer sample I* as a function of the temperature and measured on a 400 MHz NMR. The inversion pulse sequence (section 2.4.2) was used without a solid echo pulse. The time between the 180° pulse and the 90° pulse was varied between 0.001 and 6s. Equation 5.7 was obtained for the analysis. The standard deviation is given between brackets.

The *influence of the magnetic field* was also tested for the wideline measurements. The measurements were run on a 20MHz industrial NMR and its results, shown in Table 6.2, were compared with those of the 400MHz NMR (Table 6.1). As was also found for the CP/MAS measurements (Table 5.22) the relaxation times decrease for lower field NMR spectrometers. It is clear from these results that the T_{1H} minimum versus temperature changes with the magnetic field. The spin lattice relaxation time exhibits a minimum when the spectrum of thermal motions contains a preponderance of motions in the frequency region near the resonant frequency of the NMR experiment, i.e. 20 and 400MHz. This means that at lower magnetic fields the T_{1H} minimum shifts to lower temperatures. For both samples the relaxation time, measured on the 20MHz NMR, decreases with increasing temperature and the relaxation will be dominated by the backbone motions.

This implies that one can choose which motion (methyl reorientation or backbone motions) one would like to study by changing the temperature and/or by changing the magnetic field.

	40°C	100°C
B	0.235(.006)	0.111(.004)
I*	0.14(.01)	0.128(.005)

Table 6.2: T_{1H} relaxation times given in seconds for the polypropylene sample B and the ethylene-propylene copolymer I*. The measurements were recorded on a 20MHz NMR. The pulse sequence described in section 2.4.2 was used. The variable time was gradually changed between 0.001 and 1.1s. The standard deviation is given between brackets.

To *compare the different copolymer samples*, the T_{1H} measurements were run at 100°C on the 20MHz NMR to be sure that the relaxation is dominated by the backbone motions and not by the methyl reorientation. Only small differences were found between the different samples. This can be caused by the fact that no distinction can be made between the relaxation of the bulk and the ethylene-propylene copolymer part and only one relaxation time describes the T_{1H} behaviour of the whole sample.

A relaxation parameter that gives more than one relaxation time, like T_{2H}, is expected to give more accurate information.

100°C	B	J	H	I	I*
T_{1H}	0.111(.004)	0.112(.003)	0.118(.002)	0.125(0.002)	0.128(.005)

Table 6.3: The spin lattice relaxation time of the polypropylene sample B, the random copolymer J and the block copolymers H, I and I*. The relaxation time was measured at 100°C on a 20MHz with the pulse sequence described in section 2.4.2. The time between the 180° pulse and the 90° pulse was varied between 0.001 and 1.1s. The relaxation times are given in seconds and the standard deviation is given between brackets.

6.3. The spin spin relaxation time

T_{2H} was measured by using the solid echo, the Hahn echo and the CPMG pulse sequence (section 2.4.1). With the solid echo pulse sequence the component with the short relaxation time of a few microseconds is emphasised[13] while long relaxation times of some milliseconds are filtered with the CPMG pulse sequence. The Hahn echo pulse sequence is used for relaxation times in between. Ethylene-propylene copolymers contain very immobile parts, like the crystalline polypropylene and on the other hand very mobile parts, like the ethylene-propylene copolymer rubber. The mobility of the chains in the block copolymers is spread over a wide range of frequencies and therefore the spin spin relaxation times will change from some microseconds to milliseconds within one copolymer sample. Therefore, the three kinds of pulse sequences were used to study the spin spin relaxation time of the copolymers.

6.3.1. T_{2H} study with the solid echo pulse sequence

T_{2H} was measured for a polypropylene sample as well as for copolymer samples by using the solid echo pulse sequence. The analysis of such a solid echo decay curve is not an easy task. First of all it has to be noticed that it is not possible to use the whole FID. For the analysis only the data points with $t<200\mu s$ were used, i.e. until the FID intensity has decreased to about 5% of the starting intensity (Figure 6.1).

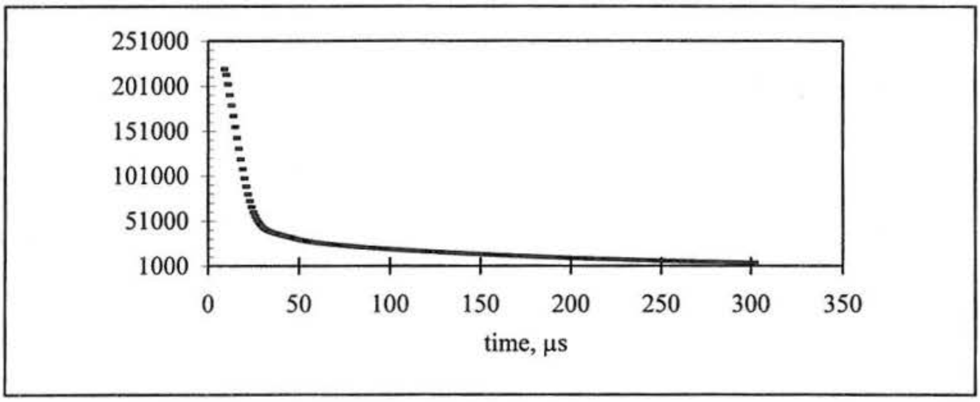

Figure 6.1: The solid echo decay curve of the ethylene-propylene block copolymer sample I at 20°C.

For the analysis of the FID some researchers[14,15] prefer to use Gaussian and exponential functions while others[4,16] use the Abragamian and the Weibullian function combined with one or two exponential functions. The Weibullian function[17] ranges between a Gaussian and an exponential function:

$$M(t) = M_o \cdot \exp\left(-\left(\frac{t}{T_2}\right)^n\right) \quad \text{with } 1<n<2. \tag{6.1}$$

The Abragamian function is a Gaussian-broadened sinc function. This function was first suggested by Abragam[18] as a phenomenological expression of the ^{19}F FID of CaF_2 and has been found to be a good representation for the FID from other regular, crystalline lattices:

$$M(t) = M_0 \frac{\sin(2\pi\nu t)}{2\pi\nu t} \exp\left(-\left(\frac{t}{T_2}\right)^2\right) \quad \text{with } \nu \text{ in Hertz and t in seconds.} \qquad (6.2)$$

The two groups of equations were evaluated. The solid echo decay was analysed in one way with an Abragamian, a Weibullian and an exponential component and in the other way with a Gaussian and two exponential functions. It has to be pointed out here that the first method is an eight parameter fit while the second method is a six parameter fit. Based on the criteria for determination of 'goodness of fit'(section 9.1.2.4), the second method was chosen. Both methods gave more or less the same T_{2H} values.

6.3.1.1. The spin spin relaxation of polypropylene measured with the solid echo pulse sequence

The results of the T_{2H} measurements of polypropylene sample B at different temperatures are shown in Figure 6.2.

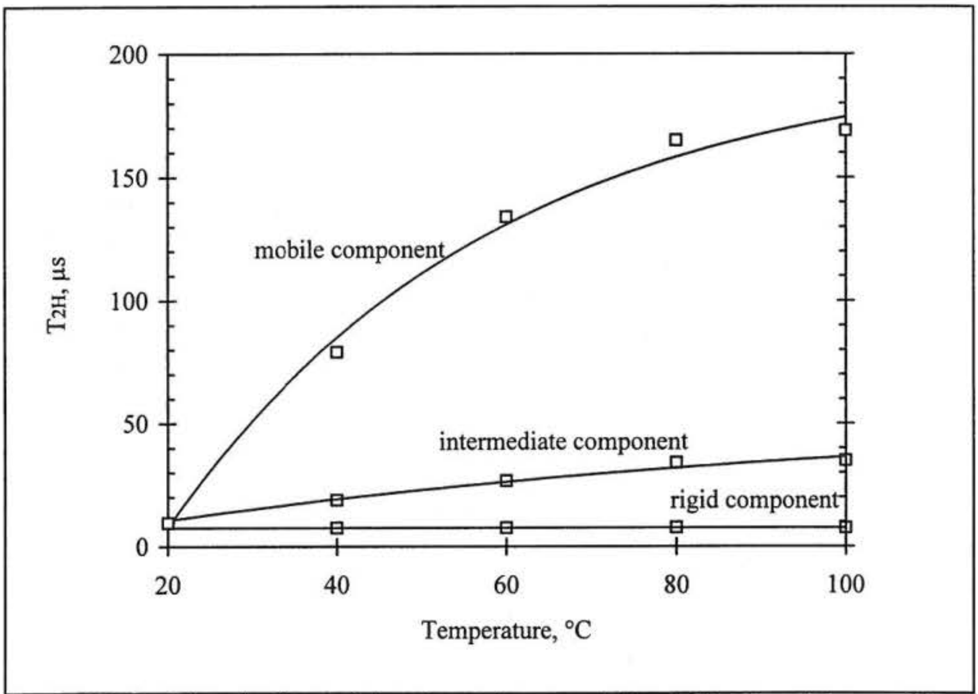

Figure 6.2: T_{2H} relaxation times of the polypropylene sample B as a function of the temperature between 20 and 100°C. The relaxation times were measured with the solid echo pulse sequence (section 2.4.1.1) with τ = 4.5µs. A Gaussian (rigid component) and one or two exponential functions were used for the analysis.

The number of components that are needed to fit the data, depends on the temperature. At low temperatures only one Gaussian function with a short T_{2H} value is needed to describe the decay. The reason is that at temperatures close to the glass transition of -1.9°C the mobility of the amorphous part of the polymer is restricted. At higher temperatures the mobility of the amorphous domain deviates more from the rigid domain, whose mobility is still restricted by the crystal lattice until the melting point. In between the rigid and the mobile domain of the polymer, there is an interphase with a mobility in between. The three components will be named as rigid, intermediate and mobile component instead of crystalline, interphase and amorphous component because at low temperatures there is no difference in the relaxation times of the crystalline, interphase and amorphous domain. The short T_{2H} relaxation time which is connected with the rigid domain stays constant over the whole temperature range while the other relaxation times increase with the temperature. The polymer chains in the amorphous domain get a higher mobility with increasing temperature, which explains the increasing spin spin relaxation time of the mobile and intermediate component.

Besides the effect of the temperature on the relaxation times, the temperature has also an influence on the fractions connected with the different relaxation times (Figure 6.3). At 20°C there is only one rigid component whose fraction decreases at higher temperatures. A rigid fraction of 100% at 20°C does not mean that the crystallinity is 100% but at that temperature it is not possible to make a differentiation with T_{2H} between the crystalline domain and the almost glassy amorphous domain. To deduce the percentage crystallinity from these measurements, the measuring temperature has to be well above the glass transition temperature. At 80° or 100°C, the fraction of the rigid domain reaches a more constant value and the mobility of the mobile domain differs much from the rigid domain. The percentage crystallinity is 55%. This value is higher than the 38.3% crystallinity determined with DSC. It has to be pointed out here that the solid echo pulse sequence is used to emphasise the initial part of the FID and to determine accurately the small relaxation times. Moreover, it is not useful for long relaxation times. This can cause a too high fraction of the rigid domain.

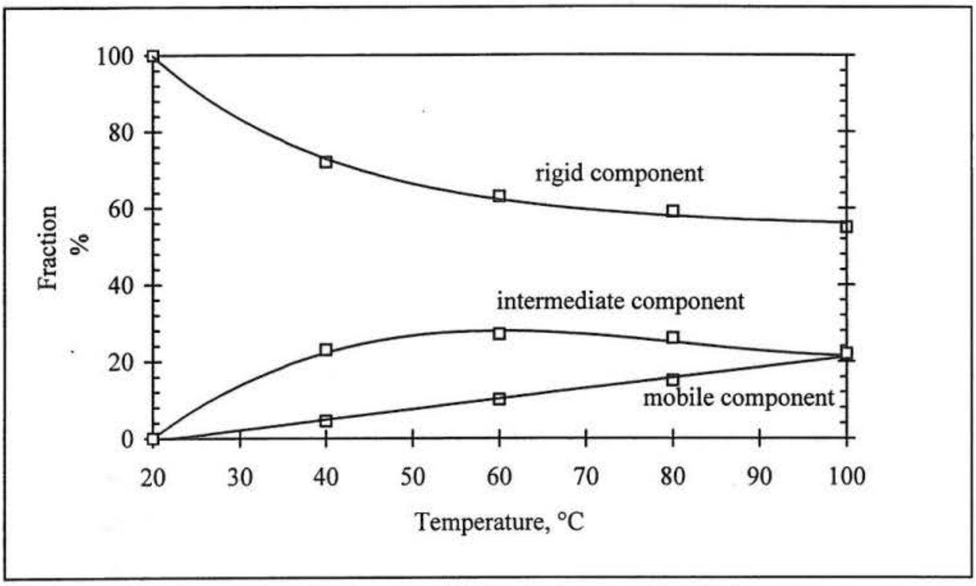

Figure 6.3: The influence of the temperature on the fractions of the different spin spin relaxation times of a polypropylene sample B measured with the solid echo pulse sequence (section 2.4.1.1). The spin spin relaxation times are shown in Figure 6.2.

6.3.1.2. The T_{2H} relaxation of block copolymers measured with the solid echo pulse sequence

As for the homopolymer, the spin spin relaxation of the *ethylene-propylene copolymer I** was measured with the solid echo pulse sequence (Figure 6.4). For the copolymer the solid echo decay is a superposition of a Gaussian and an exponential function. A third component was not found as for the homopolymer. A possible reason is that the longest component can't be seen with the solid echo pulse sequence probably because the relaxation was too slow. For the copolymer the mobility of the chain segments in the ethylene-propylene copolymer domains is higher at a certain temperature compared with the homopolymer because of its lower glass transition temperature (section 3.5). A higher mobility is reflected in higher T_2 relaxation times which can't be measured with the solid echo pulse sequence. On the other hand short relaxation times can be determined accurately with this pulse sequence. The short relaxation time of 9µs is constant over the whole temperature range and it is related with the rigid domain. This value is exactly the same as for the homopolymer sample B. Therefore it can be concluded that the short relaxation time is connected with the crystalline polypropylene. The long T_2 component is longer for the copolymer than for the homopolymer at any temperature because of the lower glass transition temperature of the copolymer domains.

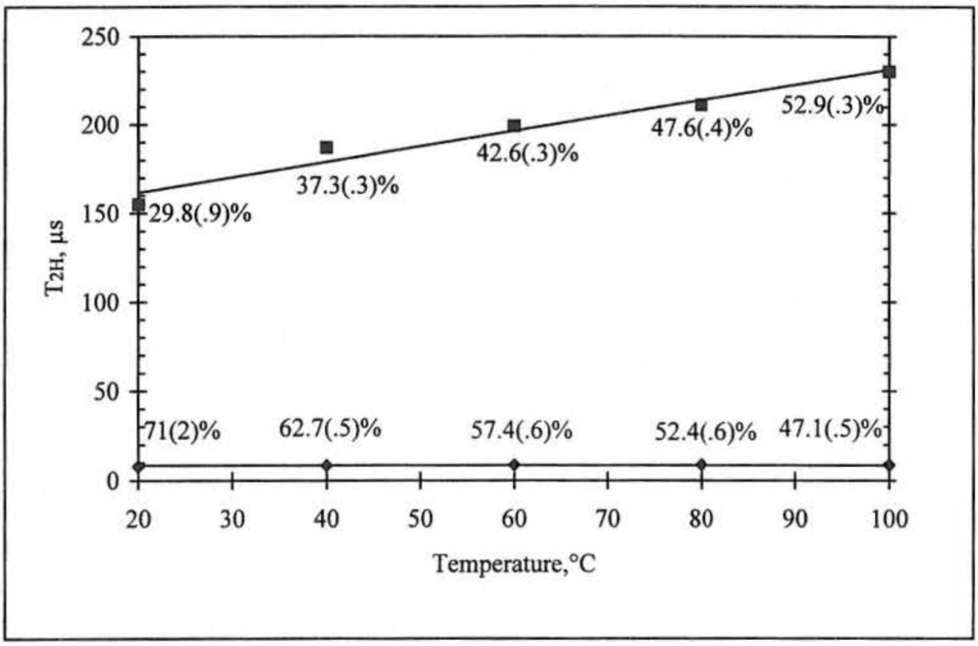

Figure 6.4: The effect of the temperature on the T_{2H} relaxation times of an ethylene-propylene sample I* measured with the solid echo pulse sequence (section 2.4.1.1: $\tau = 4.5\mu s$). A Gaussian and an exponential function were used for the analysis. The fraction and its standard deviation of each component are also given.

To get a better understanding of the long relaxation time of sample I*, the relaxation times of its xylene soluble fraction I^*_{xs} and xylene insoluble fraction, I^*_{xi} were determined and the results are given in Table 6.4. The xylene soluble fraction mainly exhibits the long component, while the short relaxation time of sample I* is mainly found in the xylene insoluble fraction. This indicates that the short T_{2H} time represents chiefly the bulk polypropylene, the crystalline as well as the amorphous polypropylene. The long T_{2H} relaxation time can be attributed to the true ethylene-propylene copolymer. This is valid at 20°C because at high temperature the T_{2H} of the mobile sample I^*_{xs} is too long to be observed by the solid echo pulse sequence. This means that the long component of sample I* at 90°C mainly represents the mobile or amorphous polypropylene.

	I^*		I^*_{xs}		I^*_{xi}	
	M (%)	T_{2H} (μs)	M (%)	T_{2H} (μs)	M (%)	T_{2H} (μs)
20°C	71(2)	8.0(.2)	4.5(.5)	9.1(.5)	89.9(.4)	9.29(.01)
	29.8(.9)	155(7)	96(1)	220(5)	10.0(.2)	85.6(.9)
100°C	47.1(.5)	8.77(.09)	[a]	[a]	51.9(.2)	8.64(.01)
					26.0(.2)	37.1(.4)
	52.9(.3)	230(2)			22.1(.2)	160.6(.7)

Table 6.4: T_{2H} relaxation times of sample I*, the xylene soluble and xylene insoluble fraction of sample I*, measured with the solid echo pulse sequence (section 2.4.1.1 with τ = 4.5μs). One Gaussian (short component) and one or two exponential functions were obtained for the analysis. The standard deviation is given between brackets. [a]The intensity of the solid echo decay of sample I^*_{xs} at 100°C was too small to determine the relaxation time.

Concerning the fractions of the two components of sample I* shown in Figure 6.4, one has to keep in mind that the pulse sequence used is useful for measuring short T_2 times and it suppresses the slow relaxation of mobile domains. The fractions of the two components change with the temperature. At higher temperatures the fraction of the rigid component decreases as was the case for the homopolymer (Figure 6.3). The percentage of the rigid component does not change to a constant value at high temperature. This implies that the percentage crystallinity can't be deduced from these measurements although measurements were done at temperatures high enough above T_g. The fact is, as was already mentioned, that the copolymers are too mobile to be completely seen with this pulse sequence. This will be pointed out in section 6.3.3.

6.3.1.3. The T_{2H} relaxation of the xylene soluble fractions measured with the solid echo pulse sequence

In Table 6.4 it is shown that the xylene soluble fraction, I^*_{xs} has a short T_{2H} time of 9.1μs for only 4.5%. This is a very small contribution and therefore it was checked that the other xylene soluble fractions exhibit a comparable relaxation time. The results are shown in Table 6.5. For three samples (H, I* and J) a small component of around 9μs was found and the contribution increased from sample I^*_{xs} to H_{xs} and J_{xs}. These samples have an immobile fraction at 20°C which can be explained in terms of the sequence distribution. Sample J_{xs} has among the xylene soluble fractions the largest percentage of propylene sequences of three or more units long, followed by sample H_{xs}, I^*_{xs} and then I_{xs}. At room temperature the polypropylene is just above its glass transition temperature and will be more or less immobile. This results in a short spin spin relaxation time.

The long relaxation time T''_{2H} increases from sample J_{xs} to sample I^*_{xs}. This matter will be later discussed when the samples are measured with the CPMG pulse sequence (Table 6.12).

	M' (%)	T'_{2H} (μs)	M" (%)	T''_{2H} (μs)
I^*_{xs}	4.5(.5)	9.1(.5)	96(1)	220(5)
I_{xs}		[a]		201(1)
H_{xs}	18.6(.2)	9.7(.1)	81.4(.2)	193.2(.4)
J_{xs}	24.7(.2)	9.20(.07)	75.2(.2)	177.6(.4)

Table 6.5: T_{2H} relaxation times of the xylene soluble fractions, measured with the solid echo pulse sequence (section 2.4.1.1: τ = 4.5μs). A Gaussian and an exponential function were used for the analysis. The standard deviation is given between brackets. [a]The contribution of the short component was too small to determine.

6.3.1.4. The spin spin relaxation behaviour of the xylene insoluble fractions measured with the solid echo pulse sequence

As the solid echo pulse sequence is used to study the immobile part of the polymer, the xylene insoluble fractions which mainly contain the crystalline polypropylene and polyethylene were analysed with this pulse sequence. The results are collected in Table 6.6.

A difference can be seen between the random and the block copolymers. The random copolymer J_{xi} has a smaller T''_{2H} compared with the others. This can be explained by the fact that it is the ethylene that locally reduces the glass transition temperature and sample J_{xi} contains only about 1.1% ethylene in comparison with about 5 to 8 percent for the block copolymer fractions. This means that the random copolymer fraction J_{xi}, can be compared better with a pure polypropylene sample which is at 20°C just above its glass transition temperature. On the other hand, sample J_{xi} has already at 20°C two T_{2H} components while the polypropylene sample B has only one relaxation time. This indicates that sample J_{xi} must have a higher mobility or a lower glass transition temperature. This is the result of the small ethylene content.

For the block copolymers, more or less the same results were found.

	M' (%)	T'_{2H} (μs)	M" (%)	T''_{2H} (μs)
I^*_{xi}	89.9(.4)	9.29(.01)	10.0(.2)	85.6(.9)
I_{xi}	90(1)	9.68(.03)	10(1)	87(1)
H_{xi}	87.9(.6)	9.69(.05)	12.1(.3)	92(3)
J_{xi}	89.1(.7)	8.5(.1)	10.9(.4)	36(1)

Table 6.6: The T_{2H} relaxation times of the xylene insoluble fractions, measured at 20°C with the solid echo pulse sequence (section 2.4.1.1 with $\tau = 4.5\mu s$). A Gausian and an exponential function were obtained for the analysis. The standard deviation is given between brackets.

6.3.1.5. Conclusions

With the solid echo pulse sequence the T_{2H} relaxation of the rigid part of the polymer was studied and the same short T_{2H} time was found for the polypropylene and for the ethylene-propylene copolymer samples. This short relaxation time is connected with the rigid polypropylene. At low temperature it represents the whole bulk polypropylene while at high temperature it is the crystalline polypropylene. The short T_{2H} relaxation time stays constant over the temperature region between 20°C and 100°C while the other relaxation times increase with the temperature.

To emphasise the more mobile phase of the polymer, like the true ethylene-propylene copolymer the Hahn echo pulse sequence can be used.

6.3.2. T_{2H} study with the Hahn echo pulse sequence

6.3.2.1. T_{2H} measurement of polypropylene with the Hahn echo pulse sequence

The spin spin relaxation time of a polypropylene sample was measured with the Hahn echo pulse sequence at different temperatures (Figure 6.5). A resemblance is found with the T_{2H} data measured with the solid echo pulse sequence: three components were needed for the fitting of the decay except at low temperature two components were found. The short rigid component of about 9μs is also fitted with a Gaussian function and is constant over the whole temperature range. The intermediate and mobile component were again fitted as exponential functions and the relaxation times also increase with the temperature. The T_{2H} of the intermediate and mobile component, measured with the Hahn echo pulse sequence, are longer than when measured with the solid echo pulse sequence. With the solid echo pulse sequence relaxation times of tens of microseconds can be best measured while the Hahn echo can be better used for longer relaxation times. Moreover, it seems that the amorphous domain consists of a wide range of mobilities. Depending on the pulse sequence used, other relaxation times represent the amorphous domain.

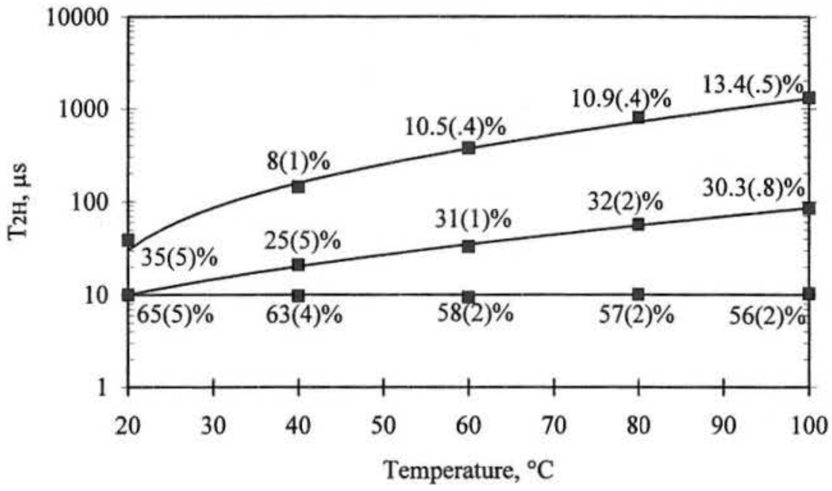

Figure 6.5: The spin spin relaxation times of the polypropylene sample B, measured at different temperatures with the Hahn echo pulse sequence (section 2.4.1.2). At 20°C the time τ was varied between 6 and 600µs, while at 90°C this time was gradually changed between 6 and 50000µs. A Gaussian (short component) and one or two exponential functions were used for the analysis. The fractions and their standard deviations are also shown.

6.3.2.2. T_{2H} measurement of ethylene-propylene block copolymers with the Hahn echo pulse sequence

As the Hahn echo pulse sequence can be better used for mobile systems than the solid echo pulse sequence, this pulse sequence gives more accurate results for the ethylene-propylene copolymers. The results are shown in Figure 6.6 for sample I*.

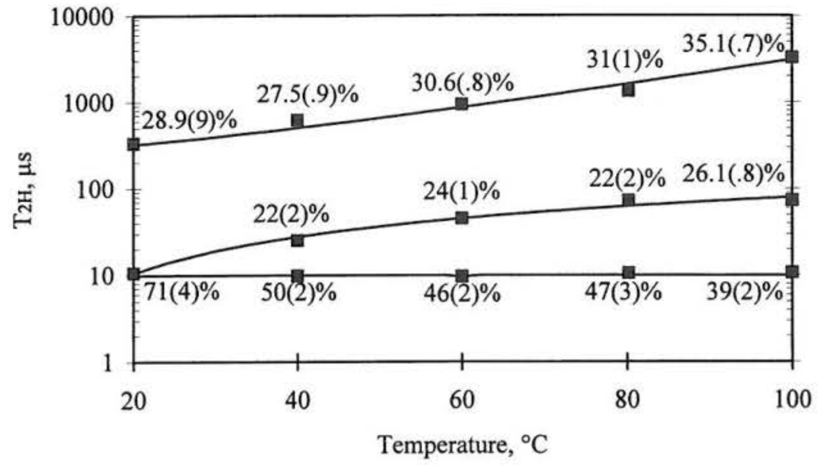

Figure 6.6: The spin spin relaxation times of the ethylene-propylene block copolymer I*, measured at different temperatures with the Hahn echo pulse sequence (section 2.4.1.2). At 20°C the time τ was varied between 6 and 1000µs, while at 100°C it was changed between 6 and 5100µs. A Gaussian and an exponential function were used for the analysis. The fractions and their standard deviations are also shown.

Now three components were used for the Hahn echo decay instead of two components as for the solid echo decay. Concerning the fractions of the components the rigid fraction decreases when the temperature increases as was found with the solid echo pulse sequence. To get a better understanding of the relaxation times of sample I* its xylene soluble and xylene insoluble fraction were measured with the Hahn echo pulse sequence. The results are collected in Table 6.7. The short relaxation times of sample I^*_{xs} and I^*_{xi} are higher than measured with the solid echo pulse sequence. This indicates that the Hahn echo pulse sequence is not as good as the solid echo pulse sequence for the determination of short relaxation times. The short relaxation time (10µs) of sample I* at room temperature is mainly found in sample I^*_{xi} and the long relaxation times can be best compared with the relaxation times of the sample I^*_{xs}. This xylene soluble fraction I^*_{xs} has a relaxation time of even more than 1ms at room temperature. This component can be associated with the most mobile part of the polymer like the low molecular weight part. As the sample I* also contains the low molecular weight fraction one can wonder why this long component of 1ms is not found in sample I*. First of all, sample I* contains 1.25% low molecular weight or oil fraction while this is 5.2% for sample I^*_{xs}. Thus, for sample I* the very slow relaxation of this small fraction can hardly be seen. The low molecular weight part causes that the long T_{2H} time (381μs) of sample I* is longer than the long T_{2H} time (183μs) of sample I^*_{xi}.

	I*		I^*_{xs}		I^*_{xi}	
	M (%)	T_{2H} (μs)	M (%)	T_{2H} (μs)	M (%)	T_{2H} (μs)
20°C	71(4)	10.6(.2)	12.4(.1)	18.5(.1)	80(4)	16.9(.9)
	28.9(.9)	381(9)	76.4(.6)	370(2)	20(2)	183(13)
			11.2(.4)	1345(35)		
100°C	39(2)	10.7(.3)			62(3)	13.5(.4)
	26.1(.8)	73(4)	39(3)	727(27)	29(1)	76(4)
	35.1(.7)	3240(244)	61(4)	3889(237)	8.5(.4)	1652(100)

Table 6.7: The spin spin relaxation times of sample I*, I^*_{xs} and I^*_{xi} measured with the Hahn echo pulse sequence (section 2.4.1.2) with the time τ varied between 6 and 1000μs at 20°C. At 90°C this time was gradually changed between 6 and 5100μs. A Gausian (short component) and one or two exponential functions were obtained for the analysis. The standard deviation is given between brackets.

At 100°C the short component of sample I* can be associated with the short component of sample I^*_{xi} and describes the relaxation of the crystalline polypropylene. The two longest relaxation times of the ethylene-propylene block copolymer I* are connected with the amorphous part of the polymer, like the amorphous polypropylene, the ethylene-propylene rubber and the low molecular weight fraction.

It has to be mentioned here that a component cannot be associated with one certain part of the polymer, like the crystalline, the amorphous domain, the interphase and the low molecular weight fraction parts. Hence, the polymer exhibits a wide distribution of mobilities and relaxation times. In fact the relaxation should be fitted with an infinite number of relaxation times. The three relaxation times given in the table give already a good representation of all the relaxation times and every component will represent one or more phases or parts of the sample. Thus, the longest component of sample I^*_{xs} does not only represent the low molecular weight as was measured from fractionation but maybe can be associated with a broader distribution of molecular weights.

6.3.2.3. The spin spin relaxation time of the different copolymer samples measured with the Hahn echo pulse sequence

The spin spin relaxation times of the different samples, J, H, I and I*, measured with the Hahn echo pulse sequence were compared and the results are given in Table 6.8. It seems that the long T''_{2H} time which mainly represents the ethylene-propylene rubber is shorter for the random copolymer J compared with the block copolymers. The random copolymer J, in which the ethylene is randomly distributed has one glass transition temperature (-14.9°C) while the block copolymers have a lower glass transition temperature (-54.8°C) of the ethylene-propylene rubber that is dispersed in the bulk polypropylene matrix with a higher T_g (Table 3.5). Hence, the block copolymers have at room temperature ethylene-propylene copolymer chains with a higher mobility than sample J. This results in higher relaxation times for the block copolymers compared with the random copolymer J.

Concerning the block copolymers (H, I and I*) the relaxation times are more or less the same but their fractions differ. Sample I* has the highest fraction of mobile component, followed by sample I and then H. Sample I* has also the highest ethylene content and short ethylene and propylene sequences, the highest xylene soluble fraction and best impact strength. Thus, it can be concluded here that the copolymer sample which contains a larger amount of ethylene, that is divided in short sequences, has the best impact strength and this is reflected in a higher fraction of mobile component in a Hahn echo experiment.

	M' (%)	T'_{2H} (μs)	M'' (%)	T''_{2H} (μs)
J	96(1)	8.2(.2)	4.4(.1)	113(12)
H	92(2)	13.4(.1)	8.3(.2)	358(15)
I	86(3)	14.1(.2)	13.9(.4)	362(16)
I*	71(4)	10.6(.2)	28.9(.9)	381(9)

Table 6.8: The spin spin relaxation times of the samples J, H, I and I* measured with the Hahn echo (section 2.4.1.2) pulse sequence at 20°C with the time τ varied between 6 and 1000μs. A combination of a Gaussian and an exponential function was used for the analysis. The standard deviation is given between brackets.

From the results of the Hahn echo pulse sequence it is known that some samples are very mobile, surely at high temperature and relaxation times of some milliseconds are found. The best way to measure such long relaxation times is by using the CPMG pulse sequence.

6.3.3. T_{2H} study with the CPMG pulse sequence

6.3.3.1. A comparison between the T_{2H} relaxation of polypropylene and ethylene-propylene block copolymers when measured with the CPMG pulse sequence

To study the relaxation times of the most mobile part of the polymer the pulse sequence of Carr Purcell Meiboom and Gill can be used (section 2.4.1.3). The relaxation times of the polypropylene sample B, the ethylene-propylene block copolymer I* and its fractions I^*_{xs} and I^*_{xi}, measured at 20°C, are given in Table 6.9. Only exponential functions were used for the analysis of the decays. Two components resulted in the best fit; except for sample B at room temperature because this sample is still very immobilised at 20°C. Only a small signal could be seen with this pulse sequence. At 20°C the relaxation times of sample I* and sample I^*_{xs} are more or less the same. This indicates that with this pulse sequence and at 20°C the relaxation of sample I* is dominated by the ethylene-propylene rubber domain.

20°C	M' (%)	T'_{2H} (ms)	M" (%)	$T"_{2H}$ (ms)
B		0.12(.02)		
I*	54(3)	0.40(.04)	46(4)	2.19(.09)
I^*_{xs}	53(4)	0.65(.04)	47(4)	2.6(.1)
I^*_{xi}	86(4)	0.085(.004)	15(1)	1.04(.09)

Table 6.9: The spin spin relaxation times of the samples B, I* and its xylene soluble fraction, I^*_{xs} and its xylene insoluble fraction I^*_{xi} measured at 20°C with the CPMG pulse sequence (section 2.4.1.3 with $\tau = 20\mu s$). At 20°C the time between the 90° pulse and the recorded echo was varied between 80µs and 9.28ms. One or two exponential functions were used for the analysis. The standard deviation is given between brackets.

Contrary, at 100°C (Table 6.10) the relaxation of sample I* is faster than that of sample I^*_{xs}. This can be explained as follows. At room temperature the amorphous polypropylene is just above its glass transition temperature and the contribution of the amorphous polypropylene to these long relaxation times is small. On the other hand, at high temperature the mobility of the amorphous polypropylene is increased and its relaxation contributes more to the relaxation times of sample I* measured with the CPMG pulse sequence.

Eventually, it can be said that the relaxation times of sample I* lie in between these of sample I^*_{xs} and I^*_{xi}.

100°C	M' (%)	T'_{2H} (ms)	M" (%)	T''_{2H} (ms)
B	46(7)	0.14(.03)	54(4)	6.0(.3)
I*	48(3)	4.0(.3)	52(4)	20.2(.9)
I^*_{xs}	49(4)	8.3(.6)	51(5)	35(2)
I^*_{xi}	57(5)	1.0(.2)	43(4)	13.8(.2)

Table 6.10: The spin spin relaxation times of the samples B, I* and its xylene soluble fraction, I^*_{xs} and its xylene insoluble fraction I^*_{xi} measured at 100°C with the CPMG pulse sequence (section 2.4.1.3 with $\tau = 20\mu s$). The time between the 90° pulse and the recorded echo was varied between 80μs and 84ms. Two exponential functions were used for the analysis. The standard deviation is given between brackets.

Comparing the results of the Hahn and the CPMG pulse sequence, it can be concluded that the longest relaxation time, measured with the Hahn echo pulse sequence, is of the same size as the shortest relaxation time when measured with the CPMG pulse sequence.

Moreover, from the CPMG pulse sequence it is known that the polypropylene sample B and the ethylene-propylene copolymer I* have relaxation times in the millisecond region at 100°C. Such long relaxation times can not be seen with the solid echo pulse sequence. This explains the too high crystalline fraction that is measured with the solid echo pulse sequence (section 6.3.1.2) because the most mobile part of the polymer can not be detected. To study the spin spin relaxation of the ethylene-propylene heterophasic copolymers, all three pulse sequences are needed to determine the total range of relaxation times accurately.

6.3.3.2. A comparison of the T_{2H} relaxation of the block copolymers when measured with the CPMG pulse sequence

The different copolymers were compared by using the CPMG sequence and the T_{2H} results are given in Table 6.11. Comparable results are found as with the Hahn echo pulse sequence although one looks at longer relaxation times with the CPMG pulse sequence: the long relaxation time of the random copolymer J deviates from the other samples because of the lower ethylene content and the higher T_g. The percentage of the long component depends on the total ethylene content of the sample. Besides, short sequences of ethylene and propylene cause higher relaxation times.

	M' (%)	T'_{2H} (ms)	M" (%)	$T"_{2H}$ (ms)
J	90(5)	0.077(.005)	10(2)	0.46(.08)
H	65(4)	0.104(.008)	36(2)	1.43(.07)
I	53(5)	0.12(.01)	47(2)	1.71(.07)
I*	54(3)	0.40(.04)	46(4)	2.19(.09)

Table 6.11: The spin spin relaxation times of the samples, J, H, I and I*, measured at 20°C with the CPMG pulse sequence (section 2.4.1.3 with $\tau = 20\mu s$). The time between the 90° pulse and the recorded echo is varied between 80 and 9.28ms. Exponential functions were used for the analysis. The standard deviation is given between brackets.

6.3.3.3. T_{2H} study of the xylene soluble fractions when measured with the CPMG pulse sequence

As the CPMG pulse sequence emphasises the most mobile part of the polymer, it is the best way to study the xylene soluble fractions of the samples. The results are shown in Table 6.12 for the amorphous xylene soluble fractions and the xylene soluble fractions. The difference between them is that the xylene soluble fraction contains besides the ethylene-propylene rubber (i.e. the amorphous xylene soluble fraction) the low molecular weight or oil fraction. For all the fractions two relaxation times were found. The relaxation times of the amorphous xylene soluble fractions are shorter than those of the xylene soluble fractions. This difference is more obvious for the random copolymer J and this is less clear for I*. This can be explained by the percentage oil fraction in the xylene soluble fractions: sample J_{xs} consists for 23% of oil, sample H_{xs} has 9.7% oil, sample I_{xs} 7.5% and sample I^*_{xs} contains only 5.2% oil (section 3.3). This means that the relaxation times of sample J_{xs} are more influenced by the oil fraction than the other xylene soluble samples and this causes a higher difference between the relaxation times of sample J_{xs} and J_{xsa}. On the other hand, sample J_{xs} that contains the largest oil fraction does not have the largest relaxation times among the xylene soluble fractions because the relaxation times are also influenced by the mobility of the true ethylene-propylene copolymer part, which is represented by the amorphous xylene soluble fraction. The shorter relaxation time is a result of the lower ethylene content and the higher glass transition temperature of sample J_{xs}. This causes less mobile polymer chains and lower T_{2H} relaxation times.

	M' (%)	T'_{2H} (ms)	M" (%)	T''_{2H} (ms)
J_{xs}	55(3)	0.20(.02)	45(3)	1.05(.06)
H_{xs}	50(4)	0.48(.05)	50(4)	2.5(.1)
I_{xs}	48(4)	0.38(.05)	52(5)	2.32(.2)
I^*_{xs}	53(4)	0.65(.04)	46(4)	2.6(.1)
J_{xsa}	71(3)	0.105(.006)	29(3)	0.52(.03)
H_{xsa}	55(3)	0.17(.01)	45(2)	1.28(.05)
I_{xsa}	40(3)	0.20(.03)	60(3)	1.63(.07)
I^*_{xsa}	57(6)	0.56(.09)	43(6)	2.0(.3)

Table 6.12: The spin spin relaxation times of the xylene soluble fractions: J_{xs}, H_{xs}, I_{xs} and I^*_{xs} which contain the oil fraction and ethylene-propylene rubber, and the relaxation times of the amorphous xylene soluble fractions without oil or low molecular weight: J_{xsa}, H_{xsa}, I_{xsa} and I^*_{xsa}. The relaxation times were measured with the CPMG pulse sequence (section 2.4.1.3 with τ = 20μs) at 20°C. The time between the 90° pulse and the recorded echo is varied between 80μs and 9.28ms. For the analysis two exponential functions were used. The standard deviation is given between brackets.

The influence of the oil fraction on the T_{2H} relaxation times of the *total samples* is small because all the samples contain maximum 2% oil and the difference in oil fraction between the samples is small. So the difference in T_{2H} relaxation times between the samples J, H, I and I* must chiefly be explained in terms of the ethylene-propylene rubber fractions and their sequence.

6.3.4. The influence of the magnetic field on the spin spin relaxation times

According to equation 2.11 of chapter 2 it seems that T_{2H} is independent of the magnetic field. This was checked by measuring T_{2H} on a 20MHz and a 400MHz NMR as was discussed for the T_{1H} in section 6.2. The results of the solid echo, the Hahn echo and the CPMG pulse sequence, measured on the 20MHz and the 400MHz NMR, are collected in Table 6.13. It seems that the relaxation times differ for the different magnetic fields, surely for the Hahn echo measurements. Very short relaxation times of 10μs cannot be determined with the Hahn echo pulse sequence on the 20MHz NMR because of the dead time of 9μs. In the Hahn echo pulse sequence the FID is acquired after a time '90° -τ - 180° - τ ' and the shortest time that an FID can be acquired after the 90° pulse is two times the dead time or after 18μs for the 20MHz NMR. For the 400MHz NMR it is only 12μs. Besides, in the Hahn echo pulse sequence there is only one 180° refocusing pulse so that spin diffusion can affect the relaxation times. Moreover, the timing of the pulses has to be very correct. When this is not correct wrong relaxation times can be found.

		20MHz		400MHz	
		M (%)	T_{2H} (μs)	M (%)	T_{2H} (μs)
solid echo	40°C	63(2)	9.5(.3)	62.7(.5)	8.55(.07)
		37(1)	264(13)	37.3(.3)	187(2)
	100°C	46(2)	10(3)	47.1(.5)	8.77(.09)
		53.9(.9)	312(14)	52.9(.3)	230(2)
Hahn echo	40°C			50(2)	9.8(.3)
		60(4)	29(1)	22(2)	25(1)
		40(2)	515(27)	27.5(.9)	613(2)
	100°C			39(2)	10.7(.3)
		53(5)	44(4)	26.1(.8)	73(4)
		47(3)	1085(106)	35.1(.7)	3240(244)
CPMG	40°C	51(3)	680(70)	52(3)	800(50)
		49(1)	4400(200)	48(4)	6690(800)
	100°C	47(3)	1700(200)	48(3)	4000(300)
		53(2)	15500(500)	52(4)	20200(900)

Table 6.13: T_{2H} times of sample I* measured with the solid echo, the Hahn echo and the CPMG pulse sequence on a 20MHz and a 400MHz NMR. The measurements and analyses were done as was described in sections 6.3.1 for the solid echo pulse sequence, in section 6.3.2 for the Hahn echo pulse sequence and in section 6.3.3 for the CPMG pulse sequence.

It can be concluded that it is not allowed to compare T_{2H} results of measurements run on different NMR spectrometers although it should give theoretically similar results.

6.4. $T_{1\rho H}$ relaxation time

$T_{1\rho H}$ was measured with the pulse sequence described in section 2.4.3. For the analysis of the data exponential functions were used. The results of the measurements of the 20MHz NMR are given in Table 6.14.

As was also found with the CP/MAS measurements (chapter 5) the long $T''_{1\rho H}$ time or rigid component of the polypropylene sample B seems to decrease with the temperature while the short relaxation time or mobile component increases.

For the xylene soluble fraction I^*_{xs} the single relaxation time describes the relaxation of the ethylene-propylene rubber and it increases remarkably with the temperature.

For the block copolymer I* the interpretation of the results is more difficult because no distinction can be made between the relaxation of the bulk polypropylene and that of the true ethylene-propylene copolymer. By comparing the results of sample I* with those of the homopolymer B and the ethylene-propylene rubber I^*_{xs} it seems that at low temperature the short relaxation time contains the relaxation of the amorphous polypropylene and of the true ethylene-propylene copolymer. At high temperature the relaxation time of the crystalline polypropylene (right to $T_{1\rho H}$ minimum) and that of the true ethylene-propylene copolymer (left to the $T_{1\rho H}$ minimum) are collected in the long relaxation time and the short relaxation time of sample I* is associated with the amorphous polypropylene.

		M' (%)	$T'_{1\rho H}$ (ms)	M'' (%)	$T''_{1\rho H}$ (ms)
40°C	B	37.5(.3)	1.8(.2)	62.5(.4)	40.8(.8)
	I*	48.2(.6)	3.4(.4)	52.1(.9)	31(1)
	I^*_{xs}		7.7(.4)		
100°C	B	53(1)	6.8(.4)	47(1)	38.2(.8)
	I*	42(1)	7.0(.6)	58(2)	45(1)
	I^*_{xs}		54(2)		

Table 6.14: The $T_{1\rho H}$ relaxation times of the polypropylene sample B, the ethylene-propylene block copolymer I* and the xylene soluble fraction I^*_{xs} measured on a 20MHz NMR at different temperatures. The pulse sequence described in section 2.4.3 was used with a rf-field of 57kHz. The spin lock time was varied between 0.5 and 100ms.

Finally, it can be concluded that one has to be careful with the interpretation of the $T_{1\rho H}$ results of ethylene-propylene block copolymers because the assignment depends on the temperature.

6.5. Conclusions

The proton relaxation times of a polypropylene sample, a ethylene-propylene random copolymer and some ethylene-propylene block copolymers were measured via wideline NMR.

For polypropylene and ethylene-propylene copolymers only *one T_{1H} relaxation time* was found. For the homopolymer it is caused by complete spin diffusion while for the copolymer it isn't the result of complete spin diffusion (see chapter 5) but there exists only a small difference between the relaxation times of the bulk polypropylene and the true ethylene-propylene copolymer.

The interpretation of the *$T_{1\rho H}$ relaxation time* of the block copolymers is complex. Only two relaxation times are found while there are at least three domains with different $T_{1\rho H}$ relaxation times (the crystalline and amorphous polypropylene and the true ethylene-propylene copolymer). Moreover, some relaxation times increase with the temperature and other decrease. This means that the assignment of the relaxation time depends on the temperature.

The mobility of commercial ethylene-propylene copolymers is spread over a wide range of frequencies. This implies that T_{2H} of these copolymers ranges between a few microseconds and some tens of milliseconds. The best way to measure this broad range of relaxation times is by using different pulse sequence: the solid-echo, the Hahn echo and the CPMG pulse sequence. Each pulse sequence can be conceived as a *direct mobility filter* for ethylene-propylene copolymers. The pulse sequence that has to be used to study a certain part of the polymer depends on its mobility.

The crystalline polypropylene in the ethylene-propylene copolymers has a T_{2H} time of about 9µs and can best be measured with the solid-echo pulse sequence. At low temperature the rigid component represents the crystalline domain and the amorphous polypropylene that is just above its glass transition temperature. At high temperature the amorphous polypropylene has a higher mobility and the rigid component can be associated with the crystalline polypropylene. With this pulse sequence the most mobile part of the polymer can not be seen. This results in a too high crystalline fraction compared with DSC results.

To emphasise the mobile part of the polymer the Hahn echo or even the CPMG pulse sequence should be used. The CPMG pulse sequence can be used to determine spin spin relaxation times in the millisecond region. The relaxation times of the low molecular weight fraction and other mobile parts of the polymer like the true ethylene-propylene copolymer can be determined. For T_{2H} relaxation times of some tens or hundreds of microseconds the Hahn echo pulse sequence gives the most accurate results. Relaxation times of domains with intermediate relaxation rates as the amorphous polypropylene and the interphase can be analysed.

The spin spin relaxation time of the rigid component stays constant over the temperature range between 20 and 100°C because the mobility of the crystalline polypropylene does not change until the melting point. The other relaxation times increase with the temperature because the amorphous phase, i.e. the amorphous polypropylene as well as the ethylene-propylene copolymer is above its glass transition temperature and its mobility increases with the temperature.

The low molecular weight part increases the T_{2H} relaxation times of the sample and the influence depends on its fraction. The effect can be best measured with the CPMG pulse sequence.

The ethylene-propylene random copolymer which is a true copolymer is compared with ethylene-propylene block copolymers which consist of a polypropylene matrix blended with ethylene-propylene copolymer. It was concluded that the random copolymer at room temperature always has smaller T_{2H} relaxation times for the amorphous part of the polymer compared with the block copolymers. One reason is that the random copolymer has less ethylene. Another reason is that the random copolymer has only one glass transition temperature of -14.5°C while the block copolymers have two glass transition temperatures:-1.9°C for the bulk polypropylene and -54°C for the true ethylene-propylene rubber. As the block copolymers have locally (in the rubber domains) a lower Tg compared with the random copolymer their spin spin relaxation times are longer.

Among the block copolymers it seems that the length of the relaxation time depends on the sequence distribution of the polymer chain. A large fraction of short sequences of ethylene and propylene results in longer relaxation times. As the true ethylene-propylene copolymer has a lower glass transition temperature than the bulk polypropylene the mobility of the ethylene-propylene copolymer chains are higher at a certain temperature than for the bulk polypropylene. This is reflected in the larger relaxation times of sample I* with the highest xylene soluble fraction and the best impact strength.

If on-line, low field NMR (industrial NMR) offers opportunities for quality control then it is via T_{2H} measurements with the Hahn echo and the CPMG pulse sequence. The CPMG pulse sequence gives the largest differentiation between our samples. To get a better idea of the correlation between the relaxation times and the macroscopic properties much more samples should be measured.

6.6. References

1. Powles, J.G.; Strange, J.H.; Proc. Phys. Soc., 82 (1983), 6.

2. Tanaka, H.; J. Appl. Polym. Sci., 28 (1983), 1707.

3. McBrierty, V.J.; Douglass, D.C.; Falcone, D.R.; J; Chem. Soc. Faraday Trans. 2, 68 (1972), 1051.

4. Dadayli, D.; Harris, R.K.; Kenwright, A.M.; Say, B.J.; Sunnetçioglu, M.M.; Polymer, 35(19) (1994), 4083.

5. Loboda-Cackovic, J.; Cackovic, H.; Hosemann, R.; J. Macromol. Sci.-Phys., 16(1) (1979), 127.

6. Tanaka, H.; Inoue, Y.; Polym. Intern., 31 (1993), 9.

7. McCall, D.W.; Falcone, D.R.; Trans. Faraday Soc., 66 (1970), 262.

8. Fujimoto, K.; Nishi, T.; Kado, R.; Polym. J., 3(4) (1972), 448.

9. Bergmann, K.; J. Polym. Sci.: Polym. Phys. Edn., 16 (1978), 1611.

10. McCall, D.W.; Douglass, D.C.; Polym. Comm., 4 (1970), 433.

11. Kawai, T.; Yoshimi, Y.; Hirai, A.; J. Phys. Soc. Japan, 16 (1961), 2356.

12. Powles, J.G.; Mansfield, P.; Polym. Commun., 3 (1962), 339.

13. Ibbett, R.N.; "NMR Spectroscopy of Polymers", Chapmann & Hall, London, 1993.

14. Tanaka, H.; Nishi, T.; J. Chem. Phys., 82(9) (1985), 4326.

15. Fukumori, K.; Kurauchi, T.; Kamigaito, O.; J. Appl. Polym. Sci., 38 (1989), 1313.

16. Ito, M.; Kanamoto, T.; Tanaka, K.; J. Polym. Sci.: Polym. Phys. Edn., 23 (1985), 59.

17. Weibull, W.; J. Appl. Mech., 18 (1951), 293.

18. Abragam, A.; in "Principles of Nuclear magnetism", Oxford University Press, Oxford, 1961.

7. SUMMARY AND GENERAL CONCLUSIONS

In this work the molecular structure and dynamics of commercial ethylene-propylene copolymers were investigated with NMR spectroscopy and NMR relaxometry.

Commercial ethylene-propylene *block* copolymers consists of polypropylene in which ethylene-propylene copolymer domains are dispersed. In *random* copolymers, in stead, the ethylene is randomly incorporated along the polypropylene chains.

As the copolymers are very complex the results of some ethylene-propylene block copolymers were compared with those of a polypropylene sample. The copolymers were also fractionated to separate the bulk polypropylene from the true ethylene-propylene copolymer in order to analyse these fractions with NMR.

In the first part of this work a physico-chemical oriented **characterisation** and a liquid-state NMR analysis of these polymers were established.

In block copolymers the true ethylene-propylene copolymer domains have a local glass transition temperature that is about 50°C lower than that of the bulk polypropylene with a T_g around 0°C. This causes an improved impact strength of the block copolymers compared to polypropylene samples. On the other hand, random copolymers do not have such copolymer domains and the global glass transition temperature is reduced by 15°C compared to pure polypropylene.

From DSC measurements it seems that the percentage crystallinity of the copolymers is lower than for the polypropylene samples as a result of the incorporation of ethylene in the polypropylene chains.

Liquid-state NMR provided information about the sequence distribution and it is obvious that short sequences of ethylene and propylene improve the impact strength. The sample with the best impact strength has also the highest xylene soluble fraction, the highest ethylene content and especially a good distribution of ethylene in short sequences.

In the second part of this work the copolymers were investigated with **solid-state NMR** towards the molecular dynamics and molecular domains of the polymer. Ethylene-propylene block copolymers posses a wide range of molecular mobilities because these copolymers consists of a complex mixture of crystalline and amorphous polypropylene, true ethylene-propylene copolymer and polyethylene.

With high resolution ^{13}C MAS NMR it is possible for ethylene-propylene block copolymers to distinguish the signals of the bulk polypropylene and the true ethylene-propylene copolymer. Some relaxation times of these phases were determined as $T_{1\rho H}$, T_{1H}, T_{1C} and T_{2H}. Contrary, with ^{1}H wideline NMR all the information of the polymer is collected in one FID. A lot of attention was paid to T_{2H}. The broad range of molecular mobilities in the block copolymers causes a broad sweep of T_{2H} relaxation times. The spin spin relaxation can be measured via wideline NMR with different pulse sequences: the solid echo, the Hahn echo and the CPMG pulse sequence. The choice of the pulse sequence is a direct mobility filter towards the ethylene-propylene rubber.

The NMR characteristics of the different domains of the polymers are summarised:
The *bulk polypropylene* in ethylene-propylene block copolymers is characterised by a single T_{1H} relaxation time which means that with T_{1H} no distinction can be made between crystalline and amorphous polypropylene as a result of spin diffusion. On the other hand, $T_{1\rho H}$ shows a bi-exponential decay: the long relaxation time is ascribed to the rigid phase as crystalline polypropylene and the short or mobile relaxation time can be mainly associated with the amorphous polypropylene. From $T_{1\rho H}$ and T_{1H} measurements it was concluded that the size of the crystalline domain lies between 4.8 and 23nm.

The $T_{1\rho H}$ relaxation time of the rigid phase is very sensitive to the thermal treatment of the sample. Since this relaxation time varies from 30ms for non annealed samples to 87ms for the best annealed sample $T_{1\rho H}$ can be used as a probe for the thermal pretreatment of the sample.. On top, annealed samples show a splitting of the methylene ($S_{\alpha\alpha}$) and methyl ($P_{\beta\beta}$) signal in the ^{13}C solid-state spectrum.

From T_{2H} measurements at room temperature it is known that just above the glass transition temperature (-1.9°C) no differences in molecular mobility between the crystalline and amorphous polypropylene can be detected. The mobility of the amorphous polypropylene is restricted 20°C above T_g and it resembles the mobility of the crystalline polypropylene. At higher temperature two or even three relaxation times are found as a result of the increase in mobility of the amorphous polypropylene. Hence, the temperature must be high enough above the glass transition temperature to measure a difference in molecular mobility between the crystalline and amorphous polypropylene. This was also reflected in the line width of the signals in the ^{13}C MAS spectrum. The line width reduces gradually as function of the temperature. Starting from 50°C a distinction can be made between the signals of the rigid and mobile methylene and methine carbons of the bulk polypropylene. The advantage is that at elevated temperatures the relaxation times of the mobile and rigid carbon atoms can be determined separately.

It was also concluded that the true ethylene-propylene copolymer domains have less or no effect on the relaxation time of the bulk polypropylene in block copolymers because in CP/MAS experiments no differences in relaxation times were discovered between the bulk polypropylene of ethylene-propylene block copolymers and the pure polypropylene sample.

As the ethylene-propylene block copolymers contain at most 25% true ethylene-propylene copolymer the signals of the *true ethylene-propylene copolymer domain* in the MAS and CP/MAS spectrum are rather small compared with the signals of the bulk polypropylene. The signals of the mobile phases, i.e. the amorphous polypropylene and the true ethylene-propylene copolymer can be emphasised in the MAS spectrum due to the short T_{1C} time. Furthermore, a selectivity can be achieved in CP/MAS spectra at higher temperatures. A short contact time of 1ms suppresses the mobile phases, while this phase is emphasised relatively with a contact time of 13ms. This improves the determination of the relaxation times of the true ethylene-propylene copolymer domain.

From $T_{1\rho H}$ measurements there was concluded that this relaxation time of the ethylene-propylene copolymer domains is strongly effected by the temperature: it varies from a few milliseconds at room temperature to almost 100ms at 90°C, while for the amorphous polypropylene not more than 18ms is reached at 90°C. This confirms that the mobility of the copolymer domains must be higher than that of the bulk polypropylene. This result is in agreement with the lower glass transition temperature of the true ethylene-propylene copolymer domains compared with the T_g of polypropylene. The higher mobility of the copolymer is also reflected in a higher T_{2H} relaxation time. The T_{2H} relaxation time of the true copolymer increases to some tens of milliseconds at 100°C.

Commercial ethylene-propylene copolymers also contains a small amount of *polyethylene* and a distinction between the mobility of the copolymer and the crystalline polyethylene can be made with $T_{1\rho H}$.

From the CPMG measurement it was concluded that the *low molecular weight* does increase the T_{2H} relaxation time and the effect depends on the fraction.

At this moment a first interpretation of the results of an **industrial NMR** can be reported.

With wideline NMR only *one T_{1H} relaxation time* was found for the ethylene-propylene block copolymers. From the CP/MAS experiments it is known that the relaxation time is not averaged out over the whole sample by spin diffusion. The relaxation times of the polypropylene and the true ethylene-propylene copolymer differ for less than 1 second and no distinction can be made with wideline NMR.

$T_{1\rho H}$ relaxation times determined from wideline NMR should be interpreted with care. Two relaxation times are found with wideline NMR while some times are determined with CP/MAS NMR. The assignment of the two relaxation times determined with wideline NMR depends on the temperature.

The spin spin relaxation of the block copolymers ranges from a few microseconds to some milliseconds. The relaxation is in fact a distribution of many relaxation times of carbon atoms with different mobilities. This distribution is represented by two or three relaxation times. Depending on the pulse sequence used certain relaxation times are emphasised and another set of relaxation times are representative for the distribution of relaxation times.

A comparison of the samples showed that the polypropylene samples have always shorter T_{2H} relaxation times compared to the copolymers due to the higher T_g of polypropylene. There exists also a difference between block and random copolymers. The random copolymer has shorter T_{2H} relaxation times compared with the block copolymers. Moreover, the results showed that there exists a relation between the T_{2H} relaxation times and other properties of the samples. Samples with more ethylene and with their ethylene divided in short sequences have the highest T_{2H} relaxation times and the best impact strength.

If on-line low field NMR offers some possibilities for quality control, it is expected that it is measured via T_{2H} via the Hahn or the CPMG pulse sequence. With the CPMG pulse sequence the most mobile part of the polymer like the ethylene-propylene rubber can be measured and it is this phase of the polymer that improves the properties (impact strength) of the bulk polypropylene.

8. SAMENVATTING EN ALGEMENE CONCLUSIES

In dit werk werden de moleculaire structuur en dynamica van commerciële ethyleen-propyleen copolymeren onderzocht m.b.v. NMR spectroscopie en NMR relaxometrie.

Commerciële ethyleen-propyleen *blok*copolymeren bestaan uit een polypropyleen matrix waarin ethyleen-propyleen copolymere domeinen verspreid zitten. In *random*copolymeren daarentegen is het ethyleen willekeurig verdeeld in de polypropyleen keten.

Daar de structuur van deze copolymeren zeer complex is werden de NMR resultaten vergeleken met deze van een polypropyleen staal. Bovendien werden de copolymeren gefractioneerd om het bulk polypropyleen en het 'echte' copolymeer apart te kunnen analyseren met NMR.

In het eerste deel van dit werk werden de polymeren aan een fysico-chemisch georiënteerde **karakterisatie** en een vloeistof NMR analyse onderworpen.

In blokcopolymeren hebben de ethyleen-propyleen copolymere domeinen een lokale glastransitieovergang die ongeveer 50°C lager is dan deze van het bulk polypropyleen met een T_g rond 0°C. De aanwezigheid van deze domeinen zorgt voor de verbetering van de slagvastheid van de blokcopolymeren t.o.v. polypropyleen stalen. Randomcopolymeren daarentegen hebben geen copolymere domeinen en de globale glasovergang is verlaagd met 15°C t.o.v. polypropyleen.

Uit DSC metingen bleek dat het percentage kristalliniteit van de copolymeren lager is dan voor de polypropyleen stalen als gevolg van de aanwezigheid van ethyleen in de polypropyleen ketens.

Met vloeistof NMR werd de sequentiedistributie bepaald. Hieruit kon afgeleid worden dat korte sequenties van ethyleen en propyleen de slagvastheid verbeteren. Stalen met een goede impactsterkte hebben ook een hoge xyleen oplosbare fractie, een hoog ethyleen gehalte en vooral een goede verdeling van het ethyleen in korte sequenties.

In het tweede deel van dit werk werd aangetoond dat **vaste stof NMR** interessante informatie kan verschaffen omtrent de moleculaire dynamica en de moleculaire domeinen van de copolymeren. Ethyleen-propyleen copolymeren bestaan uit een complex mengsel van kristallijn en amorf polypropyleen, 'echt' ethyleen-propyleen copolymeer en polyethyleen waardoor de mobiliteit van de verschillende domeinen in zo'n copolymeer sterk kunnen variëren.

Met hoge resolutie ^{13}C MAS NMR is het mogelijk een onderscheid te maken tussen de signalen van het bulk polypropyleen en het 'echte' copolymeer. Enkele relaxatietijden van de verschillende domeinen werden bepaald, zoals T_{1H}, $T_{1\rho H}$, T_{1C} en T_{2H}. Met ^{1}H wideline NMR bevat het te analyseren FID alle informatie van de verschillende domeinen van het polymeer. Met deze techniek werd vooral aandacht besteed aan T_{2H} metingen. De grote spreiding van moleculaire mobiliteiten in blokcopolymeren veroorzaakt ook een grote spreiding aan T_{2H} tijden. Deze spin-spin relaxatietijden kunnen via wideline NMR met verschillende pulssequenties onderzocht worden: de solid echo, de Hahn echo en de CPMG pulssequentie. De keuze van de pulssequentie is een directe mobiliteitsfilter naar het ethyleen-propyleen rubber.

De NMR karakteristieken van de verschillende domeinen van de polymeren zijn hieronder samengevat:

Het *bulk polypropyleen* in ethyleen-propyleen blokcopolymeren is gekenmerkt door één enkele T_{1H} relaxatietijd. Dit betekent dat het niet mogelijk is om met T_{1H} een onderscheid te maken tussen kristallijn en amorf polypropyleen als gevolg van spindiffusie. Aan de andere kant vertoont $T_{1\rho H}$ een bi-exponentiële verval curve: de lange relaxatietijd kan toegeschreven worden aan de rigide fase zoals kristallijn polypropyleen en de korte component kan geassocieerd worden met de amorfe fase. Uit de T_{1H} en $T_{1\rho H}$ resultaten kon afgeleid worden dat de kristallijne domeinen een grootte hebben tussen 4.8 en 23nm.

De $T_{1\rho H}$ relaxatietijd van de rigide fase blijkt zeer gevoelig te zijn voor de thermische voorgeschiedenis van het staal. Deze relaxatietijd varieert van 30ms voor het niet-geannealde staal tot 87ms voor het best geannealde staal. Dit betekent dat $T_{1\rho H}$ gebruikt kan worden om de thermische voorgeschiedenis van een staal te controleren. Bovendien vertonen geannealde stalen een opsplitsing van het methyleen en methyl signaal in het ^{13}C vaste stof NMR spectrum.

Uit de T_{2H} metingen bij kamertemperatuur is afgeleid dat juist boven de glastransitie temperatuur (-1.9°C) geen verschillen in mobiliteit kunnen gedetecteerd worden tussen kristallijn en amorf polypropyleen omdat bij deze temperatuur de mobiliteit van het amorf polypropyleen beperkt is. Bij hogere temperatuur verhoogt de mobiliteit van het amorfe polypropyleen waardoor twee tot drie relaxatietijden kunnen onderscheiden worden. Vandaar dat de temperatuur voldoende hoog boven de glastransitie temperatuur moet zijn om een verschil in moleculaire mobiliteit te kunnen meten tussen kristallijn en amorf polypropyleen. Dit reflecteerde zich ook in de lijnbreedte van de signalen in het ^{13}C MAS spectrum. De amorfe of mobiele signalen worden geleidelijk smaller in functie van de temperatuur. Vanaf 50°C is het mogelijk om een onderscheid te maken tussen de signalen van de rigide en de mobiele methyleen en methine koolstoffen van het bulk polypropyleen. Het voordeel van hogere temperatuursmetingen is dat de relaxatietijden van het mobiele en rigide koolstof atoom apart kunnen bepaald worden.

Verder bleek dat de ethyleen-propyleen copolymere domeinen weinig of geen invloed hebben op de relaxatietijden van het bulk polypropyleen in deze blokcopolymeren daar er met CP/MAS experimenten geen onderscheid gevonden was tussen de relaxatietijden van het bulk polypropyleen in blokcopolymeren en een polypropyleen staal.

Uit de ^{13}C vaste stof NMR spectra bleek dat de signalen van *het ethyleen-propyleen rubber* klein zijn t.o.v. de signalen van het bulk polypropyleen. De ethyleen-propyleen blokcopolymeren bevatten immers maximum slechts 25% 'echt' ethyleen-propyleen copolymeer. De signalen van de mobiele fasen - het amorfe polypropyleen en de 'ethyleen-propyleen copolymere domeinen- kunnen benadrukt worden in het MAS spectrum als gevolg van de korte T_{1C} tijd. Bovendien kan enige selectiviteit bekomen worden in CP/MAS spectra bij hoge temperatuur. Een korte contacttijd van 1ms onderdrukt de signalen van de amorfe faze terwijl deze faze relatief benadrukt wordt met een contacttijd van 13ms. Dit verbetert de bepaling van de relaxatietijden van de ethyleen-propyleen copolymere domeinen.

Uit $T_{1\rho H}$ metingen kon afgeleid worden dat de relaxatietijd van deze ethyleen-propyleen copolymere domeinen sterk beïnvloed is door de temperatuur: de relaxatietijd varieert van enkele milliseconden bij kamertemperatuur tot bijna 100ms bij 90°C. Voor het amorf polypropyleen daarentegen werden bij hoge temperatuur slechts tijden gevonden van maximaal 18ms. Dit toont aan dat de copolymere domeinen een hogere mobiliteit moeten bezitten dan het bulk polypropyleen. Dit resultaat wordt bevestigd door de lagere glastransitie temperatuur van het 'echte' copolymeer t.o.v. polypropyleen. De hogere mobiliteit reflecteert zich ook in langere T_{2H} relaxatietijden. De T_{2H} relaxatietijd van de copolymere domeinen kan gaan tot enkele tientallen milliseconden bij 100°C.

Commeriële ethyleen-propyleen copolymeren bevatten ook een kleine hoeveelheid *polyethyleen*. Er kan een onderscheid gemaakt worden tussen de mobiliteit van het copolymeer en het kristallijn polyethyleen m.b.v. $T_{1\rho H}$.

Het laag moleculair gewicht doet de T_{2H} relaxatietijd, die gemeten is via de CPMG pulssequentie, verhogen en het effect hangt af van de fractie.

Op dit moment kan een eerste interpretatie gegeven worden aan de resultaten van een **industriële NMR**.

Met wideline NMR werd slechts één T_{1H} relaxatietijd gevonden voor de ethyleen-propyleen blokcopolymeren. Van de CP/MAS experimenten is echter geweten dat de relaxatietijd niet uitgemiddeld is over het ganse staal door spindiffusie, maar dat de relaxatietijden tussen het bulk polypropyleen en het 'echte' copolymeer zo weinig verschillen dat er met wideline NMR geen onderscheid gemaakt kan worden tussen de relaxatietijden van beide domeinen.

$T_{1\rho H}$ relaxatietijden die bepaald zijn met wideline NMR moeten met de nodige voorzichtigheid geïnterpreteerd worden. Twee relaxatietijden werden gevonden met wideline NMR terwijl er meerdere tijden gevonden waren met CP/MAS NMR. De toewijzing van de twee relaxatietijden die bepaald zijn wideline NMR hangt af van de temperatuur.

Uit T_{2H} metingen bleek dat binnen een copolymeer de T_{2H} relaxatietijden van de verschillende domeinen sterk kunnen variëren. De relaxatie is in feite een distributie van relaxatietijden van koolstof atomen met verschillende mobiliteiten. Deze distributie wordt voorgesteld door twee of drie relaxatietijden. Afhankelijk van de gebruikte pulssequentie zijn er bepaalde relaxatietijden benadrukt en een ander set van relaxatietijden zal de distributie van tijden voorstellen.

Een vergelijking van de stalen onderling toonde aan dat de polypropyleen stalen dikwijls kortere T_{2H} relaxatietijden hebben in vergelijking met de copolymeren als gevolg van de hogere T_g van het polypropyleen. Er bestaat ook een verschil tussen blok- en randomcopolymeren. Het randomcopolymeer heeft kortere T_{2H} relaxatietijden t.o.v. de blokcopolymeren. Bovendien kon er afgeleid worden dat er een relatie bestaat tussen de T_{2H} relaxatietijden en andere eigenschappen van de stalen. Stalen met meer ethyleen en met hun ethyleen verdeeld in korte sequenties hebben de hoogste T_{2H} relaxatietijden en de beste slagvastheid.

Indien de on-line industriële NMR mogelijkheden biedt voor kwaliteitscontrole dan wordt er verwacht dat dit best gemeten wordt via T_{2H} met de Hahn of de CPMG pulssequentie. Met de CPMG pulssequentie wordt het meest mobiele deel van het staal gemeten zoals het ethyleen-propyleen rubber. Het is precies deze fase van het polymeer dat voor de verbetering van de eigenschappen (impactsterkte) zorgt.

9. EXPERIMENTAL PART

9.1. NMR measurements

9.1.1. Liquid-state NMR

For the liquid-state NMR measurements 1,2,4-trichorobenzene with 10% benzene-d_6 as the lock signal was used. First of all three to four pellets of the investigated polymer were put in a NMR tube and solvent was added just to cover the sample. The NMR tube was heated at 120°C so that the solvent could diffuse into the pellets. Afterwards, more solvent was added and the polymer solution was heated at 140°C until a homogeneous solution was obtained. This could be checked against light.

The quantitative 100MHz ^{13}C NMR spectra were measured at 120°C and 1000 scans were collected. A 60° pulse was used and the preparation time was 8s. A Waltz-16 modulated proton decoupling was used.

9.1.2. Solid-state NMR

9.1.2.1. Sample preparation

The polymer pellets were melt pressed in a hot press at 230°C for 5 minutes followed by quenching in ice water. The result was a polymer film of 0.7mm thickness (quenched sample). Afterwards the polymer film was heated to 100°C for one hour and cut into small particles and moulded (if that was possible) under cooling with nitrogen air.

For the study of the annealing of the polymer the quenched polymer film was cut into small particles, which were put for one hour in a thermostatically controlled oil bath. The temperature of the *oil* was: 120, 123, 126, 140, 160, 165, 168, 170, 172°C. The sample name depended on the oil temperature, i.e. I-120, I-123, …

For the study of the annealing time the polymer was annealed at 120°C during 5, 15, 30 and 60minutes.

9.1.2.2. ^{13}C CP/MAS NMR

Two NMR spectrometers were used to record the spectra: a Varian Unity 400 spectrometer was used for most of the measurements and when a Varian XL 200 NMR was used it is mentioned with the NMR results. The magic angle spinning speed was 6kHz and 3.6kHz for the 400MHz and the 200MHz NMR, respectively. The rf-field of 57kHz and 40kHz was used for the 400MHz and the 200MHz NMR. The polymer sample was put in Si_3N_4 rotors. The calibration of the temperature of the 400MHz NMR was performed with ethylene glycol.

The pulse sequences used are reported in section 2.3.3. A preparation time of 5s was used for the CP/MAS measurements. For the MAS spectra the preparation time is mentioned with the spectra in chapter 5. The length of the contact time, the measuring temperature as well as the array of the variable time in the pulse sequence are reported together with the NMR results in chapter 5.

9.1.2.3. ^{1}H wideline NMR

The measurements were obtained with a Varian Unity 400 spectrometer with a static transverse 5 mm-coil. A sweep width of $2*10^6$ was used. The temperature was calibrated by using methanol. The pulse sequences are described in section 2.4. The measuring temperature as well as the array of the variable time in the pulse sequences are given with the relaxation results in chapter 6. For all the measurements a preparation time of 4 to 5μs was used.

The 20MHz NMR measurements reported in chapter 6 were recorded with an Oxford QP20+. A spin lock field yielded 57kHz. A preparation time of 3s was used.

9.1.2.4. Analysis of the NMR spectra

Integration and deconvolution of the signals of the spectra was performed using the software of a Varian Unity 400 spectrometer.

Relaxation times were obtained by fitting the experimental data using a computer program, Kaleidograph, that is based on the Levenberg-Marquardt algorithm. Criteria that were used to determine the goodness of fit of the results were: χ^2 have to be as low as possible, the correlation coefficient R must be close to 1, the standard deviation of all the parameters have to be small. The standard deviation is related with a 60 percent confidence interval.

9.2. Differential scanning calorimeter

The apparatus used for studying the melting of the polymers was a DSC 2920 equipped with Thermal Analyst 2100 software. The sample preparation was the same as for the solid-state NMR measurements (section 9.1.2.1). During the measurement the sample was warmed up to 200°C with a heating rate of 10°C/min. For the determination of the melting temperature the maximum of the melting peak was used.

For the measurement of the glass transition temperature a DSC 2920 modulated DSC was used. The sample was cooled to -200°C and heated with a rate of 2,5°C/min. The period of modulation was 60s and the temperature amplitude of modulation was 1,00°C. A flow rate of helium of 30ml/min was obtained. The glass transition temperature was determined from the inflection point in the DSC scan.

9.3. Wide angle x-ray scattering

Wide angle x-ray diffraction patterns were obtained using a Philips PW1840 apparatus (45kV, 30mA) using Ni-filtered $CuK_{\alpha 1}$ radiation ($\lambda = 0.15405$nm). The 2Θ Bragg angle was varied between 10 to 35 degrees.

9.4. Fractionation with xylene

5g of a polymer sample was weighed in a suitable flask and 500 ml o-xylene was added. A magnetic stir bar was placed in the flask. The flask equipped with a condenser, a thermometer and a nitrogen inlet tube was placed in an oil bath and put on the electronic stirrer plate.

The solution was heated to 150°C in a period of 30 minutes, while stirring under a nitrogen blanket. As 150°C was reached, the solution was stirred at that temperature for another 30 minutes. Cooling of the solution was done in two stages. In the first stage, the solution temperature was reduced to 100°C in 10 minutes. In the second stage, the solution was cooled down to 25°C in 20 minutes without stirring. The temperature was maintained at 25°C during 20 minutes without stirring and then 10 minutes with stirring. This sample treatment was automated.

The solution was filtered through a funnel with filter paper (whatman 41). The filtered aliquot was separated into two 150 ml samples.

The precipitate was washed with xylene, heated under a nitrogen stream at 140°C and placed in an vacuum oven at 70°C until constant weight was reached. This was the *xylene insoluble fraction*.

To one of the 150 ml aliquots of filtered solution 300ml of acetone was added and the mixture was stirred at 25°C. Precipitation must be complete as evidence by a clear solid-solution separation. The solution was filtered on a tarred metallic screen and washed with acetone so that the xylene was completely removed. The filtrate was collected in tarred pans and heated under a nitrogen stream at 140°C. Afterwards, the pan was placed in the oven under a light vacuum at 70°C until a constant weight was reached. This was the *oil fraction*. The insoluble fraction was dried in a vacuum oven at 70°C until a constant weight was reached. This fraction was called the *amorphous xylene soluble fraction*.

The second 150 ml aliquot of the filtered solution was quantitatively transferred into the tarred pan and evaporated in the same way as the oil fraction. This was the *xylene soluble fraction*.

9.5. Mechanical testing

Injection moulded samples were used for the mechanical testing. The test methods are based on ISO norms. The samples are conditioned at 25°C and a relative humidity of 50% for at least 48 hours. For the determination of the Charpy and Izod impact strength the injection moulded samples were notched.

For the melt flow rate, a certain amount of polymer (3 to 6g) was brought is a cylinder heated at 230°C. The capillary had a diameter of 2.095mm and a length of 8mm. A weight of 2.16kg was used.

The rate of elongation is 50mm/min for the tensile test and the rate of deformation yielded 2mm/min for the flexural test. The tests were performed at 25°C.

ABBREVIATIONS

Ethylene-propylene block copolymer = a polypropylene matrix in which ethylene-propylene copolymer particles are dispersed.

Ethylene-propylene random copolymer = polypropylene chains in which the ethylene is randomly distributed.

iPP = isotactic polypropylene

sample names:		**percentage ethylene (%):**
A	polypropylene	0
B	polypropylene	0
H	ethylene-propylene block copolymer	8.5
I	ethylene-propylene block copolymer	14
I*	ethylene-propylene block copolymer	15.5
J	ethylene-propylene random copolymer	3.1

H_{xs}, I_{xs}, I^*_{xs}, J_{xs}	the xylene soluble fraction of respectively the samples H, I, I* and J and this fraction contains presumably the true ethylene-propylene copolymer
H_{xi}, I_{xi}, I^*_{xi}, J_{xi}	the xylene insoluble fraction of respectively the samples H, I, I* and J and this fraction contains presumably the bulk polypropylene

Chemical shift assignment

S, T, P	methylene (secondary), methine (tertiary) and methyl (primary) carbons
α, β, γ, δ	refers to the distance between the carbon under investigation and the neighbouring methine carbon

ABBREVIATIONS

NMR

B_0	main magnetic field
B_1	spin lock field
CP	cross polarisation
CT	contact time
DD	dipolar decoupling
γ	magnetogyric ratio $\gamma = 2\pi\mu/I$
I	nuclear spin quantum
MAS	magic angle spinning
M_0	magnetisation at time $t = 0$
M_∞	equilibrium magnetisation at time $t = \infty$
μ	magnetic moment
ω_0	Larmor frequency
T_{CH}	cross depolarisation time
T_1	spin lattice relaxation time
$T_{1\rho}$	spin lattice relaxation time in the rotating frame
T_2	spin spin relaxation time